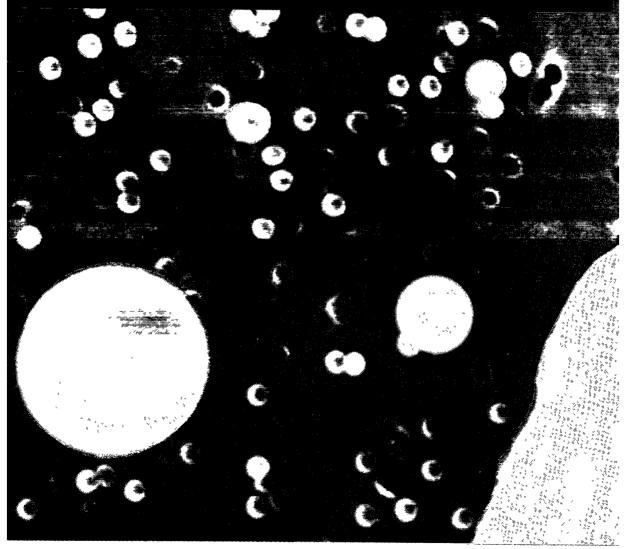# A Study on

The Affinity Cross-Flow Filtration Process

Wei Zhang

28

A Study on

The Affinity Cross-Flow Filtration Process

Proefschrift

ter verkrijging van
de graad van doctor aan de Universiteit Twente,
op gezag van de rector magnificus,
prof. dr. Th.J.A. Popma,
volgens besluit van het College van Dekanen
in het openbaar te verdedigen
op donderdag 19 augustus 1993 te 15.00 uur

door

Wei Zhang
geboren 14 maart 1954
te Dalian, China

Dit proefschrift is goedgekeurd door de promotor prof. dr. C.A. Smolders, de co-promotor prof. dr. ing. H. Strathmann en de assistent-promotor dr. ir. Th. van den Boomgaard.

Acknowledgement

I first wish to thank Kees Smolders for providing me the opportunity to undertake this Ph.D. study and for his guidance and support through out this work.

I am indebted to Thonie van den Boomgaard for his invaluable comments, suggestions and fruitful discussions during the four years period, and especially in the final stage of writing the thesis.

I would like to thank Heiner Strathmann for his thorough check of this manuscript and Marcel Mulder for his advise and support.

Many colleagues in the group deserve special thanks: to Zandrie Borneman not only for his skillful technical assistance but also for his patience in teaching me Dutch; to Richard Bouma for his strong support in mathematics; to Antoine Kemperman for his contribution in the preparation of core-shell latex and to Shuguang Li for refreshing my Chinese. I would like to thank my room mates: Arnold, Monique and Antoine for their support, understanding and many helps.

I am grateful to all members of the membrane technology group for their kindness, friendship and support during my stay in Enschede.

Outsides the group I wish to thank Bert Gebben for his persistent support, stimulating discussions and his direct contribution in chapter 2. My thanks also goes to Gert van den Berg who was the first contact I had with the University of Twente.

Outside the academic world I owe a great deal to my wife, You-Lei, and my daughter, Xin-Lan, for their love, understanding , patience and support.

Wei Zhang

CONTENTS

1

Introduction

1.1 GENERAL

In the middle of the nineteenth century, according to Geis [1], the Dutch chemist Gerardus Mulder found a common substance from plants and animal tissues which he believed to be "the most important of all substances of the organic kingdom". To this substance Mulder gave the name *protein* after the Greek word *proteios*, meaning "of first importance", together with a specific chemical formula ($C_{40}H_{62}N_{10}O_{12}$). Proteins are the most abundant of cellular components and play key roles in nearly every biological process.

Nowadays in modern society proteins are used as feed stock for different products varying from human and animal nutrients to medicines and various industrial products. In the preparation of proteins as feed stock conventional separation techniques are applied such as precipitation, extraction, drying and so on. The introduction of genetic recombinant techniques in the middle of 1970's resulted in novel protein products [2, 3]. However, these proteins are usually produced in low concentrations and in the presence of numerous contaminants, so alternative separation techniques are required. The high degree of dilution makes an extensive downstream processing necessary and makes purification a dominant part of the overall process costs (figure 1) [4-7]. Belter *et al* [8] distinguished for the separation processes of pure proteins from the animal or plant cells or cultured microorganisms four different steps. The starting point is removing insoluble material and the final separation step is polishing the purified product e.g. by crystallization or drying. Unfortunately each separation step represents a certain degree of product loss. Therefore it is desirable to reduce the number of processing steps and to enhance the product recovery in every step.

In the following section several separation processes will be discussed.
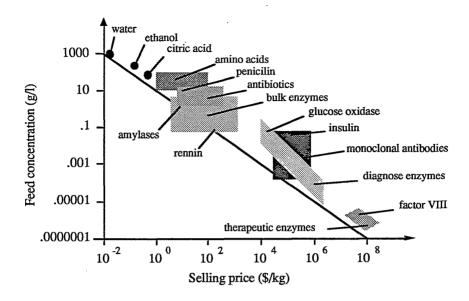
Fig. 1 The Sherwood plot for bioproducts: feed concentration versus selling price
(plotted after A.E. Rodrigues et al. [4]).

1.1.1. Purification processes

Separation processes can be categorized into three groups according to their functions[6]:

- Concentration of a small amount of desired product,
- Fractionation of comparable amount of related components,
- Purification for removing small amount of impurity.

Most of the conventional separation processes e.g. centrifugation, conventional filtration, cross-flow filtration and precipitation are not feasible to be applied as a purification process but a clarification process, and therefore are often used in early steps of a protein separation scheme. This is so because the contaminants usually have similar physicochemical properties as those of the desired protein product and because these separation processes are either lack of resolution power or economically not feasible. Adsorptive processes such as various forms of liquid chromatography and electrophoresis appear to be the only tool for protein purification. Analytical chromatography is used in a lab scale for small amounts of protein samples while preparative chromatography is generally used in an industrial production line. According to the functions of the column packing materials

chromatographic procedures can be grouped into gel permeation (or size exclusion) chromatography, ion exchange chromatography, hydrophobic chromatography and affinity chromatography. Among these chromatographic procedures affinity chromatography has the unique feature of high resolution. Therefore it would be desirable to apply this technique in an early step to deal with large quantities of the feed stream so that the total number of processing steps necessary will be decreased to reduce the protein loss.

Affinity chromatography is one of the most attractive bioseparation techniques among the various chromatographic applications. The term affinity chromatography was introduced by Cuatrecasal *et al* in 1968 [9]. At that time it was used to describe all kinds of chromatography except size exclusion, ion exchange and hydrophobic chromatography [10]. In this thesis the term affinity chromatography is used not only to include biospecific ligands but also biomimetic ligands such as dye ligands and metal chelating ligands. Affinity chromatography utilizes biospecific adsorption which includes a number of simultaneous interactions between biological molecules and their complementary ligands, resulting in strong and highly specific binding and very high purification factors (50 to 1000) [11]. Affinity chromatography is typically carried out in a column packed with porous particles (or beads) on which the affinity ligand has been immobilized. A four step procedure is normally required to operate the affinity chromatography process (see figure 2). In the first step a protein mixture is loaded into the column, allowing specific recognition by the affinity ligand. Selective binding of the protein onto the ligand-immobilized particles occurs. In the following step washing buffer will remove the
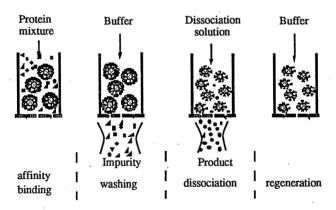
Fig. 2 A schematic illustration of a typical affinity chromatographic procedure.

unbound impurity (or contaminants) from the column. In the third step, elution buffer is applied to make the interactions between the protein and the affinity ligand no longer favorable, and in this way the product is recovered from the column. Finally, the column is regenerated with the adsorption buffer in the last step.

Although, affinity chromatography has a number of advantages over other techniques industrial application is rather limited due to the facts that: 1) it is a discontinuous process; 2) binding kinetics can be slow because of the possibility of restricted protein diffusion inside porous particles [12, 13]; 3) low flow rates and low column heights have to be employed to avoid compression of the packed porous beads in the column (due to the poor mechanical strength of the porous particles), which result in a low productivity; 4) it has difficulties in the scaling-up of the process.

Affinity binding is a powerful technique for downstream processing in biotechnology. It should be economically beneficial to employ affinity binding in early stages in a protein purification scheme, to reduce the number of the required steps. In this way the product recovery can be improved because each step of operation gives a certain portion of product loss. To this end, a large-scale affinity binding process is needed to overcome the drawbacks of affinity chromatography. Lots of efforts have been attempted to combine affinity binding with these processes which are easy in scale-up. Examples [14-16] can be given for affinity precipitation, affinity two-phase partition and affinity cross-flow filtration (ACFF). In the next paragraphs the affinity cross-flow filtration process, which will be the topic of this thesis, will be treated in more detail, together with the principles of the adsorption phenomena.

1.1.2 Affinity Cross-Flow Filtration

Very recently, four reviews on the topics of novel affinity binding-based processes for protein purification appeared in literature [17-20]. The development and the state of art of the ACFF processes have been described in these articles.

In the ACFF process a four step procedure is usually required. In the first step a mixture of substances is loaded into the system where the desired substance (target molecule) will bind to the affinity ligand carrier. In the second step the targeted molecule, which would pass freely through a porous membrane, will be retained by the membrane due to the formation of the affinity complex which has a size larger than the pores of the membrane, while unbound components in the mixture will pass through the membrane. In this way

the separation of the targeted molecule from the mixture is achieved. In the third step the isolated targeted molecule-carrier particle complex is treated with an appropriate eluant to dissociate the targeted molecule from the carrier particles. Subsequently the targeted molecules are separated from the carrier particles by means of a membrane with the right pore size and thus purified. In the last step the carrier particles are regenerated and reused. A flow scheme of the ACFF process is depicted in figure 3.
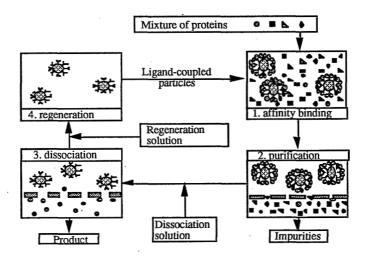
Fig. 3 A schematic illustration of the ACFF process.

The work by Mattiasson and coworkers first demonstrated successfully the ACFF process [21]. Mannans on the surface of heat-killed yeast cells were used as ligands for purifying the lectin Concanavalin A (molecular weight (MW) of 102,000 daltons) from defatted Jack beans (Canavalia ensiformis). A membrane with a nominal MW cut off of 1.000.000 daltons was used to retain the cells and to recover the lectin Concanavalin A. Total yield of the process was 70 % with high product purity [22, 23].

Luong and his coworkers have investigated the ACFF process systematically [24-28]. A water soluble ligand bound polymer (MW > 100.000 daltons) was synthesized by copolymerizing N-acryloyl-m-aminobenzamidine, a strong trypsin inhibitor, and acrylamide in the absence of oxygen for the purpose of purification of trypsin from a trypsin-chymotrypsin mixture. Batchwise operation was carried out using Millipore flat

sheet membranes with the MW cut-off of 100.000 daltons. Trypsin was dissociated from the trypsin-affinity polymer complex by the trypsin inhibitor, arginine. A capability of recovering 98% pure trypsin at 90% yield was found. Luong *et al* also performed the ACFF process in a continuous mode. Trypsin was purified from crude trypsin prepared from pig pancreas. Four UF membrane units were used in the process, resulting in a yield of 77%. A mathematical model was developed to describe the dynamic behavior of an ACFF continuous process. High retention both for the chymotrypsin in the washing step (69%) and for the trypsin in the dissociation step (93%) were encountered in the continuous process. This example further emphasizes the essential importance of the selection of a suitable membrane and a carrier particle.

Herak and Merill [29, 30] presented a more theoretical work. They used models based on the affinity interaction theory and diafiltration theory to predict the concentrations of the targeted molecule in the affinity binding and the washing step in the ACFF process . Human serum albumin (HSA) was used as a targeted molecule. Agarose beads with immobilized Cibacron blue were used as carrier particles. Millipore 0.2 μm hydrophilic microfiltration membranes were used in their experiments. Both experimental and modeling work clearly indicated that the release of the target molecules during the washing step is better described by a model assuming no release of the targeted molecules (irreversible binding) from the carrier particles rather than the one assuming an equilibrium state for the binding interaction (partial release of the bound proteins during washing).

There are many other efforts in the development of the ACFF processes which are listed in table 1. It is worthwhile to point out that in the early stage of development people tended to use the available materials in their hand rather than prepare it for a specific application, and they were limited in choosing the appropriate membranes for the protein-carrier particle system studied. With the experiences and the knowledge obtained through the last ten years or so, it is now possible to develop so-called tailor-made carrier particles and tailor-made membranes for a specific application of the ACFF process.

1.1.3 Protein adsorption

Affinity binding of a protein to a ligand shares the common features with protein adsorption at interfaces in general in the sense of molecular interactions involved. The term adsorption is defined as that material accumulates at the interface between two phases. Protein adsorption onto a solid surface is a complicate process involving numerous parameters and considerations concerning the nature of the protein, the nature of the solid

Table 1. *Proteins and enzymes recovered by affinity cross-flow filtration*

Protein purified	Carrier particle	Particle size	Membrane	Ref.
Concanavalin A	Heat-killed yeast	5 μm	1,000,000 [a]	22
ADH [b]	starch granule	1 - 10 μm		23
Trypsin	polyacrylamide	> MW 100,000	100,000 [a]	26, 27
HSA [c]	agarose particle	20 - 150 μm	0.2 μm	29
ADH and LDH [d]	fumed silica	12 nm		31
β-galactosidase	agarose particle	50 - 200 μm	20 μm	32
Trypsin	dextran T-2000	MW 2,000,000	300,000 [a]	33
Trypsin	dextran T-2000	MW 2,000,000	100,000 [a]	34
hemoglobin	agarose particle	unknown	100,000 [a]	35
Avidin	liposomes	25 - 70 nm	100,000 [a]	36

a: molecular weight cut off value of the membrane used.

b: ADH refers to alcohol dehydrogenase.

c: HSA refers to human serum albumin.

d: LDH refers to lactate dehydrogenase.

surface and the solution environment.

These basic considerations are directly related to the intra- and inter-molecular interactions important in protein structure and function: 1) ionic or electrostatic interaction between the charged groups either in attraction or in repulsion. 2) hydrophobic interaction resulting from water-structure effects adjacent to hydrophobic interfaces which is usually an entropically driven process. 3) hydrogen binding which results in high interaction energies compared to other non-covalent bonds. 4) other interactions, e. g., a charge-transfer or partial electron donor/acceptor type of interaction. The same features are applicable to the surfaces, e.g. hydrophobic/hydrophilic surfaces as well [37, 38].

Like all processes, adsorption only occurs if there is an overall decrease in Gibbs free energy of the system:

$$\Delta G = \Delta H - T \, \Delta S < 0 \qquad\qquad (1)$$

Equation 1 shows that the adsorption can be either enthalpy driven or entropy driven. The adsorption of proteins from an aqueous solution at a solid/water interface is usually endothermic, therefore it is generally accepted that the adsorption process is driven by entropy changes [39]. The equilibrium state of an adsorption process can be described by an adsorption isotherm [38, 40]. Some well-known isotherms are the Langmuir isotherm for uniform adsorption sites, the empirical Freundlich isotherm and the Temkin isotherm for nonuniform adsorption sites [41, 42]. The theory of adsorption is very well developed for small molecules at interfaces as well as for neutral and charged polymers [43-48]. In the case of protein adsorption the situation is more complex. This is attributed to several factors associated with protein adsorption processes. Protein adsorption is usually irreversible upon dilution. Exchange of protein molecules from solution to the ones adsorbed may possibly occur. When adsorption from a mixture of proteins takes place, the situation is even more complicated due to the existence of competition between proteins for the adsorption sites on the surface, which in turn depends on the concentration, the diffusion coefficient, and the interaction between the protein and the surface.

It is generally observed that proteins adsorb more strongly onto hydrophobic surfaces than onto hydrophilic surfaces. This is thought to be due to the large entropy gain through desorption of water molecules from the surface of protein molecules and the hydrophobic surface where the water molecules are adsorbed in an ordered structure with a low entropy [39]. The adsorbed proteins usually undergo a conformation change in protein structure in favor of enhancing the interaction.

Besides hydrophobic interactions, electrostatic interactions can be expected to play an important role in the interactions between proteins and charged surfaces. Proteins themselves are polyelectrolytes with charged groups, e. g. primary amines and carboxylic acids. The net charge of the proteins in solution depends on the pH of the proteins. At the isoelectric point (IEP), the net charge is zero, but there are still charged groups centered at certain locations on the proteins. As a consequence, electrostatic interaction is still possible [49, 50]. A general observation for the effect of pH is that protein adsorption goes through a maximum at the IEP [40, 51]. This can be readily explained by the fact that the electrostatic repulsion at the IEP between the protein molecules in the adsorbed protein layer is minimum. When the surface and the protein to be adsorbed are charged, it is expected that adsorption will be increased if the protein molecule and the surface have opposite charges, and decreased for equal charges. However, adsorption of negatively charged proteins onto

negatively charged surfaces has been observed [52-55]. Both ion coadsorption and conformational changes of the adsorbed protein are considered to be responsible for this type of adsorption.

The effect of ionic strength is expected to influence protein adsorption to a large extent as it is for the effect of pH. This is due to the charge screening effect. As a consequence, the thickness of the electric double layer decreases when the ionic strength of a solution increases. Moreover, the electrostatic interaction between a protein and a surface will be decreased as the ionic strength of a solution increases. This effect is often used to evaluate whether electrostatic interaction plays an important role in protein adsorption or not. Norde *et al*, found ion coadsorption in the adsorbed protein layer on negatively charged latex at neutral pH which in turn influenced the protein adsorption [51, 52].

The competition between plasma proteins in an adsorption process is an interesting phenomenon worth mentioning. Competitive adsorption is a typical kinetic process. As a result of the competition, the composition of the adsorbed layer will change in time depending on the difference between the proteins in concentration, molecular dimension and adsorption energy. This means that displacement of adsorbed proteins by the proteins in solution occurs, which is called the "Vroman" effect [56, 57]. The "Vroman" effect is characterized by a maximum in the amount of the adsorbed protein both as a function of time and as a function of concentration [58, 59]. The surface hydrophobicity is thought to play an important role in this exchange process. However, a relationship between the surface characteristics and the "Vroman" effect has yet to be found.

1.2 THE MODEL SYSTEM STUDIED

1.2.1 General

The ACFF process, as the name suggests, consists of two parts, one being affinity adsorption and the other being membrane filtration. In affinity adsorption the carrier particle on which the affinity ligand is immobilized is of essential importance. A core-shell type of latex particle with a thin porous shell is utilized in this study as an attempt to avoid pore diffusion limitation in the whole process. Porous chromatographic beads are used for reasons of comparison. The following proteins are chosen as model proteins for this study. Bovine serum albumin (BSA), bovine serum immunoglobulin G (IgG), and lysozyme are well known and have been studied extensively [37, 40, 60, 61]. Besides, these proteins are

easy to obtain and have been used in many applications e.g., in health care and food industry. It is known from literature that a triazine dye Cibacron Blue F3G-A has a high affinity for BSA and an intermediate affinity for IgG [60]. Therefore, BSA may serve as a target and IgG as an impurity in the ACFF process. For reasons of comparison lysozyme is used in this study to gain an insight into the binding mechanism between the ligand and the proteins. This is because lysozyme has a high isoelectrical point (pH = 11), and thus shows a positive charge rather than the negative charge at normal binding conditions for BSA and IgG. The group specific ligand, Procion Blue HB™ which is a analog of the well-known Cibacron Blue F3G-A, was chosen because of the high chemical stability compared with a protein ligand, and the easy accessibility so that it can be used for large scale production. The general features of the model protein-ligand-carrier particle system, together with cross-flow filtration, are described in more detail in the following paragraphs.

1.2.2 Affinity binding

In general affinity binding between a ligand and a protein is more complex than protein adsorption on a plain surface. This is so because 1) ligands normally have a position at a small distance from the solid surface and are able to make a sterical contact with protein molecules; 2) ligands usually contain various types of chemical groups, and therefore, bind protein molecules through different types of interactions.

First of all, a ligand has to be chosen specifically for an affinity adsorption process. Biological ligands, although possessing high specificity with proteins, have certain deficiencies, e. g. high cost and low stability for potential large-scale application and they show difficulties in immobilization [62-64]. Dye-ligands on the other hand, have the advantage of low cost and high durability in comparison with biological ligands. The incident finding of the affinity interaction of a triazine dye Cibacron Blue F3G-A (CB) to a number of proteins brought a rapid growth of interest both in research and applications [62, 65]. As a result, immobilized CB has found its use for the purification of over 80 enzymes and proteins [66]. Since the dyes have no biological relation to the proteins to be purified their interaction is therefore named "dye-ligand affinity" to distinguish from biospecific affinity [67]. It has been shown that commercial preparations of triazine dyes consist of several chromophoric species [68].

All the dyes share the common feature of having both charged groups and nonpolar (aromatic) ring systems in the same molecule [69, 70]. As an example, the molecular

structure of CB is depicted in figure 4. It has been confirmed that CB binds proteins mainly through the interaction with its aromatic ring. If, for example, CB is immobilized using the anthraquinonoid amino to agarose, the binding strength to a number of proteins, e.g. interferon [71, 72], serum albumin [73] and glucose-6-phosphate dehydrogenase [74] is greatly reduced or even eliminated. This is explained by the steric hindrance for approaching protein of the anthraquinone group after it is used for immobilization. To

Fig. 4 The molecular structure of Cibacron Blue F3G-A.

some types of enzymes CB binds in a biospecific manner. For instance, the binding of CB to various dehydrogenases involves the so-called "nucleotide-binding fold" on these enzymes, and elution using a natural ligand such as nicotinamide dinucleotide can be very efficient. However, the fact that CB binds to a large number of proteins which are functionally unrelated indicates that the interpretation of the binding mechanism between the dye and the proteins is very difficult and it is still not clear for most of the proteins. It is believed that dye affinity to a vast number of proteins is a combination of hydrophobic and electrostatic interaction [62, 75, 76].

Immobilization of CB onto carrier particles can be done through hydroxyl group by a nucleophilic exchange of the chlorine atom on the triazine ring to form an ether bond. Parameters like dye concentration, salt concentrations, pH and temperature, all can be optimized to give a desired amount of dye immobilized on the particles (surface ligand density) [11].

1.2.3 Carrier particles

Agarose particles

As it has been adopted in affinity chromatography an ideal carrier particle, on which the

affinity ligand is immobilized and which can be used in the ACFF process, should meet the following requirements [77-79]: mechanically and chemically stable, free of non-specific adsorption centers, presence of functional groups for ligand immobilization and resistance toward microbial and enzymatic attack. Hardly any material can fulfill these conflicting conditions. In practice, the choice of the type of carrier particle for a particular application is very often a compromise among these conditions.

Agarose is the most commonly used support material in affinity chromatography as a hydrogel and in a bead form. It is a linear polysaccharide consisting mainly of 1,3-linked -o-galactopyranose and 2,4-linked, 3,6-anhydro -o-L-galactopyranose [80]. The structure of the polysaccharide chains of the agarose is formed with a double helix, and aggregates are formed via hydrogen bonding into bundles or fibers with ordered structures resulting in large openings within the matrix. The agarose matrices are very hydrophilic and have minimal non-specific interactions with proteins. This unique feature is attributed to the water molecules which are tightly bound with the polysaccharide chains and act as a screen that keeps proteins away from the polymer chains [81]. Ligand immobilization can easily be done through a large amount of hydroxyl groups available on the polysaccharide chains. Beaded forms of agarose particles are commercially available as column packings for gel filtration and affinity chromatography. These particles are characterized by the size of the pores which exclude proteins according to their molecular weight, which can vary from 5×10^5 daltons to 1.5×10^7 daltons depending on the pore size in the particles. The variation in the size exclusion limit is achieved by varying the polymer content during the bead preparation. The particle sizes of the agarose beads range from 40-200 μm [82].

Mechanical stability of the agarose particles is one of the major draw backs. This is especially true in HPLC. Small sized, highly crosslinked agarose particles have been made and resulted in improved rigidity and chemical and physical stability [83]. One of these types of agarose particles, called Superose 6 Prep grade, is used in this work.

Core-shell latex particles

Polystyrene (PS) latex is commonly used as a colloidal model system [40, 84, 85]. Monodisperse PS latex can be prepared in a wide size range with good reproducibility [86-88]. Due to the hydrophobic nature, nonspecific protein adsorption on PS latex is inevitable. By introducing a hydrogel shell around the hard PS core, core-shell latex particles are prepared by a seeded semi-continuous emulsion copolymerisation of acrylic and vinylic monomers [89-90].The shell is water-swellable due to the presence of the vicinal hydroxyl

(generated from the hydrolysis of epoxy groups), the amide, the sulfonate and sulfate groups in the shell of the core-shell latex particles. A large amount of hydroxyl groups in the hydrogel shell is essential for eliminating nonspecific protein adsorption as well as for ligand immobilization [91]. Since the shell layer is very thin, it provides minimal or no diffusion path for proteins to adsorb onto these particles.

In contrast to porous agarose particles core-shell latex particles are designed to be less or non-porous in order to eliminate pore diffusion. This is done in the expense of losing specific surface area (per unit volume) for ligand immobilization, which may lead to low binding capacity. Core-shell latex particles are therefore prepared in a range of particle sizes from submicron to micron in order to provide comparable specific surface areas as that for agarose particles.

The core-shell latex particles are negatively charged. The negative charge comes from covalently bound sulfate and sulfonate groups during the seeded polymerization. Therefore, ionic interactions may occur between proteins and the shell layer of the particles.

1.2.4 Proteins

Bovine serum albumin

Serum albumin is a globular, ellipsoidally shaped protein which has been studied extensively [92]. One of the main reasons is that it is the most abundant protein found in blood with a high concentration of 3.5-4.5 g/l, and therefore could be prepared in large quantities with a reasonable purity in early time. As has been pointed out by Franglen in 1974 [93], preparation and storage of plasma albumin was always accompanied by formation of dimer or polymer; it is difficult to maintain albumin samples in a completely monomeric state. This is attributed to the property of albumin that it possesses a reactive thiol group per molecule, which activity decreases in time during storage. As a consequence, large deviations are found for the determination of the molecular weight of bovine serum albumin (BSA) [94]. A value of about 69,000 daltons was commonly accepted. Albumin contributes 80 % of the colloid osmotic pressure and about 10 % of protein nutrition of cells [95]. Albumin has an isoelectric point of 4.7 to 4.9. At physiological pH the net charge is about -17 units of negative charges. BSA migrates slightly faster than human serum albumin (HSA) on electrophoresis at pH 8.6. So BSA has a higher negative charge than HSA. The high charge of albumin makes it very hydrophilic and highly soluble in water. It is also known that these charges are distributed

nonuniformly in three domains over the molecule (see figure 5) [96].

Albumin binds and transports various substances, especially fatty acids [97]. Binding of one or two long-chain fatty acids is known to stabilize the native structure of albumins, and the configuration becomes more spherical and more resistant to proteolysis [98].

In general albumin binds any organic compound with at least five or six CH_2 groups
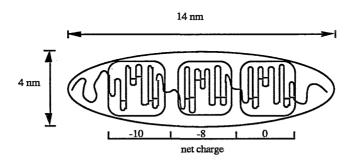
Fig. 5 The proposed structure of the albumin molecule (plotted after T. Peters Jr.[96]).

despite whether an accompanying hydrophilic group such as a carboxylate, sulfonate, sulfate or hydroxyl group exists or not [99]. The binding is dominated by the hydrophobic interactions between the alkyl chain and the hydrophobic side chains of the amino acids forming the binding site " pockets" in the albumin molecule. The binding strength can be enhanced by involving electrostatic interactions because the presence of cationic residues near the mouth of the pockets which can interact with an anionic group such as a carboxylate or sulfate group. [96, 99, 100].

A strong interaction between albumin and Cibacron Blue F3G-A (CB) has been found and utilized in affinity chromatography for the purification of albumin from Cohn fraction IV paste [7]. It has been proven that this binding interaction involves the binding sites for fatty acids [101-105]. Preparative chromatography using a 40 l column packed with CB immobilized agarose particles has been applied for the purification of BSA from Cohn fraction IV paste from 15 % to > 95 % [106].

Immunoglobulin G

Immunoglobulin G (IgG) is the major class of antibodies present in blood plasma (from

8-17 grams of IgG/liter of plasma) [107]. The basic structure of immunoglobulin is a Y-shaped molecule consisting of two heavy chains and two light chains which are interconnected by disulfide bonds [108, 109]. The two arms, named Fab fragments (F refers to fragment; and ab refers to antigen binding), contain the antigen-binding site at the top, while the base part is called the Fc fragment (c refers to crystallizable), which is more hydrophobic in nature and often adsorbs to hydrophobic surfaces [110, 111]. In adsorption studies it is found that the angle between the two Fab fragments varies from 10° to 180° when the solution environment changes ; e. g., being more extended at pH values away from the isolectric point. It is known that IgG binds CB at an intermediate level (less strongly than BSA) [60], although the exact binding sites and binding mechanisms are not known.

Lysozyme
Lysozyme is a single chain protein with a molecular weight of 14200 daltons and a dimension of 9 x 2 x 2 nm^3 [112]. The rich source of lysozyme is in egg white. As an enzyme, it catalyzes the hydrolytic cleavage of polysaccharides for some bacteria. The high isoelectric point of pH 11 makes lysozyme particularly useful, because at neutral pH most proteins have a negative charge while lysozyme is positively charged.

Studies on lysozyme-CB interaction reveal that CB binds lysozyme more strongly than BSA [30, 113]. Two types of binding interactions were distinguished by Mayes et al., one type has high binding strength and the other has low binding strength (nonspecific type) [114]. The binding mechanisms and the binding sites are not known.

1.3 MEMBRANE FILTRATION

1.3.1 General
Ultrafiltration (UF) and microfiltration (MF), are the typically pressure-driven separation processes which have been well developed for large-scale industrial applications. Membranes for UF and MF can be made of polymer materials as well as ceramics [115-118]. The separation mechanism for UF and MF is based on the so-called sieving effect which is solely dependent on the relative dimension of a solute (or particle) regarding to the size of the pore on a membrane surface. For a filtration system with the protein concentrations C_f in the feed and C_p in the permeate the observed retention coefficient R is:

$$R = 1 - \frac{C_p}{C_f} \qquad\qquad (2)$$

In the ideal case these solutes (or particles) whose sizes are smaller than the pore size will pass through without hindrance ($R = 0$), while those particles larger than the pore size will be retained by the membrane ($R = 1$). For the ACFF process it is desirable to have 100 % transmition of proteins and 100 % retention for the carrier particles. However in practice this sharp separation is usually not obtainable. A solute with a smaller dimension in comparison with the pores on a membrane will be partially retained due to the steric interaction between the solute and the pores. Thus, a zero percent retention is difficult to obtain unless the solute particles are very small with respect to pore size.

1.3.2 Dead-end filtration

Membrane filtration processes can be operated either in the forms of "dead-end" filtration or cross-flow filtration. In dead-end filtration the solution to be filtered flows in the same direction as the permeate flow, i.e. perpendicular to the membrane surface (figure 6 a) [115]. The retained solutes or particles therefore will deposit on the membrane surface
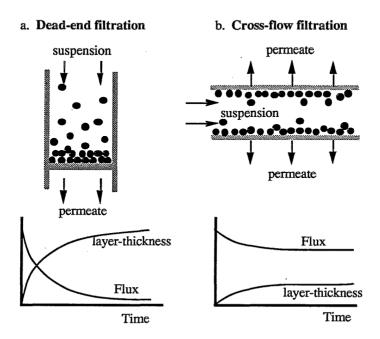
Fig. 6 The schematic illustrations of dead-end filtration and cross-flow filtration.

forming a cake layer or accumulate in the void spaces if a depth filter is used. Subsequently the filtration flux will decrease in time due to the deposition of the retained particles. As a result the filter medium is often replaced when the flux reduction becomes unacceptable. For this reason dead-end filtration is usually operated batchwise.

1.3.3 Cross-flow filtration

For the last two decades cross-flow filtration (see figure 6 b) has been developed for overcoming the drawbacks of dead-end filtration. The advantages of the cross-flow filtration over the traditional dead-end filtration lies in two aspects: 1) high shear stress can be used along the membrane surface to sweep away the retained solute (or the deposited particles). This is applicable for cross-flow filtration because the flow directions between the feed and the permeate are different so that the increase of the feed flow rate, as a means to increase the shear stress, does not necessarily bring more solutes (or particles) to the membrane surface while it is not the case for the dead-end mode. 2) back-flushing operation can be periodically used to remove the retained solutes or particles at the membrane surface.

Membrane filtration can be used for the purpose of concentration (product in the concentrate), clarification (product in the permeate) and separation (product in both streams). Besides these operation modes, diafiltration is a useful technique for removing contaminants from the processing solution while a constant concentration of a retained solute is maintained when it is expected to be so [117]. In the batch operation of the ACFF process, diafiltration is often applied.

1.3.4 Concentration polarization

During a membrane filtration process, it is usually observed that filtration flux of the membrane decreases in time, often referred to as flux decline. The flux decline can be a few percent of the pure water flux for relatively clean feed in UF, and can be more than 90 % for some cases in MF. Several phenomena are responsible for the flux decline which reflects the decreased driving force and/or the increased filtration resistance. At least five types of resistances can be distinguished [119-124]. The resistance of the membrane R_m is always present and is independent on time. The resistance caused by pore blocking R_p, the resistance due to adsorption of the solute onto the pore wall of the membrane R_a, the resistance caused by the phenomenon of concentration polarization R_{cp} and the resistance

caused by gel layer formation R_g are additive to the resistance of the membrane R_m and are time dependent. Accordingly, the filtration flux J for UF and MF can be expressed in a general form :

$$J \text{ (flux)} = \frac{\text{Driving force}}{\eta \text{ Resistance}} = \frac{\Delta P}{\eta \ R_{total}} \qquad (3)$$

where η is the viscosity of filtration solution, ΔP is the transmembrane pressure drop and R_{total} is the total resistance expressed as:

$$R_{total} = R_m + R_p + R_a + R_{cp} + R_g \qquad (4)$$

These resistances are schematically depicted in figure 7. As mentioned above, the so-called concentration polarization is a very important, and very often encountered phenomenon as long as the membrane is rejective to a solute (or a particle). Concentration
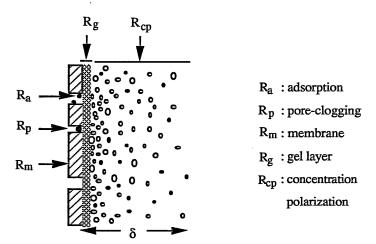
Fig. 7 *A schematic description of various resistances possibly present near a membrane surface during a filtration experiment (plotted after van den Berg* [119]*).*

polarization can be described as the accumulation of the rejected solute at the membrane interface during the filtration process, and results in a concentrated layer at the interface with a layer thickness δ. This concentrated layer may evolve into a gel layer depending on

the property of the solute (or the particle) and the operation conditions. This gel layer (or concentrated layer) reduces flux to a large extent. The phenomenon of concentration polarization is depicted in figure 8. Many models have been proposed to describe the filtration flux by taking the concentration polarization into account [125-133]. Most of the models can be grouped into two basic types. One type of the models is based on the cake-filtration theory with the assumption of a constant concentration of the solutes (or the particles) in the cake layer deposited on the membrane surface. The other type of models is derived from the mass balance between the solutes (or particles) brought to the membrane surface by convective permeation flow and the solutes taken back to the bulk solution from the surface by diffusive transport. These two idealized situations are depicted in figure 8 a and b.

a) the cake-filtration type
of description

b) the concentration profile
according to the film theory
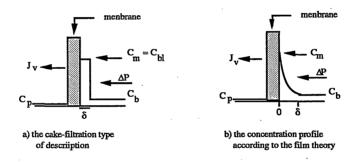
Fig. 8 Two basic models for illuminating the phenomenon of concentration polarization.

1.3.5 Choice of membranes

Some criteria for selection of membranes for filtration of protein solutions have already been mentioned by a number of investigators [16, 134] as follows:

- high hydraulic permeability to solvent (water)
- sharp MW cut-off
- good mechanical durability, chemical and thermal stability
- high hydrophilicity
- easy cleaning and sterilization

The sharp MW cut-off and low non-specific protein adsorption are two features essential for selection of membranes used in the ACFF process. In the ACFF process the

separation between proteins and the carrier particles has to be done with membranes. A suitable membrane should give 100 % transmition to proteins and 100 % retention to the carrier particles. Generally speaking, UF membranes are not considered to be suitable for the separation of macromolecules with a difference in molecular weight of less than a factor of 10. The molecular weight of a protein of interest is usually in the range of 20,000-200,000 daltons. Therefore, UF membranes with MW cut-off of 100,000-1,000,000 daltons would be a right choice. Unfortunately, the use of UF instead of MF membranes is not often recommended when both proteins (or enzymes) and particles (with particle size of submicrons) are present. This is because proteins may be retained which is not desirable [135, 136]. The membranes with narrow pore size distribution would be expected to have better performances, especially with a hydrophilic nature[137-140]. Therefore microfiltration membranes are favorable in the ACFF processes, which may have high retention for particles and low retention for proteins.

1.4 STRUCTURE OF THE THESIS

The search for large-scale separation processes in downstream processing for biotechnology has gained increasing attention over the last ten years or so. The ACFF process is one of the promising processes under extensive investigations. However, research works are limited by the accessible materials as carrier particles and membranes. This study is considered to be the first effort toward the investigation of so-called tailor-made carrier particles and tailor-made membranes for a specific application of the ACFF process.

In chapter 2 polystyrene core-shell latex and the ligand-immobilized core-shell latex complex are investigated as affinity ligand carriers for affinity separations. The core-shell latex particles are prepared by a seeded emulsion polymerization process and consisted of a hard polystyrene core surrounded by a hydrophilic shell with particle sizes ranging from submicron to micron. Covalently ligand immobilization directly to hydroxyl groups present in the hydrophilic shell of the core-shell latex particles is studied by diffuse reflection spectroscopy. Electrochemical properties of the ligand-immobilized core-shell latex particles are also studied in respect to surface charge and colloidal stability of the ligand-carrier complex. Protein binding and release is studied as well.

In chapters 3 and 4, binding experiments for singular protein as well as competitive binding with a protein mixture on the ligand-immobilized core-shell latex particles and the ligand-immobilized agarose particles are investigated for three proteins, bovine serum albumin, bovine serum immunoglobulin G and lysozyme. The effects of surface ligand density and binding conditions such as protein concentration and composition, binding time, pH and ionic strength on the binding are investigated. Binding isotherms of the proteins are determined for singular proteins. The protein binding capability Γ_m and the binding constant K_a are evaluated from the isotherms using a type of Langmuir fit, and consequently are used in the prediction of the binary binding isotherms. Dissociation experiments are carried out using solutions of NaCl, sodium octanoate or free dye. With these results the interpretation of binding mechanisms is attempted. Binding conditions for the competitive case which lead to optimized preferential binding of one particular protein are studied.

In chapter 5 the microfiltration behavior of the protein solution, the particle suspension and the mixture of both is investigated. For the case of protein solution particular attention is given to the phenomenon of protein aggregation and its consequence to flux decline. Microfiltration of the ligand-immobilized carrier particles with and without the presence of protein is studied using several types of membranes. A range of particle sizes are used to show the influence of the particle size on the steady state flux. The interactions between particle, protein and membrane are also investigated.

In chapter 6 the filtration behavior of two well-characterized proteins of different molecular dimensions, both alone and in a mixture, using two partially permeable membranes, both with a hydrophilic character is investigated. Experiments of protein adsorption on the membranes are also performed. The emphasis of this chapter lies in the aspect of the mutual interaction between proteins and interaction between proteins and membranes regarding the performance parameters such as flux reduction and retention.

In chapter 7 the ACFF process is carried out in a batchwise mode with the model protein-ligand system on the ligand-immobilized core-shell latex particles and the ligand-immobilized agarose particles using a few types of membranes. Both purity and recovery of the target protein, in the presence of a model impurity are examined for the ACFF process. Model simulation of the washing stage of the ACFF process is attempted. Emphasis of this chapter is laid on the use of nonporous particles and membrane aspects in the ACFF process.

1.5 REFERENCES

1. I. Geis, in "Biochemistry", G. Zubay (Ed.), Addison-Wesley Publishing Company, Inc., Reading, Massachusetts, 1983, pp. 1.

2. D.I.C. Wang, Biotechnology: Status and Perspectives, AIChE Monograph Series Vol. 84 (18), 1988.

3. A.S. Michaels and A.S. Michaels, Chem. Eng. Prog., 80 (1984) 19.

4. A.E. Rodrigues, M.M. Dias and J.C.B. Lopes, in "Chromatography and Membrane Processes in Biotechnology", C.A. Costa and J.S. Cabral (Ed.), NATO ASI Series E: Applied Science Vol. 204, Kluwer Academic Publishers, Dordrecht, 1991, pp. 25.

5. J.L. Dwyer, Bio/Technol., 2 (1984) 957.

6. E.N. Lightfoot, in "Protein Purification from Molecular Mechanisms to large-Scale Processes", M.R. Ladisch, R.C. Willson, C.C. Paionton, S.E. Builder (Eds.), ACS Symposium Series. 427, 1989, pp. 35.

7. E.R.A. Jeans, P.J. Marshall and C.R. Lowe, Trends Biotechnol., 3 (1985) 267.

8. P.A. Belter, E.L. Cussler and W.-S. Hu, Bioseparations: Downstream Processing for Biotechnology, Wiley, New York, 1988, pp. 1.

9. P. Cuatrecasal, M. Wilchek, C.B. Anfinsen, Proc. Natl. Acad. Sci., USA, 61 (1968) 636.

10. J. Porath, J. Macromol., Sci. Chem., 10 (1976) 1.

11. M.T.W. Hearn and B. Anspach, in "Separation Processes in Biotechnology", J. A. Asenjo (Ed.), Marcel Dekker, Inc., New York , 1990, pp. 17.

12. F.H. Arnold, H.W. Blanch and C.R. Willke, Chem. Eng. J., 30 (1985) B25.

13. P.M. Boyer and J.T. Hsu, AIChE J., 38 (1992) 259.

14. J.C. Janson, Trends Biotechnol., 2 (1984) 31.

15. C.R. Lowe, J. Biotechnol., 1 (1984) 3.

16. J.H.T. Luong, A.L. Ngugen and K.B. Male, TIBTECH, 5 (1987) 281.

17. N. F. Gordon, C.M.V. Moore and C.L. Cooney, Biotech. Adv., 8 (1990) 741.

18. J. -P. Chen, J. Ferment. and Bioeng., 70 (1990) 199.

19. D. Sii and A. Sadana, J. Biotechnol., 19 (1991) 83.

20. B. Mattiasson, in "Chromatographic and Membrane processes in Biotechnology", C.A. Costa and J.S. Cabral (Eds.), NATO ASI Series E: Applied Science Vol. 204, Kluwer Academic Publishers, Dordrecht, 1991, pp. 335.

21. B. Mattiasson and T.G.I. Ling, in "Membrane Separation Biotechnology", McGregor W.C. (Ed.), Marcel Dekker, (1986) 99.

22. B. Mattiasson and M. Ramstorp, Ann. N.Y. Acad. Sci., 413 (1983) 307.

23. B. Mattiasson and M. Ramstorp, J. Chromatogr., 283 (1984) 323.

24. K.B. Male, J.H.T. Luong, and A.L. Nguyen, Enzyme Microbial Technol., 9 (1987) 374.

25. J.H.T. Luong, K.B. Male and A.L. Nguyen, Biotechnol. Bioeng., 31 (1988) 439.

26. J.H.T. Luong, K.B. Male and A.L. Nguyen, Biotechnol. Bioeng., 31 (1988) 516.

27. J.H.T. Luong, K.B. Male and A.L. Nguyen, Biotechnol. Bioeng., 32 (1988) 451.

28. K.B. Male, A.L. Ngugen and J.H.T. Luong, Biotechnol. Bioeng., 35 (1990) 87.

29. D.C. Herak and E.W. Merrill, Biotechnol. Prog., 5 (1989) 9.

30. D.C. Herak and E.W. Merrill, Biotechnol. Prog., 6 (1990) 33.

31. T.G.I. Ling and B. Mattiasson, Biotechnol. Bioeng., 34 (1989) 1321.

32. E. Pungor Jr., N.B. Afeyon, N.F. Gordon and C.L. Cooney, Bio/Technol., 5 (1987) 604.

33. D. Adamski - Medda, Q.T. Nguyen and E. Dellacherie, J. Membr. Sci., 9 (1981) 337.

34. T.B. Choe, P. Masse and A. Verdier, Biotechnol. Lett., 8 (1986) 163.

35. J.C. Hsia, Eur. Pat. Appl. EP 229696 A1 (1987).

36. J.D. Powers, P.K. Kilpatrick and R.G. Carbonell, Biotechnol. Bioeng., 33 (1989) 173.

37. J.D. Andrade, in "Surface and Interface Aspects of Biomedical Polymers", Vol. 2, Protein Adsorption, J.D. Andrade (Ed.), Plenum Press. N.Y., 1985, pp. 1.

38. J. Israelachvili, Intermolecular and Surface Forces, 2nd ed., Academic Press, London, 1991.

39. M.A. Cohen Stuart, G.J. Fleer, J. Lyklema, W Norde and J.M.H.M. Scheutjens, Adv. Colloid Interface Sci., 34 (1991) 477.

40. W. Norde, Adv. Colloid Interface Sci., 25 (1986) 267.

41   W.J. Moore, Physical Chemistry, Lowe & Brydone Ltd., Thetford, Norfolk, U.K., 1974.

42. J.M.H.M. Scheutjens and G.J. Fleer, J. Phys. Chem., 83 (1979) 1619.

43. J.M.H.M. Scheutjens and G.J. Fleer, J. Phys. Chem., 84 (1980) 178.

44. C.A.J. Hoeve, J. Chem. Phys., 44 (1966) 1505.

45. M.J. Garvey, Th.F. Tadros and B. Vincent, J. Colloid Interface Sci., 49 (1974) 57.

46. M.A. Cohen Stuart, F.H.W.H. Waajen, T. Cosgrove, B. Vincent and T.L. Crowley, Macromolecules, 17 (1984) 1825.

47. J. Papenhuijzen, J. Van der Fleer and B.H. Bijsterbosch, J. Colloid Interface Sci., 104 (1985) 553.

48. H.A. van der Schee and J. Lyklema, J. Phys. Chem., 88 (1984) 6661.

49. J. Vila and J.L. Alssandrini, J. Theo. Biol., 134 (1988) 445.

50. Y. Ikada, H. Iwata, F. Horii, T. Matsunaga, M. Taniguchi, M. Suzuk, W. Taki, S. Yamagata, Y. Yonekawa and H. Handa, J. Biomed. Mater, Res., 15 (1981) 697.

51. H. Shirahama. and T. Suzawa., J. Colloid Interface Sci., 126 (1988) 269.

52. W. Norde and J. Lyklema, J. Colloid Interface Sci., 66 (1978) 257.

53. P. van Dulm, W. Norde and J. Lyklema, J. Colloid Interface Sci., 82 (1981) 77.

54. A.V. Elgersma, R.L.J. Zsom, W. Norde and J. Lyklema, J. Colloid Interface Sci., 138 (1990) 145.

55. A.V. Elgersma, R.L.J. Zsom, W. Norde and J. Lyklema, Colloids and Surfaces, 54 (1991) 89.

56. L. Vroman, A.L. Adams, J. Biomed. Mater. Res., 3 (1969) 438.

57. L. Vroman, A.L. Adams and M. Kings, Fed. Proc., 30 (1971) 1494.

58. J.L. Brash and P.ten Hove, Thromb Haemostasis, 51 (1984) 326.

59. P. Wojciechowski, P. ven Hove and J.L. Brash, J. Colloid Interface Sci., 111 (1986) 455.

60. G. Birkenmeier, in "Protein-Dye Interactions: Developments and Applications", M.A. Vijayalikshmi and O. Bertrand (Eds.), Elssvier Applied Science, London, 1989, pp. 253.

61. T.A. Horbett and J.L. Brash, Proteins at Interfaces. Physicochemical and Biochemical Studies, ACS Symposium Series 343, J.L. Brash and T.A. Horbett (Eds.), Amer. Chem. Soc., Washington D.C., 1987, pp. 1.

62. C.R. Lowe, in "Topics Enzyme and Fermentation Biotechnology", A. Wiseman (Ed.), Vol. 9, Ellis Horwood, Chichester, 1984, pp. 78.

63. K. Jones, Anal. Proc., 28 (1991)140.

64. M.D. Scawen, Anal. Proc., 28 (1991) 143.

65. R.K. Scopes, Anal. Biochem., 165 (1987) 235.

66. P. Mohr and K. Pommerening, Affinity Chromatography: Practical and Theoretical Aspects, Marcel and Dekker, N.Y., 1986.

67. Y.D. Clonis, in "Reactive-Dyes in Protein and Enzyme Technology", Y.D. Clonis, T Atkinson, C.T. Bruton and C.R. Lowe (Eds.), Stockton Press, N.Y., 1987, pp. 33.

68. D. Hanggi and P. Carr, Anal. Biochem., 149 (1985) 91.

69. C.V. Stead, in Protein-Dye Interactions: Developments and Applications, M.A. Vijayalikshmi and O. Bertrand (Eds.), Elsevier Applied Science, London, 1989, pp. 21.

70. S. Subramanian, in "Protein-Dye Interactions: Developments and Applications", M.A. Vijayalikshmi and O. Bertrand (Eds.), Elsevier Applied Science, London, 1989, pp. 56.

71. W. Janlowski, W. Von Muenchhausen, E. Sulkowski and E. Carter, Biochemistry, 15 (1976) 5182.

72. E. Bollin, K. Vastola, D. Oleszek and E. Sulkowski, Prep. Biochem., 8 (1978) 259.

73. J. Tarvis, D. Bowen, D. Tewksbury, D. Johnson and R. Pannell, Biochem. J., 57 (1976) 301.

74. R.S. Beissner and F.B. Rudolph, J. Chromatogr., 161 (1978) 127.

75. R.K. Scopes, in "Protein-Dye Interactions: Developments and Applications", M.A. Vijayalikshmi and O. Bertrand (Eds.), Elssvier Applied Science, London, 1989.

76. J. Carlsson, J.-C. Janson and M. Sparrman, in "Protein Purification: Principles, High Resolution Methods, and Applications", J.-C. Janson and L. Ryden (Eds.), VCH Publishers, Inc., New York, 1989, pp. 275.

77. T.C.J. Gribnau, Ph.D Thesis, Catholic University, Nijmegen, The Netherlands, (1977).

78. C.P. Lowe and P.D.G. Dean, Affinity Chromatography, John Wiley & Sons, 1974.

79. P.D.G. Dean, W.S. Johnson and F.A. Middle (Eds.), Affinity Chromatography, A Practical approach, Press, Oxford, Washington DC, 1985.

80. F.M. Nicolaisen, I. Meyland and K. Schaumburg, Acta. Chem. Scand., B34 (2) (1980) 103.

81. J. Porath, J. Chromatogr., 218 (1981) 241.

82. Data given by Pharmacia, Sweden.

83. T. Andersson, M. Carlsson, L. Hagel, P.-A. Pernemalm and J.-C. Jansen, J. Chromatography, 326 (1985) 33.

84. R.H. Ottewil and J.N. Shaw, Discuss Faraday Soc., 42 (1966) 154.

85. A. Kotera, K. Furusawa and K. Kudo, Kolloid Z.Z. Polym., 240 (1970) 839.

86. W.M. Brouwer and R.L.J. Zsom, Colloids and surfaces, 24 (1987) 165.

87. R.L.T. Zsom, J. Colloid Interface Sci., 111 (1986) 434.

88. H. Shirahama and T. Suzawa, J. Colloid Interface Sci., 104 (1985) 416.

89. J. Ugelstad and P.C. Mork, Adv. Colloid Interface Sci., 13 (1980) 101.

90. J.W. Vanderhoff, M.S. El-Asser and F.J. Micale, ACS Pol. Mat. Sci. Eng., 54 (1986) 587.

91. B. Gebben, D. van Houwelingen, W. Zhang, Th. van den Boomgaard and C.A. Smolders, Colloids and Surfaces B Biointerfaces, in preparation; chapter 2 of this thesis.

92. P.G. Squire, P. Moser and C.T. O'Konski, Biochem., 7 (1968) 4261.

93. W.L. Hughes, in "The Proteins", vol. 2, part B, H. Neurath and K. Bailey (Eds.), Academic Press Inc., N.Y., 1954, pp. 663.

94. H.E. Schultze and J.F. Heremans, Molecular Biology of Human Proteins with Special Reference to Plasma Proteins, vol. 1, Elsevier Publishing Co., Amsterdam, 1966.

95. T. Peters Jr., in Plasma Proteins, Vol. 1, F.W. Putman Acad. Press, N.Y., 1975, pp. 133.

96. T. Peters Jr., Adv. Prot. Chem., 37 (1985) 161.

97. J.D. Morrisett, H.J. Pownall, A.M. Gotto Jr., J. Biol. Chem., 250 (1975) 2487.

98. F. Soetewey, M. Rosseneu-Motreff, R. Lamote, J. Biochem. (Tokyo), 71 (1972) 705.

99. R.H. McMenamy, in "Albumin structure, Function and Uses," V.M. Rosenoer, O. Murray and M.

A. Rothschill (Eds.), Pergamon, New York, 1977, pp. 143.

100. A.A. Specter, J. Lipid, Res., 16 (1975) 165.

101. W.G. Pitt and S.L. Cooper, J. Biochem., Mat. Rea., 22 (1988) 359.

102. D.J. Birkett, S.P. Myers and G. Sudlow, Molecular Pharmacology, 13 (1977) 987.

103. U. Kragh-Hansen, J.V. Moller and K.E. Lind, Biochimica et Biophsica Acta, 365 (1974) 360.

104. W.G. Pitt, T.G. Grasal and S.L. Cooper, Biomaterials, 9 (1988) 36.

105. C. Lagerecratz and T. Larsson, Biochem. J., 213 (1983) 387.

106. J.E. More, A.G. Hitchcock, S. Price, J. Rott and M.J. Harvey, in "Protein-Dye Interactions: Developments and Applications", M.A. Vijayalikshmi and O. Bertrand (Eds.), Elssvier Applied Science, London, 1989, pp. 265.

107. L. Andersson and R. Lunden, in "Plasma Proteins", Wiley, N.Y., 1979, pp. 7.

108. G.M. Edelman, Science, 180 (1973) 830.

109. J.L. Winkelhake, Immunochem., 15 (1978) 695.

110. T. Suzawa and H. Shirahama, Adv. Colloid Interface Sci., 35 (1991) 139.

111. P. Bagchi and S.M. Birnbanm, J. Colloid Interface Sci., 83 (1981) 460.

112. J.R. Colvin, Can. J. Chem., 30 (1952) 831.

113. P.M. Boyer and J.T. Hsu, Chem. Eng. Sci., 47 (1992) 241.

114. A.G. Mayes, J.D. Moore and R. Eisenthal, Biotechnol. Bioeng., 36 (1990) 1090.

115. R.H. Davis, in "Membrane Handbook", W.S.W. Ho and K.K. Sirkar (Eds.), Van Nostrand Reinhold, New York, 1992, pp. 457.

116. H.K. Lonsdale, J. Membr. Sci., 10 (1982) 81.

117. M. Cheryan, Ultrafiltration Handbook, Technomic Publishing Co., Inc., Lancaster, 1986, pp. 1.

118. M.H.V. Mulder, Basic Princiles of Membrane Technology, Kluwer Academic Publishers, Dordrecht, 1991, pp. 198.

119. G.B. van den Berg and C.A. Smolders, Desalination, 77 (1990) 101.

120. S. Nakatsuka and A.S. Michaels, J. Membr. Sci., 69 (1992) 189.

121. W.S. Opong and A.J. Zydney, J. Colloid Interface Sci., 142 (1991) 41.

122. A.G. Fane and J.M. Radovich, in "Separation Processes in Biotechnology", J.A. Asenjo (Ed.), Marcel Dekker, N.Y., 1990, pp. 209.

123. E. Klein, Affinity Membranes: Their Chemistry and Performance in Adsorptive Separation Processes, Wiley, Corp., New York, 1991, pp. 110.

124. A.D. Marshall, P.A. Munro and G. Trägårdh, Desalination, 91 (1993) 65.

125. G.B. van den Berg and C.A. Smolders, J. Membr. Sci., 40 (1989)149.

126. G.B. van den Berg and C.A. Smolders, J. Membr. Sci., 47 (1989) 1.

127. J.G. Wijmans, S. Nakao, J.W.A. van den Berg, F.R. Troelstra and C.A. Smolders, J. Membr. Sci., 22 (1985)117.

128. W.F. Blatt, A. Dravid, A.S. Michaels and L. Nelson, in "Membrane Science and Technology", J.E. Flinn (Ed.), Plenum Press, New York, NY, 1970, pp. 47.

129. D.R. Trettin and M.R. Doshi, Ind. Eng. Chem. Fundm., 19 (1980) 189.

130. G. Belfort, J. Membr. Sci., 40 (1989) 123.

131. C.A. Romero and R.H. Davis, J. Membr. Sci., 39 (1988) 157.

132. A.L. Zydney, J. Membr Sci., 68 (1992) 183.

133. W.S. Opong and A.L. Zydney, J. Membr. Sci., 72 (1992) 277.

134. J.S. Johnson, Chem. Eng., 8 (1986) 121.

135. J.D. Henry and R.C. Allred, Dev. Ind. Microbiol., 13 (1972) 177.

136. P.N. Patel, M.A. Mehaia and M. Cheryan, J. Biotechnol., 5 (1987) 1.

137. D.E. Brown and P.R. Kavanagh, Process Biochem., 22 (1987) 96.

138. P.S.J. Cheetham, in Handbook of Enzyme Biotechnology, A. Wiseman (Ed.), Ellis Horwood Ltd., 1987, pp. 54.

139. W.C. McGregor, in "Membrane Separation Biotechnology", McGregor W.C. (Ed.), Marcel Dekker, 1986, pp. 1.

140. D. Defrise and V. Gekas, Process Biochem., 23 (1988) 105.

2

Protein Separation Using Affinity Binding
Part I Polystyrene core-shell latex as ligand carrier

B. Gebben[1], G.D.B. van Houwelingen[1], W. Zhang, Th. van den Boomgaard, C.A. Smolders

SUMMARY

Polystyrene core-shell latex particles are introduced as affinity ligand carriers for affinity separations. The particles, prepared by a seeded emulsion polymerization process, are of submicron size and composed of a hard polystyrene core surrounded by a hydrophilic shell to which affinity ligands can be covalently coupled. The reactive dye Cibacron Blue is studied as model ligand. This dye ligand covalently coupled directly to hydroxyl groups on the particle surface is studied and the amount of coupled ligand is determined quantitatively by diffuse reflection spectroscopy. The degree of coupling can be controlled by the ionic strength of the reaction medium. The binding of bovine serum albumin to the latices appeared to be proportional to the ligand density. The functionalized core-shell latices show high colloidal stability, fast protein binding/release kinetics and low nonspecific adsorption. The latex particles can find use in affinity separation techniques like affinity chromatography and affinity membrane filtration.

2.1 INTRODUCTION

Affinity separation uses the natural biological affinity displayed between biological macromolecules and complementary ligands such as enzymes and coenzymes, antibodies and antigens, receptors and hormones. The ligands are generally covalently coupled to solid supports or carrier particles to facilitate the isolation of the product (bound/free separation) and to create the possibility of recycling the often expensive ligands. The dominating

---

[1] AKZO Research Laboratory Arnhem, Arla, CRC, Arnhem.

affinity purification technique is affinity chromatography[1,2]. This technique enables a high degree of purification while providing a good recovery yield. It suffers from drawbacks like discontinuity of operation and difficulties in the scale-up process[3]. One of the novel processes being developed which take advantage of the affinity adsorption process on the one hand and attempts to overcome the above mentioned disadvantages on the other hand is the so-called affinity cross-flow filtration (ACFF) process[4-7]. This process combines affinity binding to colloidally suspended solid particles with cross-flow membrane filtration for bound/free separation.

The ideal carrier particle should meet the following requirements: insolubility, high specific surface area, mechanical and chemical stability, hydrophilicity, free of non-specific adsorption sites, functional groups for ligand coupling and resistance towards microbial and enzymatic attack[1]. Beaded agarose can be considered to be the most used carrier material. Disadvantages are poor acid, thermal and mechanical stability and macroporosity, being responsible for a rate limiting pore-diffusion.

In this study [8, 9] polystyrene latex with a core-shell structure is investigated as ligand carrier for use in an affinity cross-flow filtration process. Cibacron Blue has been chosen as model ligand for the separation of bovine serum albumin (BSA) from mixtures with immunoglobulin G (IgG). In this chapter the preparation, ligand immobilization and characterization of the carrier particles are described. Chapters 3 and 4 [8, 9] deal with the single and competitive protein binding behaviour of the ligand-immobilized carrier particles. Polystyrene latex is one of the most frequently described model systems for studying particle interaction in colloidal systems[10-12] and adsorption behaviour of various adsorbents, like proteins[13-16]. Monodisperse polystyrene latex can be prepared in a wide size range and in a physico-chemically reproducible manner[17, 18]. The core-shell latex used in this study is prepared by a seeded semi-continuous emulsion copolymerization of acrylic and vinylic monomers. As seed a polystyrene latex is used prepared by an ordinary emulsion polymerization of styrene. The process results in a crosslinked copolymeric shell around the polystyrene core. The shell properties are designed in such a way that hydrophilic groups are introduced and non-specific protein adsorption is reduced as much as possible. Functional hydroxyl groups on the particle surface can be used for ligand immobilization. The direct covalent coupling of Cibacron Blue to hydroxyl functionalized core-shell latex through triazinyl arylation is studied. The characterization of the core-shell carrier particles as well as the ligand coupled particles is performed by electrophoresis,

diffuse reflection spectroscopy, conductometric titration and BSA binding.

2.2 MATERIALS

Styrene was obtained from Merck and was extracted with an equal volume of a 5 wt% potassium hydroxide solution in water to remove the inhibitor. This extraction was followed by a four-fold rinse with deionized, distilled water. Potassium persulphate was obtained from Fluka. Aerosol-MA-80, sodium-bis-1,3-dimethylbutylsulphosuccinate (SDSS), was supplied by American Cyanamid and used as received. Sodiumvinylsulphonate (SVS) was obtained from Fluka as a 30% aqueous solution, glycidylmethacrylate (GMA), acrylamide (AAm) and N,N'-methylenebisacrylamide (NMBAm) were obtained from Janssen and used as received.

Cibacron Blue F3G-A (Procion Blue HB) was purchased from Janssen. The content of dye is about 60%. The dye was used as received.

Bovine Serum Albumin (BSA, Boseral 30 TA, 300 g/l solution) was obtained from Organon Teknika B.V. (Boxtel, The Netherlands) and used as received.

Potassium monohydrogen phosphate and potassium dihydrogen phosphate, analysis grade, were obtained from Baker.

Pure water was obtained using a Millipore Milli Q-plus system fed with distilled water.

2.3 METHODS

2.3.1 Latex preparation

Monodisperse polystyrene latex was prepared by batchwise emulsion polymerization according to earlier described procedures[13, 14] in 1 liter double walled glass reactors equipped with reflux cooler, pitch-blade stirrer and nitrogen purge in the presence of the anionic emulsifier sodium-bis-1,3-dimethylbutyl sulphosuccinate (SDSS, Aerosol MA-80), sodium hydrogencarbonate buffer and potassium persulfate initiation at 70°C. Recipes are given in table 1.

After reaction the latices were filtered over glass wool and used without further purification as seeds in a seeded semi-continuous emulsion copolymerization where a monomer feed consisting of 9.0 g sodium vinylsulphonate (SVS), 7.0 g glycidylmethacry-

Table 1 *Recipes for batchwise preparation of monodisperse polystyrene core particles*

Code	H_2O	Styrene	$K_2S_2O_8$	$NaHCO_3$	SDSS[a]	Time	T	Diameter [nm]	
	[g]	[g]	[g]	[g]	[g]	[hr]	[°C]	QELS[b]	SEM
AAJ 19	600	300	0.486	0.606	7.77	16	70	240	255
VQ 69	600	316	0.319	0.320	5.20	22	70	378	390

a: SDSS refers to sodium-bis-1,3-dimethylbutylsulphosuccinate.

b: QELS refers to quasi-elastic light scattering.

late (GMA), 1.0 g acrylamide (AAm) and 1.0 g N,N'-methylene-bisacrylamide (NMBAm) in a mixture of 37.5 ml water and 37.5 ml methanol, was dosed at constant rate to the reactor using a Pharmacia peristaltic pump. Dosing was started directly after addition of potassiumpersulphate to the reactor at 70°C. The reactions are carried out for 18 hours (inclusive monomer feed dosage time). Recipes are given in table 2.

Table 2 *Recipes for preparation of core-shell particles*
by seeded semi-continuous emulsion polymerization

Code	H_2O	Seed		$K_2S_2O_8$	$NaHCO_3$	Feed[a]
	[g]	[g]		[g]	[g]	[ml]
ALD 3	775.0	150.0	AAJ 19	0.321	0.200	75.0
ALD 8	724.5	129.1	VQ 69	0.320	0.201	47.9

a: The composition of a monomer feed is described in the text.

Purification was performed by liquid replacement using microfiltration in stirred dead-end Amicon cells equipped with 0.2 μm Nuclepore membranes, replacing the medium 30 times with pure water. Hydrolysis of the surface epoxide groups was performed by bringing the purified latex to pH 2.5 using 1 N hydrochloric acid and shaking the latex for 3 hours at 50°C followed by liquid replacement with pure water. The amount of vicinal hydroxyl groups at the latex surface can be determined by periodate oxidation and spectrophotometric detection of diacetyldihydrolutidine formed by the reaction between the released formaldehyde and 2,4 pentanedione[19].

2.3.2 Cibacron Blue immobilization (see figure 1)

In a typical immobilization experiment 20.0 g purified latex (400 nm size, solids content 5.0 wt%) was mixed with 20.0 g of an aqueous Cibacron Blue solution (14.0 g/l) followed by 20.0 g sodium chloride solution. The pH of the mixture was adjusted to 12.0 with 1 N sodium hydroxyde. The reaction mixture was transferred to a capped polyethylene bottle (100 ml) and situated in a water bath shaker at 50 °C for 3 days. The latex was extensively purified by liquid replacement with pure water using microfiltration. The filtrate was checked for presence of Cibacron Blue spectrophotometrically at 610 nm.

Fig. 1 Covalent coupling of Cibacron Blue with vicinal hydroxyl group functionalized core-shell particles.

2.3.3 Particle size

The size of the latex particles was determined by quasi-elastic light scattering (QELS), using a Malvern 4700 Zeta-sizer set-up, Scanning Electron Microscopy and Sedimentation field flow fractionation (Du Pont SF3 2000). The polydispersity index (pdi) determined by QELS approximates the square of the relative standard deviation.

2.3.4 Diffuse reflection spectroscopy

The amount of immobilized ligand was determined quantitatively by diffuse reflection spectroscopy. The blue latex, with known solids content, is placed in the sample port of an

integrating sphere (diameter 110 mm) and the diffuse reflectance is measured at 610 nm on a Varian Cary 5 spectrophotometer. The amount of ligand was calculated from a calibration curve which was obtained by adding known amounts of free Cibacron Blue to the corresponding white latex of the same solid content. A linear relation between the ligand concentration and the well known Kubelka-Munk function was obtained.

2.3.5 Conductometric titration

The amount of covalently bound ionogenic surface groups was determined by conductometric titration with sodium hydroxide (0.01 mol/l) of purified latices, which were brought in the H^+ form prior to titration by liquid replacement with a hydrochloric acid solution (pH=3) followed by liquid replacement with pure water[13].

2.3.6 Colloidal stability limits

The purified latices (0.2 ml) were mixed with sodium chloride solutions (2.0 ml) of increasing concentrations. The latex solids content after mixing was 0.5 wt%. The highest salt concentration at which the latex was still stable after 16 hr standing was expressed as the critical flocculation concentration of the particular latex.

2.3.7 Protein adsorption experiments

Protein adsorption experiments have been performed according to earlier reported procedures by Brouwer and Zsom[13, 14]. Latex, buffer and BSA solutions were mixed so that 4 mg BSA per m^2 particle surface area was present at a BSA concentration of 0.4 mg/ml. Sörensen phosphate buffer was used at a concentration of 0.067 mol/l to set the pH between 4.6 and 8.4. After gently shaking the samples were left standing for 1 hour at room temperature. The serum was isolated by centrifugation (Heraeus Sepatech, Megafuge 1.0) at 5000 rpm for 5 min., using Millipore Ultrafree-MC filter units (0.2 μm) and analysed for their protein content by HPLC-UV at an UV wavelength of 210 nm. Protein solutions which were prepared according to the above procedure but replacing the latex by water were used as references.

2.3.8 Electrophoretic mobility

The electrophoretic mobility of hydrolysed and purified latex was determined on a Malvern Zeta-sizer IIc. The pH was controlled using 0.001 N HCl and 0.001 N NaOH. The measured electrophoretic mobilities (μ) have been converted to ζ-potentials according to the Helmholtz-Smoluchowski relation.

2.4 RESULTS AND DISCUSSION

2.4.1 The carrier particles

Core-shell latices of two different particle sizes, 256 and 390 nm respectively, have been prepared by seeded emulsion polymerization using different cores. Table 3 gives an

Table 3 *Characteristics of core-shell carrier latices*

Latex	Size [nm]			Δr^c	vic.OH^d	σ^e	cfc^f [mol/l]	
	QELS^a	[pdi]^b	SEM	[nm]	[μeq/m^2]	[μeq/m^2]	NaCl	CaCl$_2$
ALD 3	256	[0.07]	255	10.5	11.3	0.21	2.0	> 1.0
ALD 8	390	[0.07]	394	6.0	6.9	0.26	0.8	> 1.0

a: QELS refers to quasi-elastic light scattering.

b: pdi refers to polydispersity index.

c: Δr refers to the shell thickness of the core-shell latex.

d: vic. OH refers to vicinal hydroxyl group.

e: s refers to negative charge density.

f: cfc refers to critical flocculation concentration.

overview of their characteristics. Electron micrographs of the particles are presented in figure 2. The polydispersity index (pdi) measured by quasi elastic light scattering (QELS) and the electron micrographs indicate a high degree of monodispersity. The increase in absolute mass of the core particles after seeded emulsion polymerization is visualized in the increased retention time after sedimentation field flow fractionation (SF$_3$). The SF$_3$ plot, presented in figure 3, shows the curves for core and core-shell particles. Besides the shift to higher retention time the SF$_3$ plot shows the absence of the formation of a second generation of shell polymer particles. The shell thickness is calculated by subtraction of the core radius, as given in table 1, from the radius of the core-shell particle determined by QELS. This shell thickness appears to be in the order of 5 to 10 nm. Since QELS determines the hydrodynamic radius the calculated thickness refers to the water swollen shell. The vicinal hydroxyl, the amide, the sulfonate and sulfate groups provide the shell with the necessary polarity for water swelling. The shell polymers protruding into the water phase are believed to provide the particles with steric stabilization. This can be deduced

figure 2 a

figure 2 b

Fig. 2 Scanning electron micrographs of core-shell latices ALD 3 [a] and ALD 8 [b].

———————— AAJ 19 core latex

· · · · · · ALD 3 core-shell latex prepared from AAJ 19

— — — ligand-coupled ALD 3 core-shell latex with
ligand density of 1.5 mg/m^2
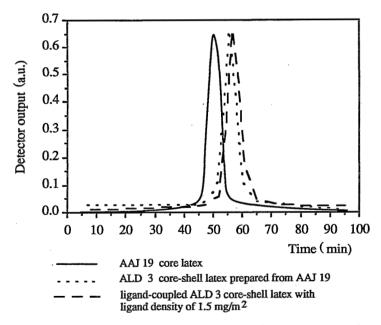
Fig. 3 Sedimentation field flow fractionation diagram for AAJ 19 core latex, ALD 3
core-shell latex prepared from AAJ 19 and ligand-coupled ALD 3 core-shell latex
with ligand density of 1.5 mg/m^2.

from the resistance against high electrolyte concentrations and the absence of an effect of the cation valency on the critical flocculation concentration (cfc), whereas polystyrene latices normally exhibit a much lower critical flocculation concentration (<1.0 mol/l)[14] especially for cations with higher valencies. Unlike the polystyrene core particles the dried core-shell particles are insoluble in toluene, indicating a complete surface coverage with hydrophilic copolymer which does not swell in toluene. The presence of N,N´-methylenebisacrylamide crosslinker in the shell composition will further enhance the mechanical stability of the shell and prevent excessive swelling of the core.

The core-shell particles are negatively charged over the entire pH range, as shown by the electrophoretic mobility measurements (see figure 4). The negative charge originates from covalently bound sulfate (initiator residue) and sulfonate groups (comonomer vinylsulfonate). The negative charge density (σ) determined by conductometric titration is in the order of 0.2 μeq/m^2 (see table 3).
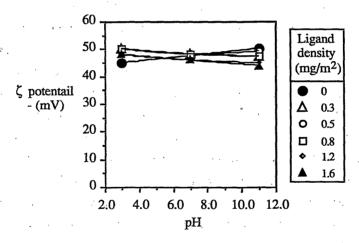
Fig. 4 Electrophoretic mobility of Cibacron Blue functionalized ALD 8 carrier latex as a function of pH and ligand density determined at ionic strength 0.17.

2.4.2 Cibacron Blue immobilization

The coupling of Cibacron Blue to hydroxyl functional core-shell latex through the triazinyl chlorine functionality of the dye is presented in figure 1. The reactive dye Cibacron Blue F3G-A consists of a chromophore group having affinity for certain proteins and a

chloro-triazine group for covalent attachment, which is not essential for the specific affinity [20, 21]. The exact composition of the commercial Cibacron Blue however is not known. Analytical evaluations by Hanggi showed commercial preparations to be composed of several chromophoric species[22]. The coupling experiments resulted in blue colored latices of different color intensity. After ligand immobilization the latices maintained their monodisperse character which can be evidenced by the SF_3 plot shown in figure 3. The curve of the ligand coupled particles shows a slight shift to higher retention time caused by the increased particle mass. The salt stability of the latex has increased after ligand coupling probably caused by the extra charge introduction which enhances both the electrostatic and steric stability. The latex can withstand more than 2 mol/l NaCl without flocculation.

The ligand density or amount of immobilized chromophores was determined spectro-photometrically by measuring the diffuse reflectance of the cleaned suspension using the absorbance of the chromophore at 610 nm. To confirm the accuracy of this method attempts have been made to compare the obtained values with those of other analytical techniques. Spectophotometric determination of the ligand after removal from the particle by acidic hydrolysis appeared impossible due to an incomplete chromophore removal from the particle. Determination of the increase in nitrogen and sulfur content by elemental analysis is strongly hampered by the fact that the amount of both elements is close to the lower limit of detection due to the relatively large contribution of the polystyrene core. In spite of this fact and the fact that the exact composition of the ligand is unknown elemental analysis confirms the order of magnitude of the values obtained with diffuse reflection spectroscopy. Conductometric titrations show an increase of negatively charged groups after Cibacron Blue immobilization. Whereas during the titration of the original latex only one equivalence point is detected, corresponding to strong acidic groups, titration of the latex with immobilized dye shows a second equivalence point probably due to the introduction of weak acidic groups. The increase in strong acidic groups can be ascribed to the introduction of sulfonate groups from the ligand molecules. The introduction of weak acidic groups is possibly the result of a side reaction during the ligand coupling at high pH, probably a hydrolytic ester splitting. After treatment of a core-shell latex under the coupling conditions in the absence of ligand a second equivalence point was indeed found by conductometric titration. Application of conductometric titration to a latex sample containing 1.8 mg Cibacron Blue/m^2, determined by diffuse reflection spectroscopy, showed an increase in strong acidic groups of 4.1 μeq/m^2. Based on 1.8 mg Cibacron

Blue/m^2 one would expect an increase of 4.2 or 6.4 μeq/m^2 for 2 or 3 sulfonate groups per ligand molecule respectively. Figure 1 presents a Cibacron Blue structure with 3 sulfonate groups per molecule, but Hanggi indicated also the presence of other species having less sulfonate groups[22]. Although conductometric titration gives no absolute evidence of the accuracy of diffuse reflection spectroscopy, just like elemental analysis it confirms the order of magnitude.

Since the coupling reaction is performed under repulsive conditions (i.e. both ligand and particle are negatively charged) the coupling should be sensitive for the ionic strength of the reaction medium. The electrolyte influence is illustrated in figure 5 showing a linear relation
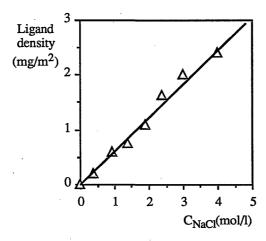
Fig. 5   Influence of the electrolyte concentration on the degree of Cibacron Blue coupling for carrier latex ALD 8. Ligand density was determined by diffusive reflectance. For details of the coupling reactions see 2.3.2 Cibacron Blue immobilization.

between the amount of immobilized ligand and sodium chloride concentration during immobilization. The electrolyte concentration can thus be used to control the ligand immobilization. Increase in reaction temperature, ligand concentration and vicinal hydroxyl surface density also showed a positive effect upon the amount of ligand immobilization in agreement with ligand coupling to polysaccharides presented in literature[20, 21].

Figure 4 shows that the electrophoretic mobility does not change with increasing ligand density despite the increase in negative charge density. This can be explained by some kind of charge saturation effect and/or by the hydrophilic, 'hairy', surface layer which causes the

hydrodynamic plane of shear to extend from the charged surface into the continuous phase. The independence of the electrophoretic mobility on pH value can be explained by the independence of the negatively charged sulfonate groups on pH value. The contribution of the weak acidic groups which were detected by conductometric titration is probably negligible in this respect.

There is no direct proof of a covalent linkage between the triazine group and the hydroxyl group on the particles but there are some strong indications for it. Firstly the amount of vicinal hydroxyl groups determined on the surface appears to be reduced and the pH of the reaction medium has decreased after the coupling reaction. Both observations are in agreement with the reaction scheme presented in figure 1. Secondly the bound Cibacron Blue could not be removed from the surface by excessive washing even under strong acidic conditions. Unfortunately the vicinal hydroxyl density could not be determined in a reproducible manner after ligand immobilization. It could therefore not be used for accurate determination of the amount of coupled ligand molecules.

2.4.3 BSA interaction studies

In figure 6 BSA adsorption is shown for polystyrene core particles, core-shell particles and Cibacron Blue functionalised particles as a function of pH. The core-shell particles, in contrast to their hydrophobic polystyrene cores, do not adsorb any BSA over a large pH range. This indicates an effective masking of the hydrophobic polystyrene surface by the shell copolymer. Only a weak adsorption below pH=5 is observed for the core-shell particles probably due to electrostatic attraction below the isoelectric point of BSA[16]. The absence of non-specific BSA adsorption is probably caused by steric repulsion of the hydrophilic surface additional to charge repulsion.

After Cibacron Blue immobilization spots with specific affinity for BSA have been introduced on an originally repulsive surface and BSA binding is again observed over the entire pH range. The level of BSA binding appears to be linearly proportional to the ligand density on the particles as can be seen in figure 7. This BSA binding takes place in spite of the increased repulsive forces between protein and particle due to the increased net negative charge of the latter. The binding is therefore believed to be caused by the specific BSA-Cibacron Blue affinity. The amount of ligand molecules that takes part in the BSA complexation, assuming a monovalent interaction, is only 1 to 5%. This low ligand efficiency is probably caused by the large size difference between protein and ligand and
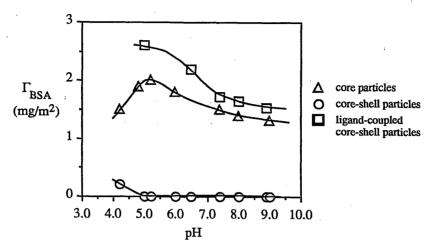
Fig. 6 *BSA binding (Γ_{BSA}) as a function of pH for polystyrene core particles, core-shell particles ALD 3 and ligand-coupled core-shell particles at ionic strength 0.17, room temperaturewith a 0.4 g/l BSA concentration. The ligand density for the ligand-coupled core-shell particles was 2.04 mg/m^2.*
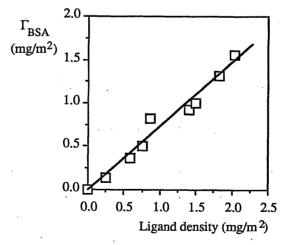
Fig. 7 *BSA binding as a function of ligand density on ligand-immobilized carrier latex ALD 3 at pH=7.4, ionic strength= 0.17 and room temperature.*

the hindered accessibility of ligands which have been immobilized in the deeper regions of the shell matrix. The increase in BSA binding with increasing ligand density for the higher ligand densities can be explained by some kind of cooperative effect of several ligands in binding one protein molecule. Figure 7 shows that a saturation level of BSA binding has not yet been reached with the ligand densities used.

Under the conditions used 70% of the maximal binding level is reached within 1 minute and maximal binding is completed within 10 minutes as can be seen in figure 8. Release of
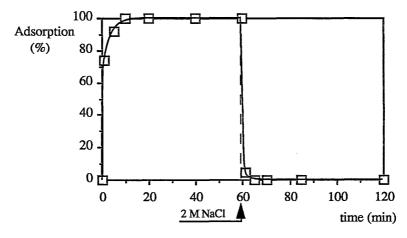
Fig. 8 BSA binding and release as a function of time. The conditions were given in the text.

the bound protein can be accomplished by increasing the sodium chloride concentration of the suspension to 2 mol/l. Complete release of BSA under these conditions is reached within 5 minutes. Under these release conditions the protein is released without flocculation of the latex particles. The fast binding and release processes suggest that the BSA-ligand interaction takes place at the outer surface of the core-shell particles. In contrast to beaded agarose there is no rate limiting pore-diffusion inside the carrier particles. Since the BSA binding takes place fast under repulsive conditions the results presented above suggest that BSA binding to the ligands is not severely hindered by steric effects of the carrier particles and the use of additional spacers between particle and ligand can be omitted.

In the following chapters the binding and release behaviour of these ligand carrying core-shell latices will be further investigated[8, 9].

2.5 CONCLUSIONS

Polystyrene particles with a core-shell structure have been prepared. The particles are sterically stabilized by a hydrophilic copolymeric shell that completely covers the hydrophobic surface of the polystyrene core. These core-shell particles are characterized by an absence of BSA adsorption over a large pH range. Cibacron Blue, as model ligand, has been coupled to these particles directly to the hydroxyl groups present in the shell. The amount of immobilized ligand could successfully be determined by diffuse reflection spectroscopy of the latex suspension. The degree of ligand immobilization appeared to be linearly proportional to the ionic strength of the coupling medium. The immobilization of Cibacron Blue is accompanied by an increase in negative surface charge and colloidal stability while the electrophoretic mobility remained unchanged. The binding of BSA to the functionalised core-shell particles was found to be linearly proportional to the Cibacron Blue surface density. BSA binding and release could be controlled by the salt concentration and appeared to be completed within 10 minutes under unstirred conditions, without loss of colloidal stability of the particles.

2.6 ACKNOWLEDGEMENTS

Mr. J. Lichtenbelt is greatly acknowledged for his contributions to the colloid chemical characterizations of the latices. Messrs T. Kemperman, Z. Borneman (University of Twente, The Netherlands), B. Meulenbrugge, J.B. Westerink, T. de Bruin and C. Bruin for their contribution to the preparation and characterization of the latices.

2.7 REFERENCES

1. T.C.J. Gribnau, Ph.D. Thesis, Nijmegen, The Netherlands (1977).
2. B. Mattiasson and T.G.I. Ling, Membrane Separation in Biotechnology, W.C. McGregor (Ed.), Marcel Dekker, New York, 1986, pp. 99.
3. E.N. Lightfoot, Protein Purification from Molecular Mechanisms to Large Scale Processes, ACS Symp. Series, 427 (1990) 35.

4. T.G.I. Ling, B. Mattiasson, Biotechnol.Bioeng., 34 (1989) 1321.

5. D.C. Herak, E.W. Merrill, Biotechnol.Prog., 6 (1990) 33.

6. J.H.T. Luong, K.B. Male, A.L. Nguyen, A. Mulchandani, Biotechnol.Bioeng., 32 (1988) 451.

7. N.F. Gordon, C.L. Cooney, Protein Purification from Molecular Mechanisms to Large-Scale Processes, ACS Symp. Series, 427 (1990) 118.

8. W. Zhang, B. Gebben, T. van den Boomgaard, C.A. Smolders, Colloids & Surfaces B: Biointerfaces, submitted (1993); chapter 3 of this thesis.

9. W. Zhang, B. Gebben, T. van den Boomgaard, C.A. Smolders, Colloids & Surfaces B: Biointerfaces, submitted (1993); chapter 4 of this thesis.

10. R.H. Ottewil, J.N. Shaw, Discuss.Faraday Soc., 42 (1966) 154.

11. A. Kotera, K. Furusawa, K. Kudo, Kolloid Z.Z. Polym., 240 (1970) 837.

12. W. Norde, Ph.D. Thesis, Agricultural University of Wageningen, The Netherlands (1976).

13. W.M. Brouwer, R.L.J. Zsom, Colloids and Surfaces, 24 (1987) 165.

14. R.L.J. Zsom, J.Colloid Interface Sci., 111 (1986) 434.

15. H. Shirahama, T. Suzawa, J.Colloid Interface Sci., 104 (1985) 416.

16. A.V. Elgersma, Ph.D. Thesis, Agricultural University of Wageningen, The Netherlands (1990).

17. J. Ugelstad, P.C. Mork, Adv.Colloid Interface Sci., 13 (1980) 101.

18 J.W. Vanderhoff, M.S. El-Asser, F.J. Micale, ACS Pol.Mat.Sci.Eng., 54 (1986) 587.

19. T. Nash, Biochem.J., 55 (1953) 416.

20. P.C.G. Dean, D.H. Watson, J.Chrom., Chrom.Rev., 165 (1979) 301.

21. H.J. Böhme, G. Kopperschläger, J. Schulz, E. Hofmann, J.Chromatogr., 69 (1972) 209.

22. D. Hanggi, P. Carr, Anal.Biochem., 149 (1985) 91.

3

Protein Separation Using Affinity Binding
Part II Binding Study with Ligand Carriers

W. Zhang, Z. Borneman, B. Gebben[1], Th. van den Boomgaard and C.A. Smolders

SUMMARY

Cibacron Blue-immobilized polystyrene core-shell latex particles (BL) have been synthesized for the potential application in affinity separation processes. In this chapter, protein binding on the BL particles was studied in order to extract the essential characteristics of the binding behavior for use in affinity separation processes. Three proteins, bovine serum albumin, bovine serum immunoglobulin G and lysozyme were used in the study. Binding isotherms of the proteins were determined. The protein binding capability Γ_m and the binding constant K_a were evaluated from the isotherms using a type of Langmuir fit. Maximum binding capacities Γ_m were found in the sequences $\Gamma_{m, \text{IgG}} < \Gamma_{m, \text{BSA}} < \Gamma_{m, \text{Lys}}$. The binding strength of the proteins to the BL particles, as indicated by the binding constant K_a, followed the order IgG < BSA < Lys. For comparison the results of BSA binding on ligand-immobilized porous agarose particles (BS) are also presented. Protein binding on the BL particles is a fast process compared to that on the BS particles. Binding of BSA and IgG was influenced drastically by variation of pH and by ionic strength. Release of the bound BSA can be accomplished by the addition of NaCl, sodium octanoate or free ligand to the solution. In contrast, release of the bound IgG can only be achieved using NaCl solution.

3.1 INTRODUCTION

Downstream processing is of growing importance in biotechnology today due to the increasing possibilities of producing many therapeutic and diagnostic proteins using genetic engineering and hybridoma technique, next to the increasing needs for industrial proteins

---

[1] AKZO Research laboratory Arnhem, Arla, CRC, Arnhem.

and enzymes. The fact that the desired products are often in dilute form makes the costs of protein purification a dominating factor in overall process economics [1, 2]. Development of large-scale process technology is becoming a major challenge and determinant for commercial success.

Progress has been achieved, for the last decade, in separation technology by exploiting the natural biospecific affinity interactions between biological macromolecules and complementary ligands. The dominating affinity purification technique on a commercial scale is affinity chromatography [3]. This technique enables a high degree of purification, while providing good recovery yield (>50 %). On the other hand affinity chromatography is suffering from the drawbacks inherently related to pore diffusion, discontinuous operation, and difficulties in the scale-up process [2].

To be able to overcome the drawbacks of affinity chromatography, a method combining affinity interaction and membrane separation is in development, which is the so-called Affinity Cross-Flow Filtration (ACFF) process [4-7]. In this process the substance to be purified (targeted molecule), when present in a crude mixture, has the ability to pass freely through a porous membrane. The targeted molecule, however, will be retained when it binds to affinity ligand carriers which have a size larger than the pores of the membrane, while unbound components in the mixture will pass through the membrane. The isolated targeted molecule-particle complex is then treated with an appropriate eluant to dissociate the targeted molecule from the particles. In the next process step the desired protein molecules are separated from the particles by means of a membrane with the right pore size and thus purified. The particles are regenerated and reused. A flow scheme of the ACFF process is depicted in figure 1.

Both membranes and particles are equally important in the ACFF process. In this study core-shell polystyrene latex particles have been applied. The particles are submicron in size and consist of a hard, non-porous core surrounded by a hydrogel shell to which affinity ligands can be covalently coupled [8]. The presence of the hydrogel shell on the particles may provide them with vanishing non-specific protein adsorption. The preparation of the core-shell latex particles and the immobilization of a triazine dye ligand Cibacron Blue (CB) through specific groups on the core-shell latex particles have been reported in chapter 2 [8]. The ligand-immobilized core-shell latex particles are indicated as BL particles. In this chapter efforts are focused on the binding characteristics of the particles. An ideal particle has to be mechanically and chemically stable and should have functional groups for ligand
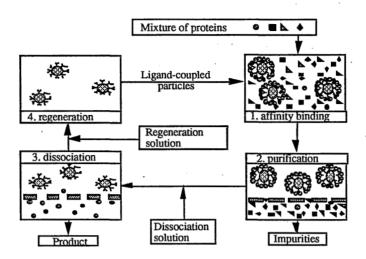
Fig. 1 A schematic illustration of the ACFF process.

immobilization. The particle should be hydrophilic and free of non-specific adsorption sites. Particles which fulfil these conditions are used in affinity chromatography. However these particles have a porous nature. For the ACFF process this can be a disadvantage due to the fact that the kinetics of the adsorption and desorption of the protein molecules should be fast, which is likely not the case in porous particles. Secondly, in the ACFF process the particles will be pumped around and it has been found that this procedure can damage e.g. some of the agarose type of particles, which are often used in chromatographic application[5]. By cross-linking the polymer matrix, however, the mechanical stability of the agarose particles can be improved to a large extent. Cross-linked agarose particles Superose 6 prep grade™ are used in this study for reason of comparison. The ligand-immobilized particles are indicated as BS particles.

The aim of the ACFF process is to purify a protein of interest from a protein mixture on a large-scale. The following proteins are chosen as model proteins for this study: bovine serum albumin (BSA), bovine serum immunoglobulin G (IgG), and lysozyme (Lys). These proteins are well known and have been studied by many investigators [9-12]. Besides, these are easy to obtain and have been used in many applications e.g., in health care and food industry. It is known in literature that a triazine dye Cibacron Blue F3G-A has high affinity with BSA and intermediate affinity with IgG [9]. Therefore, BSA may serve as a target and IgG as an impurity in the ACFF process. The reason that lysozyme is

used in this study is to gain an insight into the binding mechanism between the ligand and the proteins. Lysozyme has a high isoelectrical point (pH = 11), and thus shows a positive charge rather than the negative charge at normal binding conditions for BSA and IgG.

The group specific ligand, Procion Blue HB™ which is an analog of the well-known Cibacron Blue F3G-A, was chosen because of the good chemical stability compared with a protein ligand, and the easy accessibility so that it can be used for large scale production.

In the ACFF process it is desirable to use a ligand-immobilized carrier particle with a high binding capacity, and with a high selectivity. Binding studies with the carrier particle will provide useful information for the understanding of the binding mechanisms and for the optimization of the process parameters.

All three model proteins are globular proteins soluble in water, which distinguishes them from those "fibrous" proteins which are not soluble in water. From the view point of colloid science a globular protein in aqueous environment is regarded as a sphere with most of the hydrophobic residues centered in the interior surrounded by the hydrophilic residues. Due to the geometrical restrictions and restrictions from other interactions a fraction of the hydrophobic residues may expose to the aqueous environment and a fraction of the charged residues may be buried in the interior. Therefore, albumin can adsorb from an aqueous solution to a hydrophobic surface spontaneously through the gain of entropy by rearranging its conformation so that the hydrophobic residues in the interior of the protein molecule are exposed to the hydrophobic surface, and ice-like water at the interface is set free. Adsorption of negatively charged albumin (and IgG) onto negatively charged polymer surfaces has been reported as well [13-16]. Although adsorption of counter-ions at the interface between the polymer and the protein has been proven to play a role in the adsorption processes[15], conformational changes of the protein structure during adsorption are considered to be predominant because the adsorption patterns for the proteins on different adsorbing surfaces are similar [16]. In general, protein adsorption can result from various interactions between protein, adsorbent surface and medium (involving water-molecules and low molecular weight ions). These interactions are usually dependent on solution environment such as ionic strength, pH and temperature [10-12]. The interactions include electrostatic interactions, hydrophobic interactions, formation of hydrogen bonds, van der Waals interactions and disulfide linkage, and determine the secondary, tertiary and quaternary structures of a globular protein, and thus, the conformations of the protein molecule as a whole.

Sometimes the term binding is used instead of adsorption. Biochemists prefer to use

the first mentioned term when a few specific molecular interactions between two different molecules take place. For example, the interactions between the triazine dye Cibacron Blue and a number of enzymes are considered to be an interplay of hydrophobic and ionic interactions which is favoured in those regions of the protein molecule which bind both natural and artificial ligands bearing aromatic and ionic residues [17]. These interactions are therefore called biospecific. BSA and IgG bind the dye in a less specific manner because they are not related to those categories of the enzymes mentioned above [18]. Lysozyme is less exploited in this respect. In colloid chemistry studies the term adsorption prevails.

In this chapter, the characteristics of protein binding on the BL particles are presented. For reasons of comparison protein binding was also performed with the porous BS particles. In the next chapter the features of competitive binding of proteins on the BL particles will be given.

3.2 EXPERIMENTAL

3.2.1 Materials

Bovine serum albumin (Boseral pur™, 40030) and bovine immunoglobulin G (Bovine Gamma Globulin™, 41979) were kindly supplied by Organon Technika, The Netherlands. Lysozyme from hen egg was obtained from Fluka, Switzerland. The characteristics of these proteins are listed in table 1. Procion Blue HB™ was purchased from Janssen, Belgium. All other chemicals used were analytical grade.

Table 1 *Physicochemical properties of the proteins BSA, IgG and lysozyme.*

Protein	MW (Dalton)	I.E.P.	Monomer (%)	Dimer (%)	Dimension (Å)	Refs.
BSA	69000	4.7	84 [a]	16 [a]	140 * 38 * 38	15
IgG	156000	6.8	84 [a]	ND	234 * 44 * 44	15
Lys	14600	11	ND	ND	90 * 18 * 18	16 - 18

a: The values were measured by HPLC with a Water's Protein 300™ column.
ND: not determined.

The core-shell PS latices have been described in detail elsewhere [8]. The characteristics of the BL particles are summarized in table 2, column 2. The surface ligand densities of the BL particles presented in table 2 were determined by the diffuse reflection spectroscopy.

Table 2 *The characteristics of the BL particles.*

Type of BL	Ligand density (mg/m^2)	Γ^a $(nmol/m^2)$			Ligand utility (%)		
		BSA	IgG	Lys	BSA	IgG	Lys
BL-0	0	0	0	270	-	-	-
BL-1	0.26	1.7		260	0.5		-
BL-2	0.54	5.3	2.9		0.8	0.5	
BL-3	0.75	7.5	2.7		0.8	0.3	
BL-4	0.90	12.4		340	1.2		6
BL-5	1.39	13.5	5.1		0.8	0.3	
BL-5A	1.50	14.5			1.0		
BL-6	1.84	19.0		460	0.9		9
BL-7	2.04	22	6.5	430	0.9	0.3	7

a: Γ refers to experimentally obtained value at pH 7.4, ionic strength 0.17 and with 1.0 g/l protein.

Note: Ligand utilities for BSA and IgG are calculated by dividing the mole binding capacities of the proteins with the corresponding mole ligand densities (taking the molecular weight of the dye as 840 g/mole), and assuming a monovalent interaction between the proteins and the ligands. Ligand densities for lysozyme are calculated in the same as that for BSA and IgG except the binding capacities are subtracted by the amount bound on the bare shell of the latex particles (BL-0).

Other analytical methods, e.g. X-ray photoelectron spectroscopy (XPS) and acid hydrolysis, were applied for the determination of the surface ligand density. However the results obtained by these methods are not as satisfactory as that by the diffuse reflection spectroscopy. This is so because the surface ligand density determined by XPS analysis for nitrogen differs from that obtained for sulphur (both nitrogen and sulphur are the specific elements for the dye molecules) although it is a non-destructive method. Acid hydrolysis is unable to remove all the bound dye molecules.

Superose 6 prep grade™ was purchased from Pharmacia, Sweden. The particles have a average diameter of 17 μm determined with SEM. Ligand immobilization onto this particle was performed according to the procedure described by Böhme [23], which is similar to

the procedures for the BL particles. The characteristics of these particles are presented in table 3, column 2. The surface ligand densities of the BS particles are determined by the hydrolysis of the particles using a certain amount of sulphuric acid at 45 °C for one hour. The dye concentrations were calibrated using the same acid concentration.

Table 3 *The characteristics of the BS particles(diameter 17 μm).*

Type of BS	Ligand density (mg/m^2)	Γ_{BSA} $(nmol/m^2)$	Ligand utility (%)
BS-1	0.52	6.7	1.1
BS-2	0.52	6.1	1.0
BS-3	0.68	10.1	1.2
BS-4	0.82	12.9	1.3
BS-5	0.87	13.1	1.3
BS-6	1.00	16.1	1.4
BS-7	1.36	21	1.3
BS-8	1.40	22	1.4

Note: Ligand utilities for BSA are calculated by dividing the mole binding capacities of the protein with the corresponding mole ligand densities (taking the molecular weight of the dye as 840 g/mole), and assuming a monovalent interaction between the protein and the ligand.

Γ refers to experimentally obtained value at pH 7.4, ionic strength 0.17 and with 1.0 g/l protein.

3.2.2 Methods

Binding studies

Protein powder was dissolved in a buffer solution with stirring about 16 hours before use. The protein solution was stored at 4 °C. Just before use the solution was stirred for a short period of time (5 minutes). This procedure was followed in order to prevent shear induced aggregates [24].

Binding experiments were carried out by bringing together known amounts of protein and particle solutions (pH = 7.4 and ionic strength = 0.17, 0.067 M Sörensen phosphate buffer solution). The samples were equilibrated for 2 hours at room temperature; preliminary experiments had shown that the amount bound reaches a steady value within this time. Initial protein concentration was 1.0 g/l. These binding conditions were kept as standards unless specified otherwise.

After binding, samples were centrifuged with a Millipore Ultrafree filter to remove the

particles. Protein concentrations were analysed by means of a Waters HPLC system combined with a UV detector.

Release of the bound proteins

To release the bound proteins three different types of reagents have been explored: 2 M NaCl (solution A), 20 mM sodium octanoate (solution B) and 2.9 mM Cibacron Blue (solution C). The experiment was performed by addition of a sufficient amount of reagent to the solution rich in particles when the binding experiment has been completed. After 10 minutes contact time samples were taken, centrifuged and analysed for protein content by means of HPLC. A calibration curve with known amounts of protein in the solution containing a known amount of desorption reagent was used for the analysis of protein concentration. Release time experiments had shown that the release was complete after 10 minutes.

3.3 RESULTS AND DISCUSSION

3.3.1 Binding isotherms

A typical result of the binding of BSA, IgG and Lysozyme on the BL particles (batch BL-7 with a ligand density of 2.04 mg/m^2) are given in figure 2 a. The amount bound (in nmol/m^2) is plotted against the equilibrium concentration in g/l after binding. For reasons of simplicity the surface area of the core-shell particles used for the calculation of either surface ligand density or binding capacity is simply the outer surface. All isotherms have a Langmuir-like appearance: the amount bound increases with increasing protein concentration in solution until a plateau value is reached. Lysozyme shows the largest binding level on the particles compared to BSA and IgG. In figure 2 b the results for BSA and IgG alone are given at a different scale. It is shown in figure 2 b that IgG hardly binds onto the BL particles, but BSA does show considerable binding.

Several investigators have shown that the relationship between free and bound adsorbate in steady state can be described by a Langmuir-type equation [25-29]. This is applicable to specific adsorption by an immobilized ligand. Assuming that the immobilized ligand L on an adsorbent has an affinity for only one species of adsorbate P, the interaction can be described in a form of equilibrium relationship:
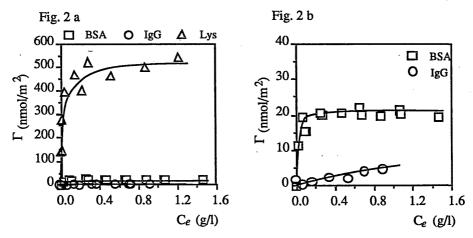
Fig. 2 Binding isotherms of BSA, IgG and lysozyme on the ligand-coupled latex BL-7 determined at pH 7.4 and ionic strength 0.17.

$$P \;+\; L \; \underset{k_2}{\overset{k_1}{\rightleftharpoons}} \; PL \tag{1}$$

where PL is the bound complex, k_1 and k_2 are the forward and reverse rate constants, respectively. A equation, also used by Chase [25], can be shown in steady state to describe the binding isotherm:

$$\Gamma = \Gamma_m \frac{K_a\, C_e}{1 + K_a\, C_e} \tag{2}$$

where the binding constant is $K_a = k_1 / k_2$, K_a represents the binding strength between the protein and the ligand, Γ_m corresponds to a monolayer coverage of the adsorbate molecules, C_e is the protein concentration at equilibrium. Both Γ_m and K_a are determined by fitting of a linearized form of the equation.

The model-fitted values of K_a and Γ_m obtained from the binding isotherms for the three proteins of figure 2 are given in table 4. The binding strength of the proteins, as indicated by the experimentally obtained values of K_a, followed the order IgG < BSA < Lysozyme. The Γ_m values for these proteins BSA, IgG and lysozyme were in the following order:

$$\Gamma_{m, IgG} < \Gamma_{m, BSA} < \Gamma_{m, Lys}$$

The binding data in figure 2 are obtained for latex particles with a ligand density of 2.04 mg/ m^2. The ligand density is most important for the binding features and will be discussed in the next paragraph.
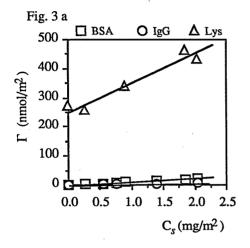
Table 4 *The characteristics of the binding isotherms of BSA and IgG and Lys on BL-7.*

Protein	Γ_m (nmol/m²)	K_a (l/g)
BSA	23	25
IgG	12	1.1
Lys	513	40

3.3.2 Binding capacities of the BL particles

Plateau values for all the latices mentioned in table 2 are obtained by bringing together an excess amount of protein and particles. One has to note that there is a minor difference in Γ and in Γ_m. The experimentally obtained value of Γ is sometimes lower than the theoretically determined value of Γ_m. The results of the experimentally obtained values of Γ for the BL particles are given in table 2 and in figure 3, they are plotted as a function of the surface ligand density. In general, a linear relation was found for BSA, IgG and lysozyme. For BSA and IgG this indicates that the increase of binding capacities results from the increase of the number of binding sites available for proteins to accommodate, which are reflected by the surface ligand densities. The particles fulfill their purpose: in the absence of ligands no detectable binding of BSA or IgG could be measured. This is a strong evidence that non-specific adsorption of BSA and IgG was eliminated by the introduction of the hydrogel shell onto the polystyrene core, on which, otherwise, adsorption could be found [8, 30-32]. In the adsorption experiments with the polystyrene core latex, the polystyrene core-shell latex and the ligand-immobilized core-shell latex particles, Gebben *et al.* [8] found that over a large pH range BSA did adsorb on the core latex, did not adsorb on the core-shell latex and but did bind again on the ligand-immobilized core-shell latex particles, which fully agrees with the experimental results obtained here. .

The ligand Cibacron Blue contains negatively charged groups. An increase of surface ligand densities will increase the surface charge of the particles. This has been confirmed by Gebben *et al.* by conductometric titration [8]. However an enhancement of the electrophoretic mobility of the BL particles as a function of the ligand density could not be
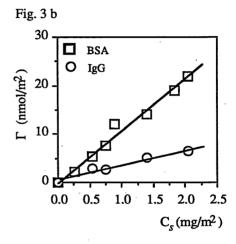
Fig. 3 a   Fig. 3 b

Fig. 3 The relation of protein binding capacities and surface ligand densities C_s on the ligand-coupled latices (BL-1 to 7). The binding experiments were carried out with a 1.0 g/l initial BSA concentration at pH 7.4 and ionic strength 0.17.

observed. This was attributed to the "hairy" surface layer which could bury the negative charges. However ions can move into this layer as the titration results showed and it is assumed that proteins will also move into this layer. Under the applied binding conditions both proteins BSA and IgG are bearing a negative charge as their isoelectrical points are below 7.4. This rules out that the binding is only governed by electrostatic interactions between the dye and the protein molecules. As suggested in literature the interactions between the ligand and the protein molecules may be better viewed as an interplay of hydrophobic and electrostatic interactions occurring at a specific region of the surface of the protein molecules. In the case of BSA the binding sites for fatty acids are thought to be involved [33]. Further discussion regarding these points will be given in the section of effects of pH and ionic strength.

In the case of lysozyme electrostatic interaction does play an important role. This is due to the high isoelectrical point of lysozyme, around pH = 11, so that lysozyme molecules

are positively charged at pH = 7.4. Thus, it is not surprising that a high intercept was found when the binding capacity of lysozyme is plotted against the surface ligand density, as shown in Figure 3 a. It implies that a certain amount of lysozyme will adsorb onto the latex on which no dye molecules are present. The presence of charge groups in the shell part of the particles is considered to be responsible for the non-specific adsorption of lysozyme onto the non-ligand-coupled latices. The increased adsorption of lysozyme as a function of surface ligand densities is then regarded as the result of the increase of charge densities; these charge groups are carried by the immobilized ligands. Consequently, it is concluded that also the dominating type of interaction between lysozyme and the ligand is of coulombic nature.

From the geometric data of the protein molecules a theoretical monolayer at the outer surface of the shell can be calculated. For lysozyme this gives a value of about 100 nmol/m^2, if the lysozyme molecules lie on their side. However the experimentally obtained value is about 5 times higher than that of the theoretical monolayer. The surface can accommodate such a large amount only if the molecules are adsorbed in an end-on orientation in a monolayer, or if the protein molecules are not only adsorbed at the outer surface of the shell but can also be accommodated inside the shell. This latter possibility is more realistic because the amount of lysozyme adsorption does increase after introduction of the ligand molecules in the shell. These ligand molecules are supposed to be buried inside the layer as can be deduced from the increase in negative charges found by conductometric titration in combination with absence of any change of the electrophoretic mobility of the particle. For BSA a theoretical monolayer gives a value of about 31 nmol/m^2 when the BSA molecules take a side-on orientation on the surface. The fact that the experimentally determined value for BSA is 74 % of this theoretical monolayer value indicates that the BSA molecules bind on the BL particles in a side-on state, and approach a monolayer coverage. Moreover, this fact suggests that the binding sites are located on the sides of the BSA molecules. For IgG the amount of 16 nmol/m^2 is obtained for a theoretical monolayer of the IgG molecules adsorbed on their side, which is in reasonable agreement with the experimentally determined value (12 nmol/m^2). However, IgG adsorption is usually considered to be in an end-on state (85 nmol/m^2 for a theoretical monolayer) rather than a side-on state with the F_c chain (see chapter 1) attached to the surface and the two F_{ab} arms extending into bulk solution with a certain angle in between them depending on the solution environment, e.g. pH and ionic strength [31, 34]. Therefore

IgG binding on the BL particles is far away from a monolayer, which can be regarded as a result of less strong interaction between the IgG molecules and the immobilized ligands in comparison with the other two proteins.

Comparing the binding capacities with the surface ligand densities on a mole basis, the ligand utility, i.e. the percentage of the immobilized ligands which binds protein molecules can be calculated and they are given in table 2. This value varies from 0.5 to 1.2 % for BSA and from 0.3 to 0.5 % for IgG, while for lysozyme 6 to 9 % of the ligands seems to be utilized in protein binding, assuming a one to one interaction between the lysozyme molecule and the ligand. The seemingly high values for lysozyme may be explained by the molecular size of this protein in comparison with the others, which may therefore result in high accessibility to the binding sites on the particles. Another explanation may result from the comparison of the relative sizes between the protein and the dye molecule that the surface area covered by one single protein molecule is much bigger than that for a dye molecule. Consequently, there are more dye molecules accommodated in this protein-occupied area as the increase of surface ligand density, while still only one dye molecule in this area is taken into account for ligand utility because of the assumption of monovalent interaction between the protein and the ligand. Assuming a monolayer coverage of the dye molecules lysozyme will cover less dye molecules, and thus, have high ligand utility with respect to other proteins. It is interesting to note that for all the three proteins the ligand utility does not vary with the surface ligand density within the estimated experimental error. This may imply that even though the surface ligand density is increased, a certain percentage of the immobilized ligand may be located in those locations in the particles that are not accessible to these proteins at all.

3.3.3 Binding capacities of the BS particles

To be able to compare the results of protein binding on the porous BS particles with the binding on the BL particles, the specific surface area of the BS particles has to be determined. The B.E.T. method gives a value of 0.53 m^2/g gel which is only corresponding to a specific surface area of the BS particles taken as non-porous particles. The binding of a dye methylene blue on Superose particles resulted in a value of 4.0 m^2/ml drained gel when taking the surface area of one single molecule of methylene blue as 0.6 nm^2. However, the specific surface area calculated from the highest value in the surface ligand densities which were determined by acid hydrolysis is 23.2 m^2/ml. This value is taken as the specific surface area for the calculation of binding capacity per unit area of the

BS particles. The results of the plateau values of BSA binding, obtained by bringing together an excess amount of protein and the BS particles, are given both in table 3 and in figure 4 as a function of the surface ligand density. As a comparison the plateau values of
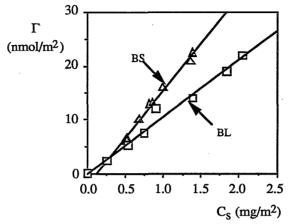

Fig. 4 *The relation of protein binding capacities and surface ligand densities C_s on the BS particles (BS-1 to 8). The binding experiments were carried out with a 1.0 g/l initial BSA concentration at pH 7.4 and ionic strength 0.17.*

BSA binding on the BL particles are also presented in figure 4. A linear relation was found for the BSA binding on the BS particles as it was observed for the BL particles. This result indicates that the BSA binding on the BS particles is also a result of the increase of the number of binding sites available for proteins, which are reflected by the surface ligand densities. The difference in slope between the two types of particles may be explained by the difference in accessibility of the binding sites between these two particles; also the ligand utility for the BS particles is about 1.3 % while the value for the BL particles is about 0.9 %. The different techniques applied for the measurements of surface ligand density for the different particles may also account for this difference between the two types of the particles.

3.3.4 Binding kinetics

One of the drawbacks of affinity chromatography is the time necessary for diffusion of the targeted molecules into the pores of the binding materials. One of the objectives of the ACFF process is to diminish the process time by using convective flow around non-porous particles. Therefore the binding kinetics of the proteins onto the BL particles has

been studied. The core-shell particles consist of a thin hydrophilic layer with specific affinity spots. The binding kinetics of proteins onto agarose beads with the same ligands coupled to it (BS) are studied as well. These type of beads are used in affinity chromatography. In figure 5 the results for the three different proteins are given for BL-7. From the results of figure 5 it can be seen that the binding was completed after 10 minutes
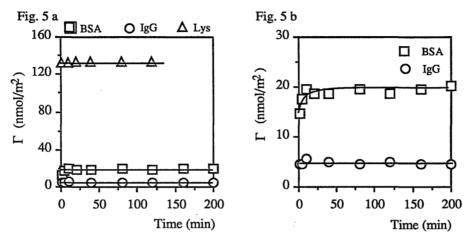

Fig. 5 *Time dependences of the protein binding/adsorption on the ligand-coupled latex BL-7. The binding experiments were carried out with an 1.0 g/l initial concentration for BSA and IgG and a 0.2 g/l initial concentration for lysozyme at pH 7.4 and ionic strength 0.17.*

for all proteins. These results indicate nicely that an equilibrium time of 2 hours is justified. Comparison of the binding kinetics onto the ligand-coupled latex (BL-7) and the porous Superose beads (BS-2) shows indeed in figure 6 that the plateau value for the BL particles is reached more quickly than for the Superose. In both cases however equilibrium values are obtained within two hours. The porous structure of Superose sterically hinders protein molecules to quickly find access to the binding sites inside the pores, resulting in a slow kinetic process.

To get an idea to which extent protein diffusion is restricted in an agarose particle a simple calculation is given. An empirical equation derived by Boyer and Hsu [35] is used to evaluate the effective diffusivity of a protein molecule (e.g. BSA) in the agarose particle Superose as given below:

$$\ln \left(\frac{D_e}{D_o}\right) = -0.1307 \, (M_w^{1/3} + 12.45) \, C_f^{1/2} \qquad (3)$$

where D_o is the diffusion coefficient of a protein in solution, D_e is the effective diffusion coefficient of a protein in the agarose matrix, M_w is the molecular weight of the protein and C_f is the polymer concentration of the agarose matrix in the gel, which is 0.07 g/cm³ for
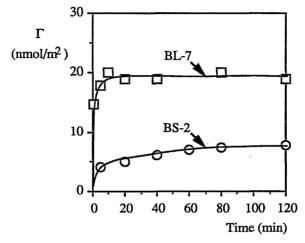
Fig. 6   A comparison of the binding kinetics of BSA on the ligand-coupled latex (BL-7) and on the dye-coupled Superose (BS). The binding experiments were carried out with a 1.0 g/l initial BSA concentration at pH 7.4 and ionic strength 0.17.

the agarose. For BSA, its $M_w = 69000$ (Dalton) and $D_o = 6.9 *10^{-7}$ (cm²/s). Applying these data in equation 2 results in $D_e = 1.12 * 10^{-7}$ (cm²/s). With this effective diffusion coefficient in hand one can estimate the mass flux of the protein from the outer surface to the center of the agarose particle, using the following expression of Fick's law, and assuming that the resistance in the hydrodynamic boundary layer around the particle is negligible [36]:

$$N_s = \frac{D_e \, (C_1 - C_0)}{Z_1 - Z_0} \qquad (4)$$

where N_s is the mass flux of the protein in (kg/m².s), C_0 and C_1 are the protein concentrations at the outer surface and at the center of the particle, respectively. Z_0 and Z_1

are the locations in Z direction at the outer surface and at the center of the particle with Z_1 - Z_0 as the radius of the particle. With the boundary conditions:

$$C_0 = C_{bulk} = 1.0 \ (g/l),$$
$$C_1 = 0 \ (g/l),$$
and $$Z_1 - Z_0 = 8.5 * 10^{-6} \ (m),$$

one obtains $N_s = 2 * 10^{-6}$ (kg/m^2.s) = 2 (mg/m^2.s), which means that it only takes one second for a BSA molecule to diffuse into the center of the particle (2 mg BSA corresponding to a theoretical monolayer per square meter). The above calculation is, of course, oversimplified. In practice, these protein molecules which arrive early will accommodate at the places near the outer surface resulting in the narrowed diffusion path, and thus further restricting diffusion for the newly coming protein molecules. The time needed for all the protein molecules, which can finally accommodate inside the particle, to diffuse in must be longer than the calculated value of 1 second. When applying the same calculation to the hydrogel shell of the core-shell latex particle, with a thickness of ca. 10 nm, the diffusion process for a BSA molecule is two orders of magnitude faster than that in the agarose particles.

What can be concluded from the calculation is that although diffusion of the protein molecules into the pores of the binding materials can be a rate limiting factor for affinity chromatography, it may not cause a severe problem in the ACFF process. This is so because a protein molecule will only diffuse in and out of one single particle in the ACFF process, while in the case of a chromatographic operation a protein molecule will not only diffuse in and out of one single particle but nearly all the particles along the column length.

3.3.5 Effects of pH and ionic strength

It is well-known that the protein - ligand interaction can be influenced by different variables such as pH, ionic strength and temperature. Since both BSA and IgG interact with the ligand it is necessary to investigate the effects of pH and ionic strength to find binding conditions that are favorable for BSA binding but not for IgG. Studying the effect of pH and ionic strength on the protein-ligand interaction can also give an insight of the kind of binding mechanism involved.

Binding plateau values have been obtained for BSA and IgG onto different BL particles with varying ligand densities as a function of pH (figure 7). From this figure it is clear that

the binding for both proteins decreases as the pH increases.

Generally, the effect of variation of the pH mainly reflects the role of the electrostatic interaction rather than any other interaction. However, over the whole pH range studied binding occurs for both proteins. The largest amount BSA bound is in the vicinity of its isoelectric point (4.7). Not many experimental data are available at lower pH values. In the case of IgG the bound amount increased at lower values of the isoelectric point. If this trend is the same for both proteins this means that electrostatic interaction will play a
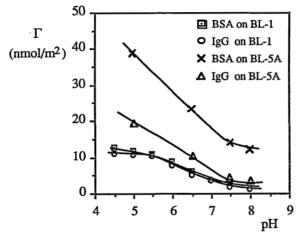

Fig. 7 *The effect of pH on the binding plateau values of BSA and IgG on the ligand-coupled latices BL-1 and BL-5A at ionic strength 0.17, room temperature and protein concentrations of 1.0 g/l for BL-1 and 0.4 g/l for BL-5A.*

role in the binding. If the overall charge of the proteins is opposite of the particle (below the isoelectric point) binding is favoured, while at an increase of electrostatic interaction between the protein and the particle the binding is diminished.

In the case of entropical driven protein adsorption a maximum at the isoelectric point is found, indicating a minimum in size of the adsorbing protein. This has not been found in this study indicating that electrostatic interaction is important. In the absence of any charge of the protein (at the isoelectric point) still binding has been found stemming from other type of interaction.

The protein-ligand interaction is in general influenced to a large extent by ionic strength: small concentrations of electrolytes promote adsorption, while larger concentrations promote desorption [37, 38]. In affinity chromatography these phenomena are used to

operate the process. Therefore, it is of interest to examine these effects for the ACFF system studied here. The results of BSA and IgG binding on two types of the BL particles as a function of ionic strength are presented in figure 8. It is clearly shown that protein binding is very sensitive to ionic strength. For example, BSA binding on BL-5A decreased from 15 nmol/m² to less than 4.0 nmol/m² when ionic strength increased from 0.17 to 0.48. The reason that much less BSA is bound at higher ionic strength may be explained as a result of the charge-shielding. Assuming that electrostatic interactions are important for the binding between the proteins and the ligand, the increase of the ionic strength will shield the charges both on the ligand and on the surface of the proteins, resulting in a weakened charge interaction. Therefore the binding capability decreases as can be seen in figure 8. The fact that the protein binding at pH above the isoelectric point decreases, as has been shown in figure 7, may only partially support the assumption of binding by charge because
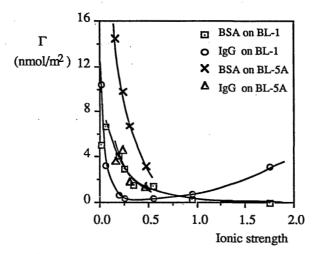
Fig. 8 The effect of ionic strength on the binding of BSA and IgG on the BL particles BL-1 and BL-5A at pH 7.4, room temperature and protein concentrations of 1.0 g/l for BL-1 and 0.4 g/l for BL-5A.

the protein binding was also found at pH around the isoelectric point where the protein molecules bear zero net charge. One can argue that the charges on and inside the protein molecules may not distribute evenly so that there are some high charge density centers localized both at the exterior and in the interior of the protein molecules. Thus, it is possible that at the isoelectric point the protein molecules bear no net charge as a whole but those

centered charges may still be present. As a consequence the binding may be driven by the electrostatic interaction even at pH close to the isoelectric point. However, the fact that the negatively charged BSA and IgG bound onto the negatively charged BL particles, and the fact that such an binding increased as the increase of the ligand density of the BL particles, as has already been shown in figure 3, rule out the domination of the electrostatic interactions in the binding process.

To summarize the discussion of the results of effects of pH and ionic strength on the protein binding, together with the correlation between the binding capacity and the surface ligand concentration, one may indeed come to the conclusion that the binding interactions are an interplay of both hydrophobic and electrostatic interactions localized on certain regions (binding sites) of the surface of the protein molecules. Upon a change in the ligand environment the protein molecules tend to response with a conformational change to balance the various interactions both in the interior and at the exterior of the molecule. This conformational change means the rearrangement of the protein tertiary and quaternary structure. As a result the exposure of the binding sites may change either in a favorable or an unfavorable way toward the ligand interactions. Consequently, the ligand binding either increases or decreases. This idea is depicted in figure 9.
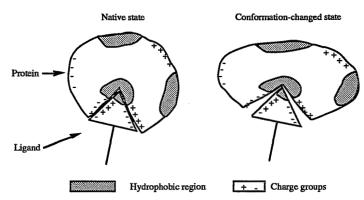

Fig. 9 Schematical illustration of the influence of the conformational change of a protein structure, as a response to a change in solution environment, on the binding interactions between the protein and a ligand.

3.3.6 Release of the bound proteins

It has been generally accepted that protein adsorption is an irreversible process due to

multi-site interaction with the adsorbent surface [10-12]. In this study protein release upon dilution has been investigated. BSA and IgG solutions, with an initial concentration (C_0) of 1.0 g/l, were diluted after the adsorption process had ended with an equal volume of the adsorption buffer. BSA and IgG desorption was not observed. Therefore, it was evident that binding of BSA and IgG on the ligand-coupled latices is an irreversible process under the binding conditions applied here. However one has to bear in mind that protein release can be achieved by changing the binding conditions such as pH, ionic strength and addition of reagents. A number of reagents may be used for this purpose e.g. NaCl, sodium octanoate and Cibacron Blue solutions. The release mechanisms with these reagents are essentially different from one another. The application of NaCl to the binding solution is considered as a kind of displacement effect of the ions at high ionic strength [39-41]. This displacement effect can be regarded as a two-folded effect: at high ionic strength the ions are capable of changing the local environment on the binding surface so that it is no longer favorable from an energetic point of view for the protein molecules to bind. On the other hand at high ionic strength the protein molecules themselves undergo a conformational change which makes the steric structure of the protein molecules unfavorable for binding, and therefore, they are displaced by the ions from the surface. Since the interactions between Cibacron Blue and BSA involve the binding sites for fatty acids [32], sodium octanoate is used as a kind of biomimetic effect. Free Cibacron Blue in solution is a competitive ligand to the immobilized ones. Therefore, protein release using these three reagents is expected to provide an insight into the mechanisms of the protein-ligand interactions. The results of percentage of the released protein are shown in Table 5. All

Table 5 *The percentages of proteins released from the particles using NaCl, sodium octanoate, and free Cibacron Blue.*

Protein type	C_0 (g/l)	NaCl 2 M	Octanoate 20 mM	CB 2.9 mM
BSA	1.0	~ 100	~ 100	~ 100
IgG	1.0	~ 100	0	14

three reagents can release BSA rather efficiently, to nearly 100 %. For the case of IgG, 2 M NaCl released the bound protein to about 100 %. Neither sodium octanoate nor free Cibacron Blue could release the protein to a satisfactory extent. This difference may

indicate that the binding interactions for IgG tend to be the non-specific type, whereas the binding interactions for BSA tend to be much more specific on a certain location.

3.4 CONCLUDING REMARKS

The binding isotherms of three proteins on Cibacron Blue-coupled PS core-shell latices were determined. The protein binding capabilities were found in the sequence $\Gamma_{m, IgG} <$ $\Gamma_{m, BSA} < \Gamma_{m, Lys}$. The binding strength of the proteins to the functionalized particles, as indicated by the binding constant K_a, followed the order IgG < BSA < Lys.

Protein binding on the ligand-coupled particles of variable surface ligand density revealed that the binding capacities of the three proteins were linearly related to the surface ligand density. For the nonligand-coupled latex particle, BSA and IgG did not show any binding, which was an indication of the absence of non-specific adsorption sites on the particles. However, lysozyme adsorbed substantially onto the nonligand-coupled latex particle. This was attributed to the presence of opposing charged groups on the interacting species: since lysozyme is positively charged and the ligand is negatively charged under the adsorption condition, it was concluded that the dominating interaction between lysozyme and the ligand has coulombic nature. It was found that protein binding on the BL particles is a fast process with respect to that on the porous BS particles. Binding of BSA and IgG was influenced drastically either by the change of pH or by a change of ionic strength. Release of the bound BSA can be achieved by addition of NaCl, sodium octanoate, and free dye to the solution. In contrast, release of the bound IgG can only be achieved using NaCl solutions.

3.5 REFERENCES

1. J.L. Dwyer, Bio/Technol., 2 (1984) 957.

2. E.N. Lightfoot, in Protein Purification from Molecular mechanisms to Large-scale Processes, ACS Symp. Series, 427 (1990) 35.

3. B. Mattiasson. and T.G.I. Ling, in Membrane Separation in Biotechnology, W.C. McGregor (Ed.), Marcel Dekker, N.Y., (1986) pp. 99.

4. N.F. Gordon and C.L. Cooney, in "Protein Purification from Molecular mechanisms to Large-scale

Processes", R.C. Willson, C.C. Paionton, S.E. Builder (Eds.), ACS Symp. Series 427, M.R. Ladisch, 1990, pp. 118.

5. D.C. Herak and E.W. Merrill, Biotechnol. Prog., 6 (1990) 33.

6. T.G.I. Ling and B. Mattiasson, Biotechnol. Bioeng., 34 (1989) 1321.

7. J.H.T. Luong, K.B. Male and A.L. Nguyen, Biotechnol. Bioeng., 32 (1988) 451.

8. B. Gebben, D. van Houwelingen, W. Zhang, Th. van den Boomgaard and C.A. Smolders, Colloids and Surfaces B Biointerfaces, in preparation; chapter 2 of this thesis.

9. G. Birkenmeier, in "Protein-Dye Interactions: Developments and Applications", Vijayalakshmi M.A. and O. Bertrand (Eds.), Elsevier Applied Science, London and New York, 1989, pp. 253.

10. J.L. Brash and T.A. Horbett (Eds.), Proteins at Interfaces. Physicochemical and Biochemical Studies, ACS Symposium Series 343, Amer. Chem. Soc., Washington D.C., 1987.

11. W. Norde, Adv. in Colloid and Interface Sci., 25 (1986) 267.

12. J.D. Andrade, in Surfaces and Interfacial Aspects of Biomedical Polymers, J.D. Andrade (Ed.), Plenum Press, New York, 1985, pp. 1.

13. A.V. Elgersma, R.L.J. Zsom, W. Norde and J. Lyklema, Colloids and Surfaces, 54 (1991) 89.

14. A.V. Elgersma, R.L.J. Zsom, W. Norde and J. Lyklema, J. Colloid Interface Sci., 138 (1990) 145.

15. P. van Dulm, W. Norde and J. Lyklema, J. Colloid Interface Sci., 82 (1980) 77.

16. W. Norde, F. MacRitchie, G. Nowicka and J. Lyklema, J. Colloid Interface Sci., 112 (1986) 447.

17. C.R. Lowe, in Topics in Enzyme and Fermentation Biotechnology, A. Wiseman (Ed.), Vol. 9, Ellis Horwood, Chichester, 1984, pp. 78.

18. Y.D. Clonis, in "Reactive Dye in Protein and Enzyme Technology", Y.D. Clonis, T. Atkinson, C.J. Bruton and C.R. Lowe (Eds.), Stockton Press, New York, 1987, pp. 33.

19. B.D. Fair B.D. and A.M. Jamieson, J. Colloid Interface. Sci., 77 (1980) 525.

20. Data given by the manufacturer.

21. C. Tanford and M.L. Wagner, J. Am. Chem. Soc., 76 (1954) 3331.

22. J.R. Colvin, Can. J. Chem., 30 (1952) 831.

23. H.-J. Böhme, G. Kopperschläger, J. Schulz, and E. Hofmann, J. Chromatogr., 69 (1972) 209.

24. A.C.M. Franken, J.T.M. Sluys, V. Chen, A.G. Fane and C.J.D. Fell, Proc. in 5th World Filtration Congress, Nice, France, 1990, pp. 207.

25. H.A. Chase, J. Chromatogr., 297 (1984) 179.

26. P.C. Wankat, Anal. Chem., 46 (1974) 1400.

27. J.W. Eveleigh and D.E. Levy, J. Solid-Phase Biochem., 2 (1977) 45.

28. B.J. Horstmann, C.N. Kenney and H.A. Chase, J. Chromatogr., 361 (1986) 179.

29 G.L. Skidmore and H.A. Chase, J. Chromatogr., 505 (1990) 329.

30. M.A. Cohen Stuart, G.J. Fleer, J. Lyklema, W. Norde and J.M.H.M. Scheutjens, Adv. Colloid Interface. Sci., 34 (1991) 477.

31. T. Suzawa and H. Shirahama, Adv. Colloid Interface. Sci., 35 (1991) 139.

32. A.G. Mayes, J.D. Moore and R. Eisenthal, Biotechnol. Bioeng., 36 (1990) 1090.

33. C. Lagercrantz and T. Larsson, Biochem. J., 213 (1983) 387.

34. P. Bagchi and S.M. Birnbaum, J. Colloid Interface Sci., 83 (1981) 460.

35. P.M. Boyer and J.T. Hsu, AIChE J., 38 (1992) 259.

36. F.H. Arnold, H.W. Blanch and C.R. Wilke, Chem. Eng. J., 30 (1985) B25.

37. C.R. Lowe and Dean P.D.G., Affinity Chromatography, John Wiley & Sons, London, 1974.

38. S. Ostrove, in "Guide to Protein Purification", M.P. Deutscher (Ed.), Method in Enzymology, vol. 182, Academic Press, San Diego, 1990, pp. 357.

39. D. Mislovicova, P. Gemeiner, E. Stratilova and M. Horvathova, J. Chromatogr., 510 (1990) 197.

40. M.P. Henry, in "HPLC of Macromolecules: a practical approach", R.W.A. Oliver (Ed.), Press, Oxford, 1989, pp. 37.

41. R.R Drager and F.E. Regnier, J. Chromatogr., 359 (1986) 147.

Appendix to chapter 3

Stability of Immobilized Cibacron Blue on Carrier Particles

W. Zhang, Z. Borneman, Th. van den Boomgaard and C.A. Smolders

SUMMARY

In the Affinity Cross-Flow Filtration process a ligand-immobilized particle is used for the selective adsorption of a specific protein in a mixture. The process efficiency of Affinity Cross-Flow Filtration is directly related to the function of the immobilized ligand (Cibacron Blue). Therefore, the importance of stability and stabilization of ligands in the ACFF process shares the same features as the stability and stabilization of enzymes in biotechnology.

In this chapter the stability of the ligand carrier will be discussed.

INTRODUCTION

In the Affinity Cross-Flow Filtration (ACFF) process, a carrier particle to which a specific ligand is immobilized is employed for the selective separation of a protein of interest from a protein mixture with the aid of cross-flow filtration to remove impurities. Protein binding onto the ligand-immobilized carrier particles (e.g. Cibacron Blue on agarose and on a core-shell latex in our case) is the starting point in the ACFF process, and has been described in detail elsewhere [1, 2]. Binding capacity, i.e. the amount of bound protein per unit area of the carrier particles, is a function of the amount of ligand immobilized on the particles (i.e. surface ligand density), and can be directly related to the process yield. Therefore, the stability of the immobilized ligand is an important parameter for the application of the ACFF process. Furthermore, recent investigation by Stewart and coworkers [3] indicates that the release of the group-specific ligand, Cibacron Blue, is

dependent to a large extent on the types of support materials and the immobilization chemistry. In this study the stability of the immobilized ligand is investigated. The influence of the release of the ligand on the binding capacity of the particles is also studied. The ligands are immobilized on core-shell latex particles or on agarose particles.

EXPERIMENTAL

Materials

Bovine serum albumin (BSA) (Boseral pur™, 40030) was kindly supplied by Organon Technika, The Netherlands. Procion Blue HB™, which is an analog to Cibacron Blue F3G-A, was purchased from Janssen, Belgium. All other chemicals used were analytical grade.

The preparation and the characteristics of the ligand-immobilized PS core-shell latices have been described in detail elsewhere [1, 2]. The characteristics of the ligand-immobilized particles, cited as Blue-Latex (BL), used in this stability study are given in table 1. After the immobilization procedure the particles with the coupled ligands were rinsed with deionized water obtained from a reverse osmosis unit. In total the amount of water displaced was 100 times the original volume.

Table 1. *The characteristics of the ligand-immobilized BL particles.*

Type of Blue-Latex	Latex code	Ligand density (mg/m^2)	Binding capacity $(nmol/m^2)$	Ligand leakage (%)	Days of storage
BL-1	AAJ 48	0.26	1.7	4.6	455
BL-2	ALD 3c	0.54	5.3	2.9	382
BL-3	ALD 3c	0.75	7.5	4.4	374
BL-4	ALD 3c	0.90	12		
BL-5	ALD 3c	1.39	14	2.0	374
BL-6	ALD 3c	1.84	19		
BL-7	ALD 2	2.04	22	2.3	333
BL-8	AMZ 27	1.44		2.7	129

Superose 6 prep grade™ was purchased from Pharmacia, Sweden. The ligand-immobilized Superose, cited as Blue-Superose (BS), was prepared according to the procedure described by Böhme [4].

Determination of ligand immobilization

Three types of methods were employed to determine the amount of ligand immobilized on the particles. The first method is a hydrolysis to release the immobilized ligand from the surface. A solution with a known amount of the BL particles were dried and redissolved in a fixed amount of sulphuric acid and stored for 3 days in a closed vessel at room temperature. After that period the dispersion is diluted with a two times larger amount of water. The diluted dispersion is then filtered with a Nuclepore 0.05 μm polycarbonate membrane. The amount of released ligand was spectrophotometrically determined in the clear permeate at 610 nm. The whole procedure was also performed on core-shell latex particles without any immobilized ligand to check the procedure.

A variation of this hydrolysis method was used for the determination of the ligand density on the agarose (BS) particles. In this case the hydrolysis was performed in 6 M HCl at elevated temperature (45 °C). To obtain comparable results this method has also been applied for some latex particle solutions. In the case of the agarose beads the particles have been removed by centrifugation and in the case of the latex particles a clear solution could be obtained by filtration.

The second method employed to measure the surface ligand density immobilized onto the particles was a direct one. X-ray photoelectron spectroscopy (XPS) was used for the analysis of the surface of the particles. Known amount of samples was dried and analyzed for the presence of the elements nitrogen and sulphur which are the specific elements for the ligand only. The spectrograms of the ligand powder and core-shell particles without ligands immobilized are used as blanks.

The third method for the determination of the amount of immobilized ligand is the diffuse reflection spectroscopy which has been described in chapter 2.

Determination of the stability of the immobilized ligand

Long term stability of the carrier ligand complex was determined by measuring the loss of the immobilized ligand as a function of time. The concentration of free ligand in solution can spectrophotometrically be determined after removing the particles. Therefore particles were separated from the dispersion using a DynaGard cartridge filter (Microgon Inc., CA,

USA) which can be mounted on a syringe. The concentration of free ligand was determined in the filtrate at 610 nm. The obtained ligand concentrations in this way were converted into loss of surface concentration.

Influence of free ligand on the binding capacity

When ligands are released from the carrier complex these molecules free in solution will compete with the immobilized ligands for the binding of the proteins. Therefore experiments have been performed to measure to which extent the released ligands will interfere in the total process. Binding of BSA onto BL-7 was studied in the presence of different amounts of free ligands while all other conditions were kept the same (0.067 M phosphate buffer at pH = 7.4). The free ligand concentration was adjusted before addition of the protein. After 2 hours the amount of unbound BSA was separated from the medium by filtration and centrifugation. The concentration of BSA was measured by means of a HPLC method in the usual way.

RESULTS AND DISCUSSION

Determination of ligand immobilization

In affinity chromatography the ligand immobilized on agarose beads is usually released by hydrolysis of the complex in HCl at elevated temperatures. Firstly this method was applied to analyse the amount of immobilization on the latex as well. However this attempt was unsuccessful. In the case of much stronger acids, like sulphuric acid, ligands could be partly released from the particles. It was visually observed that the particles remain blue indicating that the release was not complete. Therefore the surface ligand density determined by this method will give an underestimation of the actual value.

Ligand density values obtained with the hydrolysis analysis are given in figure 1 as a function of the concentration of sodium carbonate used in the immobilization procedure. Since the ligand immobilization reaction generates hydrochloric acid as one of the end products an increase in the OH^- concentration, by the addition of sodium carbonate, will enhance the ligand immobilization. This is illustrated by the linear relationship between the ligand density and the concentration of sodium carbonate used during the ligand immobilization reaction.
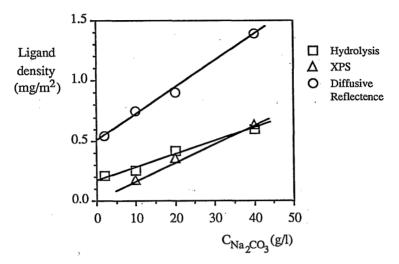
Fig. 1 *The amount of ligand immobilized onto the core-shell latex particles as a function of the concentration of sodium carbonate during the coupling reaction, determined by hydrolysis, XPS and diffusive reflectance methods.*

The second applied method XPS is a powerful tool for the elementary analysis of the chemical composition on a solid surface. This technique is non-destructive and it can provide information on elements that are buried some nanometers beneath the sample surface. However the obtained XPS results are somewhat inconsistent with each other. The concentration of the ligands at the surface found from the nitrogen peak was larger than the concentration calculated from the sulphur signal. This discrepancy made the interpretation of the results difficult.

In figure 1 the results of the nitrogen analysis are given. The same trend as for the hydrolysis analysis has been found. The trend for the sulphur analysis is the same but the absolute values are lower.

Diffuse reflection spectroscopy is a non-destructive method and the measurement is carried out in solution form. As shown in figure 1, the surface ligand density measured by this method was twice as high as that measured by the other two methods. The data for ligand densities obtained by the method of diffuse reflection spectroscopy was used throughout this thesis.

Ligand stability

In figure 2 the release of ligand is given, expressed in the loss of ligand density. Agarose-ligand complex was hydrolyzed in 6 M HCl at 20 °C and 45 °C. Only at 45 °C a considerable amount of ligand could be released, which stays constant after about 2 hours of hydrolysis. However the same procedure for the latex-ligand·complex did not result in release of ligand.
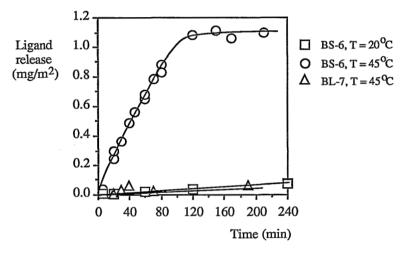

Fig. 2 The amount of ligand released from the BS particles (BS-6) and from the BL particles (BL-7) determined by hydrolysis using 6 M HCl at different temperatures. The amount released has been expressed in terms of surface concentration.

This result indicates that there is a strong chemical stability of the hydrogel shell in comparison with the agarose matrix. This result could also indicate that the agarose matrix is (partly) broken down.

After the accomplishment of the immobilization procedure, the ligand-immobilized particles must be subjected to an appropriate washing process in order to remove non-covalently attached ligands. Although various washing protocols do exist, distilled water alone is probably the best washing medium effective on hydrophilic dye-ligands [5]. In general, if ligand-immobilized particles are used in non-extreme pH media, as is normal for most protein fractionation protocols, and at temperature ranges from 4 °C to 10 °C,

then the ligand release is negligible.

More *et al.*[6] studied ligand release for a period of one and a half year with (^{14}C) labelled Cibacron Blue coupled on Sepharose 6B-CL. Total release of the immobilized ligands over one and a half year under continuous flushing with a solution of 10 mM phosphate buffer, pH 7.5 containing 150 mM sodium chloride was 1.4 % of the initial coupled ligand level. Capacity of the carrier-ligand complex for albumin remained unchanged. It was noticed that extended washing of the carrier-ligand complex with low ionic strength buffer or water increased ligand release by at least a factor of 10 when compared to the buffer solution (of 10 mM phosphate buffer, pH 7.5 containing 150 mM sodium chloride) used.

In this study ligand release was found for the ligand-coupled particles stored at 4 $^{\circ}$C. The concentrations of the released ligand molecules were determined for six types of the BL particles with different storage times. The percentages of ligand release, related to the total amount of the ligands immobilized on the particle surface initially, are given in table 1 and figure 3. The results of ligand release as a function of time for three of these particles are shown in figure 3. One observation is that for all the types of the BL particles the immobilized ligands release in time. The percentages of ligand release, for 6 types of the BL particles, are below 5 %.
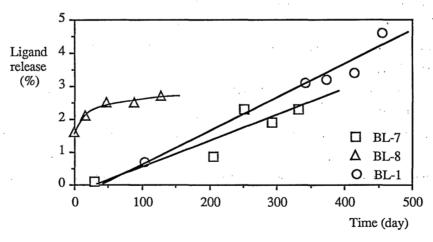

Fig. 3 The plot of ligand release in time for three types of latex particles.

It is interesting to compare the results of ligand release in this study with that obtained

by More *et al.* although the experimental conditions and the particles used are different from each other. More *et al.* applied a flushing method which removes the released ligand continuously, and thus keeps the concentration of free ligand in solution at very low level. In contrast particle solutions are placed on shelf without flushing in this study, and therefore the free ligand concentration increases in time. If ligand release is dependent on the free ligand concentration in such a way that a higher concentration of free ligand prohibits ligand release while a lower ligand concentration promotes the release, one may expect that the flushing method will result in more ligand release in comparison with a purely storage treatment for the particle solution as it is used in this study. However the solution environment also play a role in ligand release. More *et al.* used a buffer solution containing 150 mM salt while in our case the particles are stored in water. As has been mentioned above washing of the carrier-ligand complex with water may increases ligand release by at least a factor of 10 when compared to the buffer solution used in the flushing method, which implys a 14 % ligand release in our case. Since we did not apply the flushing method and the particles used are also different from that used by More *et al.*, it is reasonable to have a ligand release of less than 5 % for these particles which have been placed on shelf for at least 9 to 15 months. According to this study it is expected that ligand release will not severely influence the binding capacity of the particles.

Influence of free ligand concentration on BSA binding on the particles
The results of the influence of free ligand concentration on BSA binding on the particles are shown in figure 4. The arrow, in the figure, indicates the concentration of free ligand present originally in the BL-7 solution. The binding capacity of the particles decreased with an increase of free ligand concentration in the binding solutions. At ligand concentrations lower than 0.01 mg/ml, only slight decrease of the binding capacity was observed, while at the ligand concentrations higher than 0.01 mg/ml, the binding capacity decreased dramatically. This decrease can result from the stronger interaction between BSA and free ligand in comparison with the immobilized ligand whose mobility is sterically restricted by the immobilization.

Causes of ligand instability and future improvement
The causes of the ligand release, although being in the low level, may be attributed to three factors. One is the hydrolysis of the coupled ligand to hydroxyl groups on the particles [7].

It is suggested to use an amine group instead of a hydroxyl group for the ligand linkage to a particle because a coupled amine group is chemically more stable than a coupled hydroxyl group. Another reason could be that the release does not stem from immobilized
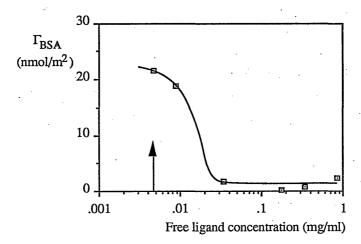

Fig. 4 BSA binding capacity of the BL particles (BL-7) as a function of added free ligand concentration in the adsorption solutions.

ligands but simply adsorbed ones. The hydrophilic shell of the particles can also be subject towards hydrolysis during a long period of storage time resulting in loss of immobilized ligand.

CONCLUDING REMARKS

For all the preparations of the ligand-coupled latex particles, it was found that the concentration of free ligand in bulk solution increased slowly with storage time. The ligand immobilized on the latex particles is however more stable towards acidic hydrolysis at elevated temperature compared to that on the agarose particles.

The percentages of loss of the immobilized ligands for the longest time period measured, about one year, were found to be less than 5 %. This amount of ligand loss is too low to give any significant influence on the binding capacity of the particles, but might cause undesired contamination of the product.

REFERENCES

1. B. Gebben, D. van Houwelingen, W. Zhang, Th. van den Boomgaard and C.A. Smolders, Colloids and Surfaces B Biointerfaces, in preparation; chapter 2 of this thesis.

2. W. Zhang, Z. Borneman, B. Gebben, Th. van de Boomgaard and C.A. Smolders, Colloids and Surfaces B Biointerfaces, in preparation; chapter 3 of this thesis.

3. D.J. Stewart, D.R. Purvis, J.M. Pitts and C.R. Lowe, J. Chromatogr., 623 (1992) 1.

4 H.-J. Böhme, G. Kopperschläger, J. Schulz, and E. Hofmann, J. Chromatogr., 69 (1972) 209.

5. Y.D. Clonis, in Reactive Dyes in Protein and Enzyme Technology, Y.D. Clonis, T. Atkinson, C.J. Bruton and C.R. Lowe (Eds.), Stockton Press, New York, 1987, pp. 33.

6. J.E. More, A.G. Hitchcock, S. Price, J. Rott and M.J. Harvey, in Protein-Dye Interactions: Developments and Applications, M.A. Vijayalakshmi and O. Bertrand (Eds.), Elsevier Applied Science, London, 1989, pp. 265.

7. C.R. Lowe, in Topics in Enzyme and Fermentation Biotechnology, A. Wiseman (Ed.), Vol. 9, Ellis Horwood, Chichester, 1984, pp. 78.

4

Protein Separation Using Affinity Binding
Part III Competitive Binding

W. Zhang, Z. Borneman, B. Gebben[1], Th. van den Boomgaard, C.A. Smolders

SUMMARY

A ligand-coupled PS core-shell latex has been used for the affinity cross-flow filtration process. Competitive binding between bovine serum albumin (BSA) and bovine immunoglobulin G (IgG), and between BSA and lysozyme, onto ligand-coupled latices was studied. It was found that BSA bound preferentially with respect to IgG throughout a range of protein mixing compositions studied. Preferential binding of lysozyme, with respect to BSA, was found for a range of protein compositions. Dilution of the total protein concentration in the applied mixture, with fixed protein ratios, did not influence the preference of BSA binding at initial BSA concentrations above 0.2 g/l. The competitive binding of BSA over IgG on the ligand-coupled latices was sensitive to the ionic strength of the solution. The prediction of competitive binding isotherms is attempted using a competitive binding model.

4.1 INTRODUCTION

A novel separation process, Affinity Cross-Flow Filtration (ACFF), is being developed for large-scale protein purifications. The preparation and the characterization of the dye-immobilized polystyrene core-shell latex particles (BL) and the binding study of single protein solutions with the BL particles are presented elsewhere [1, 2]. In this chapter the study on competitive binding of the model protein system on the ligand-coupled latex particles will be described.

Competitive adsorption occurs when two or more proteins are simultaneously mixed

---

[1] AKZO Research Laboratory Arnhem, Arla, CRC, Arnhem.

with an adsorbent. Two types of the studies on simultaneous competitive adsorption can be distinguished. One makes use of one kind of protein with varying molecular size, e.g. monomer, dimer and oligomer of the same protein molecules. Preferential adsorption of the higher molecular weight has been reported in literature: oligomers adsorb preferentially over dimers and, and dimers preferential adsorb over monomers. Most studies have been performed with albumin [3-5]. The second type of research deals with adsorption from a mixture of different proteins. In general the adsorbed amount of a specific protein from a mixture in competition with other proteins is less than the adsorbed amount of the same protein without competition. In competitive adsorption studies involving fibrinogen, IgG and albumin, it is always observed that the preference for the adsorbent decreases in this order, i.e. fibrinogen > IgG > albumin. To give an example, the competitive adsorption of the tertiary protein mixture albumin, IgG and fibrinogen on a polystyrene latex was started with the initial protein ratio (wt % in solution) of 24 : 62 : 14, and ended up with the protein ratio (wt % in the adsorbed layer) of 0 : 29 : 71 [4]. Another example can be given for the competitive adsorption of the same tertiary protein mixture on a hydrophilic grafted polyetherurethane: the initial protein ratio (wt % in solution) was 75 : 20 : 5, and the protein ratio (wt % in the adsorbed layer) at the end was 41 : 26 : 33 [6]. The reason for these shifts is attributed to the ability of conformational changes upon adsorption. Protein molecules with large conformational changes, meaning that large entropy gains can occur, show high adsorption affinity to the surface.

Several investigators have shown that the equilibrium relationship between free and bound adsorbate can be described by a Langmuir-type isotherm [7-11]. In practice, bio-separations often deal with multicomponent systems. Competition for the same binding sites, on the adsorbent, between two or more different species of proteins can occur. A competitive model can be derived by introducing a fractional occupancy of the adsorption capacity for each type of protein i into the equation [12]:

$$\Gamma_i = \frac{\Gamma_{m,i} \, K_{a,i} \, C_{e,i}}{1 + \sum_{j=1}^{n} K_{a,j} \, C_{e,j}} \quad (1)$$

where $\Gamma_{m,i}$ corresponds to a monolayer coverage of the bound molecule i, $C_{e,i}$ is the protein concentration at equilibrium, $K_{a,i}$ is a binding constant and $j=1 \cdots i \cdots n$. A high

value of $K_{a,i}$ means a high binding strength between the protein i and the ligand. Therefore the incorporation of the parameter K_a into equation 1 brings the binding preference of each protein into account in the prediction of Γ_i. Both Γ_m and K_a are determined by fitting of experimental data as described in chapter 2 [2]. Equation 1 has frequently been used in model simulation of competitive adsorption for multicomponent systems [11-14]. In this study, prediction of competitive binding for the pairs of BSA and IgG, and for BSA and lysozyme, is attempted using equation 1.

Competitive binding is studied in test tube experiments in order to see the binding/adsorption preference of the chosen model protein system on the ligand-couple latex particles (i.e. the BL particles) under various binding/adsorption conditions. The feasibility of the competitive model is tested for the purpose of further applying the model in the ACFF process.

4.2 EXPERIMENTAL

4.2.1 Materials

The same proteins (BSA, IgG and lysozyme) as have been described in chapter 3 are used in competitive binding study [2].

The core-shell PS latices have been described in detail elsewhere [1].

The filling for a Protein G column for the analysis of protein mixtures, protein G Sepharose 4 Fast Flow was obtained from Pharmacia, Sweden.

4.2.2 Binding of single proteins

The procedures for the binding experiments with the single proteins have been described in chapter 3.

4.2.3 Competitive protein binding

Competitive binding was performed by bringing together protein mixtures with different compositions but with a fixed total concentration (1.0 g/l) and the BL particles. Other experimental conditions for competitive binding experiments were kept identical to that for single protein binding experiments. After the binding experiments the remaining of the protein solution was analyzed with a Waters HPLC system, with a Shodex™ W803F size exclusion column. Protein concentration was determined with UV detection at 214 nm.

However, in the case of competitive binding studies the concentration of the different proteins could not be obtained separately. Therefore, protein mixtures were analyzed with a column filled with Protein G Sepharose 4 Fast Flow (Pharmacia, Sweden) as a pretreatment. This column binds IgG of many species specifically. Thus, IgG is retained in the Protein G column when a mixture of BSA and IgG passes through it. In this way, therefore, only the BSA concentration is measured. The IgG concentration in the mixture can be obtained by subtracting the BSA concentration from the total protein concentration which is measured with the Protein G column disconnected. To estimate the errors inherent to the measurements, a series of standard protein solutions with different compositions of BSA and IgG was evaluated. At BSA concentrations above 0.2 g/l, the standard deviation of the measurements was found to be less than 5 %.

Both protein concentrations of BSA and lysozyme could be obtained separately with the normal HPLC procedure.

4.2.4 Influence of protein concentration and composition

Experiments were performed with a range of total protein concentrations at fixed protein ratios in addition to the standard binding/adsorption conditions. The total protein concentrations varied from 0.1 g/l to 1.5 g/l with BSA / IgG ratios of 4/1 and 1/4, respectively, and from 0.1 g/l to 1.6 g/l for the ratio of BSA / IgG of one.

4.2.5 Effect of ionic strength

The ionic strength was varied in some binding experiments by diluting the buffer solution (low ionic strength) or by adding NaCl (high ionic strength). The initial protein concentration was 1.0 g/l. The initial protein ratio of BSA to IgG, on a weight basis, was one.

4.3 RESULTS AND DISCUSSION

4.3.1 Binding of single proteins

Isotherms of single protein binding for the proteins BSA, IgG and lysozyme have been discussed in detail elsewhere [2]. The characteristics of the binding isotherms, i.e., the binding constant K_a and the maximum in bound mass Γ_m obtained for single protein binding are used for the model prediction of a binary binding isotherm in the following

section.

4.3.2 Competitive binding isotherms

Bringing together two proteins and one adsorbent simultaneously will lead to competition for the binding sites. This is called competitive binding in this chapter. The results of the competitive binding isotherm for the proteins BSA and IgG onto the BL particles are depicted in figure 1. As adsorbent the BL particle BL-7 has been used. The abscissa in figure 1 shows the mole fraction of BSA in the bulk solution at equilibrium,
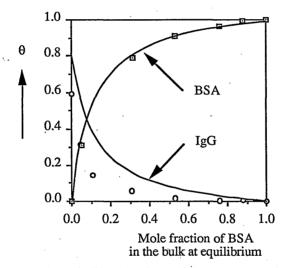

Fig. 1 Competitive binding of BSA and IgG on the ligand-coupled latex BL-7 at pH 7.4, ionic strength 0.17 and room temperature. The solid lines represent the model fit. $\theta_i = \Gamma_i / \Gamma_{m,i}$ for protein i.

and the ordinate shows for the single component mole ratios with respect to monolayer binding of the bound proteins, $\theta_i = \Gamma_i / \Gamma_{m,i}$ where Γ_i means the experimentally bound amount of protein i at equilibrium concentration $C_{e,i}$ in competitive binding, $\Gamma_{m,i}$ is the fit constant determined in single protein binding. Although the shapes of the curves for θ_{BSA} and θ_{IgG} are quite different, both θ_{BSA} and θ_{IgG} show an increase in binding with an increase of the individual fractions of BSA and IgG, respectively.

Binding of BSA is superior to that of IgG at lower mole fractions of BSA at equilibrium, while binding of IgG only takes place at a surplus of IgG and nearly in the

absence of BSA molecules. This is due to the difference in binding affinity as is indicated by the binding constant K_a for the two proteins: for a protein, like IgG, with a lower affinity, i.e., a lower K_a value, the increase of θ_i will show an exponential behavior as a function of its bulk mole fraction. For high affinity (BSA) a Langmuir type of isotherm with early saturation shows up. The solid lines in figure 1 for θ_{BSA} and θ_{IgG} are calculated by equation 1 for a 2 component system. The values for $\Gamma_{m,BSA}$, $K_{a,BSA}$, $\Gamma_{m,IgG}$ and $K_{a,IgG}$ are obtained in chapter 3 of this thesis. The values of $C_{e,BSA}$ and $C_{e,IgG}$ are the experimental values obtained in the competitive binding experiment. The calculated values for θ_{BSA} fit nicely with the experimental ones, while the calculated values for θ_{IgG} give an overestimation. The possibility of an extra displacement of bound IgG by BSA is suspected to be the reason for this disagreement, which will be discussed later in this chapter.

The results of competitive binding between BSA and lysozyme are given in figure 2. In
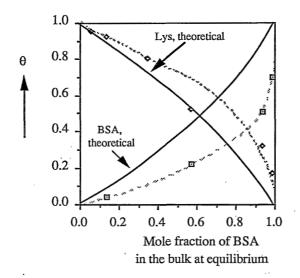

Fig. 2   The competitive binding of BSA and lysozyme on the ligand-coupled latex BL-7 at pH 7.4, ionic strength 0.17 and room temperature. The solid lines represent the model fit. $\theta_i = \Gamma_i / \Gamma_{m,i}$ for protein i.

contrast to the Langmuir-type of isotherm for the competition between BSA and IgG, BSA shows an exponential increase in competition with lysozyme, while lysozyme follows a Langmuir-type of isotherm. This is in agreement with the K_a values of the components because the $K_{a,\,BSA}$ value is smaller than $K_{a,\,Lys}$. The predicted amounts for the

competitive binding isotherms for both BSA and lysozyme are presented as solid lines in figure 2. The binding isotherm for BSA is overestimated and the binding isotherm for lysozyme is underestimated. The large discrepancy between the experimental data and the model calculation may be attributed to the possibility of an extra displacement of bound BSA by lysozyme which is not included in equation 1.

In figure 3 the competitive binding between BSA and IgG (curve a) and between BSA and lysozyme (curve b) are given. In this figure the relative bound amount of BSA is plotted as a function of the mole fraction of BSA of the two proteins present in solution. From this figure the trend of preferential binding can be clearly shown. In case of no preferential binding a linear relation should be found as indicated by the straight line in figure 3. Deviation above this line means preferential binding of BSA and below this line means the opposite. For the system BSA/IgG preferential binding of BSA is found as expected. The ligand used should show preference for BSA over IgG. By using the BL particles, more than 95 % purity of BSA in the adsorbed state can be obtained with an equilibrium mole fraction of BSA in the bulk phase as low as 0.2. When the competitive binding occurred between BSA and lysozyme, lysozyme showed much more pronounced
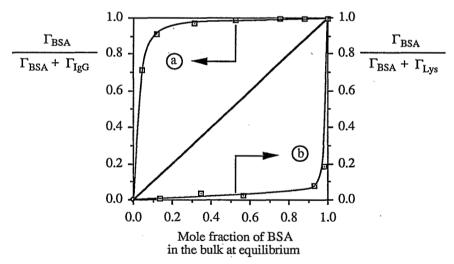

Fig. 3 The plot of surface mole fraction of BSA against its molar fraction in the bulk for the competitive binding between BSA and IgG, and between BSA and lysozyme with a 1.0 g/l total protein concentration and a mixing ratio of 1 on the ligand-coupled latex BL-7 at pH 7.4, ionic strength 0.17 and room temperature.

preferential binding to BSA. This can be readily explained by the difference in $\Gamma_{m,i}$ rather than the difference in $K_{a,i}$ for the two proteins. According to the results given in chapter 3 $\Gamma_{m,Lys}$ is 513 (nmol/m^2) while $\Gamma_{m,BSA}$ is only 23 (nmol/m^2). It is this factor 513 / 23 that exaggerates the normal surface molar fractions of the proteins.

4.3.3 Competitive kinetics

In the ACFF process kinetics of adsorption can play an important role in the competitive binding of the different proteins onto the particles. Therefore the kinetics of the protein binding has been studied in the presence of a second protein. The results are given in figure 4. For the purpose of comparison, the results of the binding of BSA and IgG separately, as a function of time are also given in figure 4. The binding of BSA and IgG, individually, on ligand-coupled latex (BL-7) is a fast process so that both Γ_{BSA} and Γ_{IgG} reach the plateau values within a few minutes of contact time in the initial stage of the binding. In the competitive binding Γ_{BSA} shows a fast increase in the initial stage of the binding process followed by a gradual increase in time. The slowly increased binding of BSA in the later stage of the competitive binding, although representing a small portion of the total bound amount, may be regarded as an indication of the presence of the competition between BSA and IgG for the binding sites.
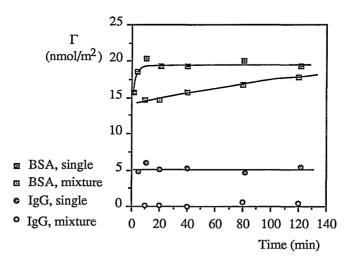

Fig. 4 Time dependence of the competitive binding between BSA and IgG with a 1.0 g/l
total protein concentration and a mixing ratio of 1 on the ligand-coupled latex
BL-7 at pH 7.4, ionic strength 0.17 and room temperature.

4.3.4 Influence of protein concentration and mixing weight ratio

To illustrate the influence of initial protein concentration and initial mixing weight ratio on the binding preference, competitive binding experiments were performed for a fixed binding time of 2 hours. The results of the competitive binding of BSA and IgG as a function of initial BSA concentration are given in figure 5. The preference of BSA binding on BL-7, with respect to IgG, at the three initial protein ratios i.e. 1/4, 1/1 and 4/1, is constant for initial BSA concentrations above ca. 0.2 g/l. However, the preference of BSA binding on the BL particles decreases at low protein concentration for all the protein ratios
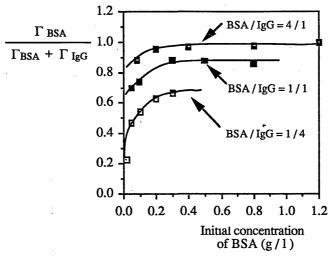

Fig.5   Influence of protein concentration on the competitive binding between BSA and IgG for various mixing ratios of BSA and IgG on the ligand-coupled latex BL-7 at pH 7.4, ionic strength 0.17 and room temperature.

tested. Theoretically, according to the prediction of equation 1, the preference of BSA binding must be independent of the initial protein concentration applied under the condition of fixed initial mixing ratio. The decreased preference can be explained as follows. The surface areas of the latex particles provided for protein binding were kept constant in the experiments. When the initial BSA concentration is lower than 0.2 g/l, the surface of the BL particles can not be saturated with the BSA molecules, which means that there is relatively more space left for the IgG molecules to accommodate. Therefore the binding preference decreases when the total protein concentration becomes low.

4.3.5 Effect of ionic strength

Protein binding depends on the difference in free energy of the protein molecules bound at the surface and free in solution. If this free energy difference is negative binding will occur. This difference can be influenced in various ways by changing the adsorbent surface characteristics, e.g. the amount of binding sites, the nature of the surface. Another possibility is changing the solution environment. The same applies for competitive binding. By using the same particles the difference in free energy for each type of protein individually can be altered, under the assumption that the nature of the surface will not be modified to a large extent due to this different solution environment. Competitive binding studies of BSA and IgG (at a ratio of 1) on the BL-7 particles has been performed at pH 7.4 and room temperature with different ionic strengths. The results of the molar binding as a function of ionic strength are shown in figure 6. As can be seen the binding of the two proteins follows different patterns upon the change in ionic strength. The binding of BSA
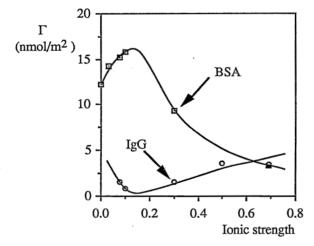
Fig. 6 Influence of ionic strength on the competitive binding between BSA and IgG with a 1.0 g/l total protein concentration and a mixing ratio of one on the ligand-coupled latex BL-7 at pH 7.4 and room temperature.

undergoes a maximum while the binding of IgG shows a minimum. Coincidently, the maximum and the minimum happened to occur at about the ionic strength of 0.17, which was used as a standard condition for protein binding. It is known for most of the proteins which interact with the ligand that at high ionic strength the ligand-protein interactions are

weakened [15-18]: a one to three moles NaCl solution is often used to elute the bound BSA molecules from a dye adsorbent. This effect has been discussed thoroughly in chapter 3 of this thesis. Briefly, upon a change in ionic strength the protein molecules tend to respond with a conformation change to balance the various interactions both in the interior and at the exterior, which results in a decreased binding capability. At low ionic strength down to zero, the solubility of BSA decreases which may influence the BSA binding. In the study of the effect of ionic strength on BSA binding from plasma onto an agarose adsorbent, on which the ligand Cibacron Blue was immobilized, a maximum of the bound BSA at the ionic strength 0.15 was observed by Harvey *et al.* [19]. This observation is in agreement with the results found here. The maximal value of the BSA binding may be explained as follows. The ionic strength of solutions in living cells and living bodies is approximately 0.15. This value has been referred to as *the optimum physiological ionic strength* [20]. The reason of being called optimal is because it maintains a normal water balance in living cells. In this accordance it may not be unacceptable to see that at the ionic strength around 0.17 the BSA molecule may fully keep their biological functions, while away from this value the molecular structure may be engaged more or less in a conformational change.

The mechanism of ligand-IgG interaction is much less explored in literature compared to the case of ligand-BSA interaction. Although a few references can be found in literature which describe adsorption (or binding) of IgG on negatively-charged latex particles, contradictory results are found for studies of the effect of ionic strength on IgG adsorption on such negatively charged particles. For example, Suzawa and Shirahama [21] studied the adsorption of bovine IgG (concentration not stated) onto PS latices (ζ = -85 mV at pH > 6.0). A slight increase in the adsorption of IgG was found when the ionic strength in the solution increased from 0.115 to 0.154 through a wide range of pH values. However, Kondo et al [22] found a decrease in bovine IgG adsorption on PS latices (ζ = -75 mV at pH > 6.0) upon the increase of ionic strength from ca. 0.01 to 0.2 at pH = 7.0. In general electrostatic interaction is weakened at high ionic strength. Consequently, hydrophobic interaction must becomes relatively enhanced under such circumstances. Further experiments are needed to get an insight in the effect of ionic strength on IgG adsorption in relation to the interaction mechanisms.

4.3.6 Model prediction of competitive binding

The experimental data of binding of proteins, separately, can be fitted to a large extent by

the Langmuir-type model, as it is shown in figure 1. The parameters K_a and Γ_m obtained from the isotherms were used in the competitive binding model for the prediction of the binary competitive binding of BSA and IgG. The prediction of the binary isotherms by the competitive binding model for BSA and IgG is in a good agreement with the corresponding experimental data, especially for BSA, as shown in figure 1. An overestimation of the molar binding for IgG was found in figure 1. One possible explanation is the extra displacement of IgG by BSA.

It is known in literature that plasma proteins in solution are able to displace other proteins preadsorbed on a surface [6, 23-27]. In competitive binding, for example, proteins with small size and high concentration will come to a surface first and adsorb onto the surface from a solution mixture because they diffuse faster when compared with large proteins and low concentrations. However, the large proteins at low concentrations may displace the proteins already on the surface as long as they have higher affinity for the surface. It has been observed that for the competitive adsorption between fibrinogen, IgG and albumin on polymer surfaces with non-specific adsorption sites the adsorption preference decreases in this order [26]. Studies on the displacement of preadsorbed proteins by Bale et al.[27] shows that the effectiveness for the proteins fibrinogen, IgG and albumin as displacement agents is in the order fibrinogen > IgG > albumin which is the same as the adsorption preference. In this study the binding preference of BSA over IgG is found because the binding results from the interaction between the proteins and the specific ligand immobilized. Although no direct evidence has been obtained yet to show the effect of displacement, one may expect that the effectiveness for protein displacement follows the same trend as the binding preference. The effect of protein displacement may explain the discrepancy between the experimentally determined binary isotherm and the predicted one, and has yet to be taken into account into predictive models. From a practical point of view the effect of protein displacement is of importance for the study of the ACFF process.

4.4 CONCLUSIONS

The binding isotherm for the binary mixture of BSA and IgG confirms that BSA bound preferentially onto the BL particles in comparison with IgG throughout a range of protein compositions. The variations of the total protein concentration in the mixture, when protein

ratios were fixed, did not influence the preference of BSA binding onto the ligand-immobilized latices at initial BSA concentrations above 0.2 g/l. This result implies that during the washing stage in the ACFF process where the total protein concentration in the mixture decreases, the binding preference of BSA will not be influenced. The prediction of competitive binding isotherms is done using a competitive binding model. Deviations of the predicted isotherms from the experimentally determined ones were observed.

4.5 REFERENCES

1. B. Gebben, D. van Houwelingen, W. Zhang, Th. van den Boomgaard and C.A. Smolders, Colloids and Surfaces B Biointerfaces, in preparation; chapter 2 of this thesis.

2. W. Zhang, Z. Borneman, B. Gebben, Th. van de Boomgaard and C.A. Smolders, Colloids and Surfaces B Biointerfaces, in preparation; chapter 3 of this thesis.

3. R.J.L. Zsom, J. Colloid Interface Sci., 111 (1986) 434.

4. H.G.W. Lensen, D. Bargeman, P. Bergveld, C.A. Smolders and J. Feijen, J. Colloid Interface Sci., 99 (1984) 1.

5. R.G. Greig and D.E. Brooks, J. Colloid Interface Sci., 83 (1981) 661.

6. B. Jansen and G. Ellinghorst, J. Biomed. Mat. Res., 18 (1984) 655.

7. H.A. Chase, J. Chromatogr., 297 (1984) 179.

8. P.C. Wankat, Anal. Chem., 46 (1974) 1400.

9. J.W. Eveleigh and D.E. Levy, J. Solid-Phase Biochem., 2 (1977) 45.

10. B.J. Horstmann, C.N. Kenney and H.A. Chase, J. Chromatogr., 361 (1986) 179.

11 G.L. Skidmore and H.A. Chase, J. Chromatogr., 505 (1990) 329.

12. T.-Y. Gu, G.-J. Tsai and G.T. Tsao, AIChE J., 37 (1991) 1333.

13. F.H. Arnold, H.W. Blanch and C.R. Wilke, Chem. Eng. J., 30 (1985) B9.

14. B.H. Arve and A.I. Liapis, Biotechnol. Bioeng., 32 (1988) 616.

15. J. Carlsson, J.-C. Janson and L. Ryden, in Protein Purification: Principles, High Resolution Methods, and Applications, J.-C. Janson and L. Ryden (Eds.), VCH Publishers Inc., N.Y., 1989, pp. 275.

16 G. Birkenmeier, in Protein-Dye Interactions: Development and Applications, M.A. Vijayalakshmi and O. Bertrand (Eds.), Elsevier Applied Science, London and N.Y., 1989, pp. 253.

17 R.K. Scopes, in Protein-Dye Interactions: Development and Applications, M.A. Vijayalakshmi and O. Bertrand (Eds.), Elsevier Applied Science, London and N.Y., 1989, pp. 97.

18. Y.D. Clonis, in Reactive Dyes in Protein and Enzyme Technology, Y.D. Clonis, T. Atkinson, C.J. Bruton and C.R. Lowe (Eds.), The MacMillan Press Ltd., London, 1987, pp. 33.

19. M.J. Harvey, R.A. Brown, J. Rott, D. Lloyd and R.S. Lane, in Separation of Plasma Protein, J.M. Curling (Ed.), Pharmacia AB, Uppsala, 1983, pp. 79.

20. P. Douzou and P. Maurel, Trends Biochem. Sci., 2 (1977) 14.

21. T. Suzawa and H. Shirahama, Adv. Colloid Interface Sci., 35 (1991) 139.

22. A. Kondo, S. Oku and K. Higashitani, Biotechnol. Bioeng., 37 (1991) 537.

23. Y.F. Missirlis and W. Lemm (Eds.), Modern Aspects of Protein Adsorption on Biomaterials, Kluwer Academic Publishers, Dordrecht, 1991.

24. K.K. Chittur, D.J. Flink, R.I. Leiniger and T.B. Hutson, J. Colloid Interface Sci., 111 (1986) 419.

25. H. Shirahama, J. Lyklema and W. Norde, J. Colloid Interface Sci., 139 (1990) 177.

26. M.D. Bale, D.F. Mosher, L. Wolfarht and R.C. Sutton, J. Colloid Interface Sci., 125 (1988) 516.

27. M.D. Bale, S.J. Danielson, J.L. Daiss, K.E. Goppert and R.C. Sutton, J. Colloid Interface Sci., 132 (1989) 176.

5

Protein Separation Using Microfiltration
Filtration of Particle Suspensions
in The Presence and Absence of Protein

W. Zhang, Z. Borneman, Th. van den Boomgaard and C.A. Smolders

SUMMARY

In this study purification of BSA in a mixture of IgG and BSA was obtained by preferential binding on specially designed polystyrene (PS) latex particles and porous agarose particles with specific ligands using microfiltration. The process is called Affinity Cross-Flow Filtration (ACFF). The microfiltration behavior of the protein solution, the particle suspension and a mixture of both is investigated. It was found that aggregates and / or particulates present in the crude protein solution, governed the flux decline. Prefiltration of the protein solution prevents flux decline to a large extent. However, pumping of the protein solution seems to alter the characteristics of the protein: after some time aggregates are formed again resulting in a severe flux decline.

Microfiltration of the ligand-immobilized carrier particles shows for the large agarose particles little influence on the flux, while for smaller PS latex particles a dramatic flux decline is found. This can be explained by the difference of the configurations of the cake layers formed on top of a membrane.

This study makes it clear that in the ACFF process microfiltration membranes with large pore sizes should be used and that the optimum particle size for the affinity carrier can be expected to be in the range of microns.

5.1 INTRODUCTION

A novel separation process, Affinity Cross-Flow Filtration (ACFF), is being developed to meet the demands for large-scale separation of proteins. The ACFF process takes the

advantage of high resolution from affinity binding and of large processing capacity in a continuous way from cross-flow filtration. The ACFF process can be divided into four stages. In the first stage a mixture of proteins is introduced into a container in which a ligand-immobilized carrier particle is present. The target protein will be bound to the ligand-immobilized carrier particle. In this way an affinity complex is formed. In the second stage purification of the protein of interest takes place by using a cross-flow microfiltration unit to wash out the impurities. In the third stage a reagent is introduced into the system to release the target protein. A filtration unit is used to recover the target protein. In the final stage the carrier particle is regenerated and ready for the next cycle.

In this study, core-shell polystyrene latices and porous agarose particles are used. The latex particles are of submicron size and consist of a hard, non-porous core surrounded by a hydrogel shell to which affinity ligands can be covalently coupled [1 - 2]. For reasons of comparison results are given also for porous agarose particles which are often used in affinity chromatography.

In the ACFF process proteins having dimensions in the nanometer range will be separated from particles with dimensions in the micrometer range. Theoretically, a microfiltration membrane should give free pass to the macromolecular solutes. In practice, however, it has often been encountered [3] that filtration of a protein solution with a microfiltration membrane shows severe flux decline. It is therefore important for practical applications to investigate systematically the filtration behavior of protein solutions, particle suspensions, and mixtures of both. This will be described in this chapter.

5.2 EXPERIMENTAL

5.2.1 Materials

Two types of membranes are used in this study. Membrane A is a 0.1 μm flat sheet membrane from Millipore, USA. Membranes B is in a hollow fiber form, and has been supplied by X-Flow B.V., The Netherlands. Bovine serum albumin (Boseral pur™, 40030) and bovine immunoglobulin G (Bovine Gamma Globulin™, 41979) [4] were supplied by Organon Technika, The Netherlands. Procion Blue HB™ (a commercial brand of Cibacron Blue F3G-A) was purchased from Janssen, Belgium.

Superose 6 prep grade™ and DEAE Sepharose Fast Flow™ were purchased from

Pharmacia, Sweden and used as examples of porous particles. The ligand-immobilized Superose was prepared according to the procedure described by Böhme [5]. The number averaged particle size of the ligand-immobilized Superose (cited as BS), determined by SEM, was 17 μm, and for DEAE Sepharose Fast Flow it was 38 μm.

The polystyrene core-shell latices were obtained from AKZO, Arnhem and were used as an example of nonporous particles. The number averaged particle sizes obtained by electron micrographs are 0.22 μm, 0.39 μm, 0.82 μm, 1.2 μm and 1.96 μm, respectively. The preparation of the ligand-immobilized latex particles (cited as BL) has been given in chapter 2.

5.2.2 Pore size distribution

The pore size distribution of the membranes is determined by a Coulter Porometer and also estimated from electron micrographs (JEOL JSM-T220A Scanning Microscope).

5.2.3 Filtration

An Amicon stirred cell (model 8050), with an effective membrane area of 14.2 cm^2, was used for the dead-end filtration of protein solutions by membrane A. A stirring speed of 300 r.p.m. was used. All the protein solutions in the experiments were used immediately after a prefiltration took place with a Millipore 0.1 μm membrane, except otherwise stated.

The experiments of cross-flow filtration were performed using lab-made modules of X-flow hollow fibers with a total internal surface area of 230 cm^2. For each experiment a new module was used. The permeate was recirculated.

The operating pressure in the filtration system was 0.1 bar unless otherwise specified.

5.2.4 Protein solutions

All protein solutions were prepared in 0.067 M Sörensen phosphate solution, pH = 7.4, ionic strength = 0.17. A known amount of protein was dissolved in a buffer solution and kept overnight in a fridge without stirring. The prepared protein solution was used within one day. Protein concentration was determined using a normal HPLC procedure.

5.3 RESULTS AND DISCUSSION

5.3.1 Characteristics of the membranes

A volumetric averaged pore size of 0.24 μm was determined for membrane A using the Coulter Porometer (see table 1). For membrane B only a bubble point of 0.08 μm could be measured. Pore sizes measured with SEM or given by the manufacturers, and water fluxes are shown in table 1 as well. Comparing the results of the pore sizes measured with the porometer and with SEM, it can be concluded that these values are consistent, but not with the data given by the manufacturers.

Table 1 *The characteristics of the two membranes used in this study.*

Type	Manu-facturer	Material	Pore size (μm)			Water flux
			Manufacturer	Porometer	SEM	$(l/m^2h.bar)$
A	Millipore	Modified PVDF	0.1	0.24	< 0.8	3,400
B	X-flow	PES & PVP blend	0.2	0.08 *	< 0.2	1,100

* Only the bubble point is measured with a Coulter Porometer.

5.3.2 Prefiltration of protein solutions

The influence of prefiltration of a 0.5 g/l IgG solution on the flux decline can be seen in figure 1 for a stirred dead end filtration using membrane A. If no prefiltration was applied a
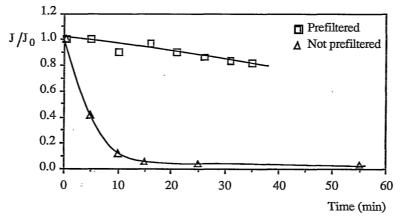

Fig. 1 The flux reduction through membrane A in a stirred cell during filtration of IgG solution prefiltered and not prefiltered at an operating pressure of 0.5 bar.

severe flux decline could be observed. The same IgG solution showed only slight decrease in flux after prefiltration which should be expected with microfiltration. In both cases the protein concentration in the permeate was constant. This indicates that only a small part of the protein causes this fouling behaviour, which can have however a large impact on practical application of the ACFF process. A similar fouling phenomenon was observed in the case of BSA.

In the case of cross flow filtration (membrane B) flux decline was observed even with a prefiltered protein solution. Adsorption of the protein molecules is thought to be the cause of the occurrence of flux decline [6]. Direct comparison between membrane A and B is not possible due to the difference in membrane configuration (flat and hollow fiber), mode of operation (stirred cell and cross-flow), membrane materials (modified PVDF and polyethersulphone with PVP as a polymer additive) and different pore characteristics. Nevertheless this example implies that membrane B would not be a desirable choice for the ACFF process.

An important aspect of the ACFF process is the continuous way of operating. This implies that protein solutions have to be pumped through various parts of the total equipment. From literature [7] it is known that pumping can have some effect on the behaviour of the proteins. In figure 2 results are presented obtained in dead end filtration of
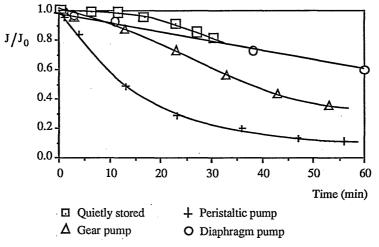

Fig. 2 *Filtration of BSA solutions in a stirred cell with membrane A. The solutions were prefiltered and pumped for 20 hours before flux measurement, and compared with that of a quietly stored solution.*

prefiltered BSA solutions which were treated differently. Three solutions were pumped with three different types of pumps for 20 hours, while the fourth solution was stored for 20 hours at room temperature. During the 20 hours period a dramatic decrease in flux can be seen for the solution which was pumped by the peristaltic pump. A more gradual decrease in flux was measured for the solutions pumped by the gear pump and the diaphragm pump. Also the fourth solution showed some flux decline after 20 hours storage which could indicate that aggregate formation took place even during storage. This hypothesis could not be supported by the light absorbance measurements of these protein solutions because these were constant within experimental error. Only the solution pumped with the peristaltic pump showed a gradual increase in absorbance (up to 30 %) in time. Protein concentrations, determined by HPLC, were constant for all four solutions. This is not surprising because common practice in HPLC is filtering out large aggregates to prevent clogging of the column. According to these results it can be concluded that protein aggregation can be induced by pumping and that only small amounts of protein must be involved in the process of aggregation.

5.3.3 Interactions between proteins, particles and membranes

The most interesting part for the ACFF process is the combination of particles and proteins in relation to the flux behaviour. Therefore experiments have been performed where first the flux behaviour of the particles alone is studied and after one hour proteins were added, imitating a part of the ACFF process.

Flux results are given in figures 3 and 4 for membrane A and membrane B, respectively. Two stages can be identified in both figures. In the first 60 minutes only particle solutions were filtered. After a steady state in flux behaviour was reached a certain amount of protein was added to the particle solution to give a total concentration of 0.5 g/l BSA. Due to the fact that protein binding took place in the system the final concentration of BSA would be somewhat lower but it gave hardly any influence to the flux results. In figures 3 and 4 the relative flux, i.e. the ratio of the steady state flux to the initial (water) flux J / J_0, is plotted as a function of time to obtain a better comparison between the different experiments. The results of the particles alone clearly show that for both types of membranes flux decline occurs related to the size of the particles used. The larger the particle size, the larger is the steady state flux. This observation has been summarized in figure 5 where the relative steady state flux (before addition of proteins) is plotted as a
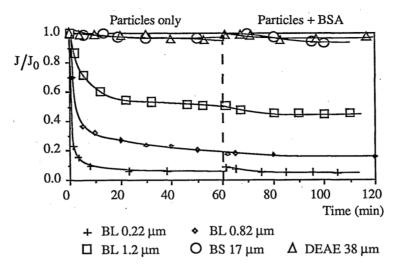
Fig. 3 *The fluxes through membrane A (average pore size 0.24 μm) obtained in a stirred cell during filtration of particle suspensions alone and after addition of BSA (0.5 g/l total concentration).*
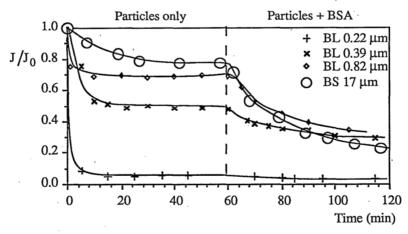

Fig. 4 *The fluxes through membrane B (max. pore size 0.08 μm) obtained during filtration of particle suspensions alone and after addition of BSA (0.5 g/l total concentration).*

function of particle size for both membranes. From this figure it is clear that the steady state flux is hardly influenced by the variation in particle size for large particles. However

when particle size gets close to the size of the pores of the membrane, the effect of particle size becomes pronounced and flux decreases drastically. The decrease in flux can be directly related to the configuration of the cake layer formed on top of the membrane. Assuming a cubic-packing of the particles, the radius of the pores r (or the radius of the channels) in the cake is simply proportional to the radius of the particles with a factor of 0.424 (a factor of 0.153 for a tetrahedric packing). A cake layer formed out of large particles may possess pores larger than the pores of the membrane so that it gives hardly any hydrodynamic resistance to solvent permeation. On the other hand, the hydrodynamic resistance of a cake layer formed with small particles can be very high so that the membrane resistance will be of minor importance. This hypothesis is supported by the results given in figure 5. For the same particle of BL 0.82 µm a flux reduction of 80 % was
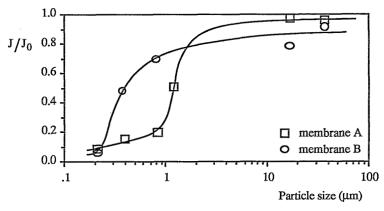

Fig. 5 The effect of particle size on the steady state flux for membrane A and B during filtration of particle suspensions without protein present.

observed for membrane A, while a flux reduction of only 30 % for membrane B was found. This is so because membrane A has a larger pore size, and a smaller membrane resistance, compared to membrane B. Similar results were obtained using the well characterized Nuclepore membranes, which have pore sizes of 0.05 µm and 0.2 µm, respectively, as cited by the manufacturer. The results are given in figure 6. Apart from the cake layer resistance, the effect of pore blocking on flux reduction can not be ruled out, especially when the particle sizes are close to the pore sizes of the membranes.

   In filtration of particle suspensions a so-called cake layer is usually deposited on top of a membrane surface resulting in a hydrodynamic resistance R_c in addition to the membrane
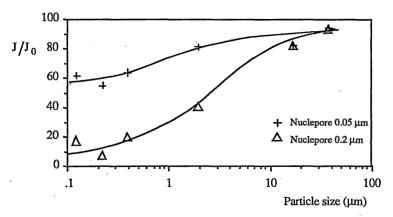
Fig.6 Relative fluxes of two types of Nuclepore membranes as a function of particle sizes.

resistance R_m. The filtration flux J for particle suspensions can be described by the cake-filtration model [8]:

$$J = \frac{\Delta P}{\eta\,(R_m + R_c)} \qquad (1)$$

where R_c is the cake layer resistance, R_m is the membrane resistance, ΔP is the transmembrane pressure drop, η is the viscosity of the solution, and J is the steady state flux. The cake layer resistance R_c can be related to the deposited mass m and the specific resistance α of the cake layer by the Kozony-Carman relationship:

$$R_c = \alpha\, m \qquad (2)$$

The specific resistance α of the cake layer can be given as:

$$\alpha = \frac{180\,(1 - \varepsilon)^2}{\rho\, D_p^2\, \varepsilon^3} \qquad (3)$$

where ε is the porosity of the cake layer, ρ is the density of the particles which form the cake layer and D_p is the particle diameter. The deposited mass m is proportional to the product of the cake layer thickness δ and the density of the particles ρ:

$$m = \delta\, \rho\, (1 - \varepsilon) \qquad (4)$$

The membrane resistance R_m can be obtained by substituting the experimentally determined values of J_o (the pure water flux) into the following equation:

$$R_m = \frac{\Delta P}{\eta \; J_o} \tag{5}$$

Using equations 1 to 5 a theoretical flux can be calculated as a function of the particle diameter D_p, assuming the porosity ε to be either 0.25 for a densely packed layer or 0.36 for a randomly packed layer, and the cake layer to be 1 and 10 µm thick. Tables 2 and 3 show the results of the calculated values of J / J_o for Nuclepore 0.2 µm and 0.05 µm membranes in comparison with the experimentally determined values, respectively. For

Table 2 *Comparison of the model calculated J / J_0 values with the experimentally determined J / J_0 values for Nuclepore 0.2 µm membrane. D_p is the particle diameter.*

D_p (µm)	J/J_o	$\delta = 10^{-6}$(m)		$\delta = 10^{-5}$ (m)	
		ε=0.25	ε=0.36	ε=0.25	ε=0.36
0.124	0.173	0.12	0.35	0.013	0.051
0.22	0.072	0.29	0.63	0.039	0.144
0.39	0.20	0.59	0.86	0.127	0.37
1.96	0.40	0.92	0.98	0.54	0.83
17	0.82	0.99	0.99	0.99	1.00
38	0.93	1.00	1.00	1.00	1.00

Nuclepore 0.2 µm membrane the calculated values of J / J_o fit reasonably to the experimental ones for the case of a cake layer thickness 10 µm and a cake porosity of 0.25. For Nuclepore 0.05 µm membrane the fit with a cake porosity 0.25 and a cake layer thickness 10 µm is close to the experimental values. The model calculation suggests that the cake layers are packed in the form of a dense packing with a layer thickness of about 10 µm. A general trend can be realized in the model calculation that for small particles the fit gives a underestimation while for large particles the fit shows an overestimation. This deviation may be related to the simplification of the cake-filtration model. For example the model does not include the effect of pore blocking and the layer thickness of 10 µm may not hold for all the cake layers formed with particles of different sizes. Nevertheless, the

Table 2 *Comparison of the model calculated J / J_0 values with the experimentally determined J / J_0 values for Nuclepore 0.05 μm membrane. D_p is the particle diameter.*

D_p (μm)	J / J_o	$\delta = 10^{-6}$ (m)		$\delta = 10^{-5}$ (m)	
		$\varepsilon = 0.25$	$\varepsilon = 0.36$	$\varepsilon = 0.25$	$\varepsilon = 0.36$
0.124	0.60	0.56	0.84	0.114	0.35
0.22	0.55	0.81	0.94	0.29	0.63
0.39	0.64	0.91	0.98	0.51	0.81
1.96	0.81	0.99	1.00	0.94	0.98
17	0.83	1.00	1.00	0.99	1.00
38	0.94	1.00	1.00	1.00	1.00

model calculation shows that the effect of particle size on the filtration characteristics of a membrane is important and has to be taken into consideration in the ACFF process.

Using an Amicon PM 30 membrane for a stirred dead-end filtration of particle suspensions of four different particle sizes, Fane [9] found that as particle size increased from 25 nm to 20 μm the flux passed through a minimum. This phenomenon was explained by assuming the polarization control changed from diffusive (important at small particle sizes) to non-diffusive (increasing with particle size). The diffusion and polarization effects are not considered to be important in this work using larger particles.

After addition of proteins the results for the flux behaviour is different for the too membranes (figures 3 and 4). One should keep in mind that there will be interaction between the protein molecules and the particles so the concentration what will be seen by the membrane will be smaller than in the case of the filtration of the proteins alone. For membrane A the fluxes are constant after addition of BSA. For membrane B, however, the fluxes decreased further indicating a strong interaction between membrane, protein and particles.

The results obtained sofar clearly show the importance of particle size to be chosen in an ACFF process, besides many other requirements for an ideal particle carrier. On the one hand particle size can determine flux and retention of a given membrane-protein system. On the other hand for the non-porous core-shell latices, the particle size determines the specific surface area available for protein binding. Large particles have hardly any influence

on either flux or retention. However the disadvantage of using a large non-porous particle is that a low specific surface area is available for ligand immobilization as well as for protein binding. For small particles the argumentation is reversed. Therefore, an optimal particle size should be chosen for a given ACFF process. For the system studied in this chapter the particle size of a few microns seems to be an optimum size.

5.4 CONCLUSIONS

It is found that the choice of the membrane itself is very important for filtration of protein solutions. Probably aggregates present in the crude protein solution governed the flux decline. Prefiltration of the protein solution prevents flux decline to a large extent. However, pumping the protein solution seems to alter the characteristics of the proteins: after some time aggregates are formed again resulting in flux decline.

This study makes it clear that in the ACFF process the size of the particle and the pore size of the membrane have to be optimized to give good flux and retention performance while keeping the binding capacity of the particles at a satisfactory level.

5.5 REFERENCES

1. B. Gebben, D. van Houwelingen,W. Zhang, Th. van den Boomgaard, C.A. Smolders, Colloids and Surfaces B Biointerfaces, in preparation; chapter 2 of this thesis.

2. W. Zhang, Z. Borneman, B. Gebben, Th. van den Boomgaard, C.A. Smolders, Colloids and Surfaces B Biointerfaces, in preparation; chapter 3 of this thesis.

3. J.A. Howell, M. Lojkine, M. Pritchard, in 'Chromatography and Membrane Processes in Biotechnology', Eds. C.A. Costa and J.S. Cabral, NATO ASI Series E: Applied Sci. Vol 204, Kluwer Academic Publishers, Dordrecht, 1991, pp. 237.

4. Brochure Organon Tecknika, The Netherlands.

5. H.-J. Böhme, G. Kopperschläger, J. Schulz, and E. Hofmann, J. Chromatogr., 69 (1972) 209.

6. H.D.W. Roesink, M.A.M. Beerlage, W. Potman, Th. van den Boomgaard, M.H.V. Mulder and C.A. Smolders, Colloids and Surfaces, 55 (1991) 231.

7. A.S. Chandavarkar, Ph.D Thesis, M.I.T., 1990.

8. A.G. Fane, in Progress in Filtration and Separation 4, R.J. Wakeman (Ed.), Elsevier, Amsterdam, 1986, pp. 101.

9. A.G. Fane, J. Membr. Sci., 20 (1984) 249.

6

Protein Separation Using Microfiltration
Filtration of Protein Mixtures

W. Zhang, Z. Borneman, Th. van den Boomgaard and C.A. Smolders

SUMMARY

In this study the filtration was performed of two well-characterized proteins of differing molecular dimensions, both singly and in a mixture, using two partially permeable membranes. Membranes with a hydrophilic character were chosen. The emphasis in this chapter lies on the mutual interaction between proteins and the interaction between proteins and membranes studied by performance parameters such as flux reduction and retention.

It is confirmed that the retention of BSA in the presence of IgG by membrane B is enhanced by an increasing IgG concentration. It is found that the relative flux reduction of membrane B, during the filtration of BSA and IgG solutions, is related to increased retentions in the presence of IgG. In contrast, the increase in BSA concentration does not influence the retention of IgG. Adsorption experiments reveal that both BSA and IgG do adsorb onto membrane B. The influence of IgG adsorption on flux reduction and retention is more pronounced compared to that of BSA.

For membrane C it is found that the retention of BSA and IgG increases with an increase in IgG concentration, while a slight decrease in the retention of BSA and IgG is realized when the BSA concentration is varied. The results are interpreted on the basis of a model for the protein concentrated layer adjacent to membrane surface. Since it has been experimentally proven that membrane C is basically a non-adsorptive type of membrane for both proteins used, it is concluded that the increase in retention as a function of protein concentration is solely resulting from the phenomenon of concentration polarization.

6.1 INTRODUCTION

As has been described in the previous chapters [1-3], a new separation process, Affinity Cross-Flow Filtration (ACFF), is in development for large-scale production of proteins and enzymes. In the ACFF process an affinity ligand immobilized on carrier particles is used to bind a protein of interest from a protein mixture, and the separation of the protein-bound particles from the protein mixture is accomplished by means of cross-flow filtration.

In the ACFF process proteins having dimensions in the nanometer range will be separated from particles with dimensions in the micrometer range. Both proteins and particles will interact with the membranes, and in turn, these interactions will interfere with the filtration process. Thus, it is necessary to study the filtration behavior of protein solutions and particle suspensions separately, in order to unravel their combined effect.

In literature it has been observed that for a partially permeable membrane solutes with molecular dimensions small enough to permeate the membrane freely are substantially or completely retained by that same membrane when a larger (and normally retained) solute is present [4-9]. A number of hypotheses have been proposed to explain these observations. Among these it is believed that both gel-layer formation and pore obstruction by macrosolute adsorption are responsible for major reductions in the hydraulic permeability of partially permeable membranes. Recently, it has been summarized that the hydraulic resistance formed during filtration of macrosolutes probably consists of four parts [10-12]: The first is pore narrowing or clogging due to solute adsorption on the pore walls; the second is the formation of a dense, partially denatured protein layer (with a thickness of around 100 nanometers); the third is the formation of a loosely packed concentrated protein layer with a thickness of several micrometers; and the fourth is a concentration polarization layer with a decreasing concentration profile down to the bulk solution phase. This picture has been observed not only for ultrafiltration membranes but also for microfiltration membranes [13-15]. Precisely how these four components of hydraulic resistance interact to control macrosolute transport through the "fouled" membrane remains to be demonstrated and clarified.

In previous chapters the preparation and characterization of ligand-immobilized PS core-shell latex particles (as well as agarose particles) for the application in the ACFF process have been presented, together with binding studies of proteins on the particles [1, 2]. The

first experiments with filtration of particle suspensions, in the presence and absence of protein [3], have shown that the choice of the membrane is very important for filtration of proteins and particle-protein mixtures. In the present study the filtration of two well-characterized proteins of different molecular dimensions, both as single proteins and in a mixture, using two partially permeable membranes is performed. The two membranes are hydrophilic in nature. The emphasis of this chapter lies on the aspect of the interaction between the proteins and between proteins and membranes regarding the effects on flux reduction and increase of retention.

6.2 EXPERIMENTAL

6.2.1 Materials

Two types of membranes are used in this study. Membrane B is in a hollow fiber form, and has been supplied by X-Flow B.V., The Netherlands. Membrane C is the Amicon YM-100 flat sheet membrane from Amicon Inc., USA. Bovine serum albumin (BSA) and bovine immunoglobulin G (IgG) were supplied by Organon Technika, The Netherlands. The physicochemical properties of these proteins are given in table 1.

Table 1 *Physicochemical properties of the proteins BSA and IgG*

Protein	MW (Dalton)	I.E.P.	Dimension (Å)	Refs.
BSA	69000	4.7	140 * 38 * 38	2
IgG	156000	6.8	234 * 44 * 44	2

Membrane B was characterized using a Coulter Porometer [16]. A bubble point leading to a maximum pore size of 0.08 μm was determined for membrane B. Membrane C has a molecular weight cut off value of 100,000 Dalton as given by the manufacturer. Water flux for membrane B was 1100 (l/m^2.h.bar), and 700-1000 (l/m^2.h.bar) for membrane C. The characteristics of these membranes are given in table 2.

Table 2 *Characteristics of the membranes used in this study..*

Type	Manu-facturer	Material	Pore size (μm)	Water flux ($l/m^2.h.bar$)
B	X-flow	PES&PVP blend	0.08 [a]	1,100
C	Amicon	cellulose	100,000 [b]	700-1000

a - the bubble point, i.e. maximum pore size measured by a Coulter Porometer.

b - molecular weight cut off value given by the manufacturer.

6.2.2 Protein solutions

All protein solutions were prepared in 0.067 M Sörensen phosphate buffer, pH = 7.4, ionic strength = 0.17. A known amount of protein was dissolved in a buffer solution and kept overnight in a refrigerator without stirring. The prepared protein solution was used within one day. Protein concentration was determined using a normal HPLC procedure.

6.2.3 Protein adsorption

The effect of protein adsorption is determined indirectly by measuring the relative permeate flux, i.e. the relative flux reduction of buffer solution as that used by Mattiasson [17] and Roesink *et al.* [18]. The buffer flux (J_0) was measured for each membrane. The membranes were then removed from the filtration setup and placed in a BSA solution at room temperature for 20 hours adsorption time. After the BSA adsorption the membranes were rinsed with the same buffer for 5 min, placed in the filtration setup and the buffer flux (J_1) was measured again. The buffer flux of the membranes before the adsorption experiments (J_0) was constant for at least 0.5 hour. The buffer flux after the adsorption experiments was measured after a constant value (J_1) was reached. The relative flux reduction for buffer solution: $1 - RF_b = 1 - J_1 / J_0$ is used as a measure of the effect of protein adsorption on flux reduction.

6.2.4 Filtration

The experiments of cross-flow filtration were performed using lab-made modules of membrane B with a total internal surface area of 12 cm^2. For each experiment a new module was used. The permeate was recirculated.

An Amicon stirred cell with an effective membrane area of 40 cm^2 was used for the dead-end filtration of protein solutions by membrane C. A stirring speed of 300 r.p.m. was applied unless otherwise specified. For each experiment a new piece of membrane was used.

All protein solutions in the experiments were used immediately after prefiltration with a 0.1 μm Durapore™ membrane from Millipore. The prefiltration was necessary to avoid interference by protein aggregates.

The operating pressure in the filtration system was 0.1 bar unless otherwise specified.

6.3 RESULTS AND DISCUSSION.

6.3.1 *Flux / rejection behavior of membrane B*

A set of filtration experiments for the protein mixture of BSA and IgG was carried out using membrane A to study the interactions between the membrane and the proteins. In these experiments protein concentrations were arranged in such a way that for one protein the bulk concentration varied while for the other it was kept constant. This enables one to find the influence of concentration of a particular protein on flux / rejection behavior of the membrane for another protein.

The results of such an experimental set up start with a study of the time effect on flux and retention. In figure 1 results are given for a protein concentration of 0.5 g/l for BSA and 0.86 g/l for IgG. The flux decreases in time and tends to level off within 2 hours. The retention for both BSA and IgG increases during the filtration process, and also levels off within 2 hours filtration time. It is evident that interactions occur during the filtration process with the protein mixture of BSA and IgG. It is noted that the retention values for BSA and IgG are close to each other. The type of fouling on this membrane will be discussed later on.

To illustrate the influence of the concentration of a larger-sized protein on the retention of a smaller particle, the retention values for BSA, taken at the end of each filtration experiment i.e. after 2 hours, together with the retention for IgG, as a function of the IgG concentration were plotted in figure 2. It is demonstrated that the retention for BSA increased with an increase of the IgG concentration. These results are consistent with those of prior investigators [4, 7]. It is noted again that the retention for BSA is close to that for
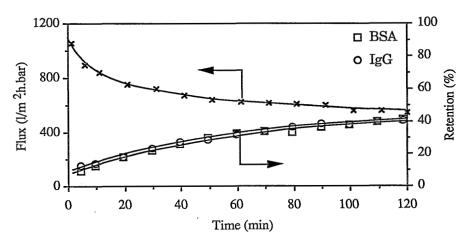
Fig. 1 Flux and retention for membrane B with a protein mixture of 0,5 g/l BSA and 0.86 g/l IgG, as a function of time.
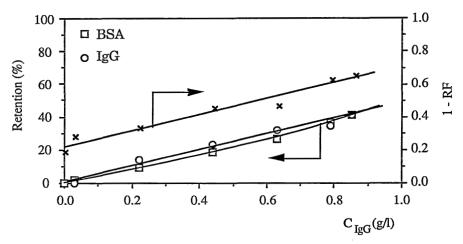

Fig. 2 Retention coefficient and relative flux reduction for membrane B, during the filtration of protein mixtures, as a function of the IgG concentration in the feed with a fixed 0.5 g/l BSA concentration.

IgG despite the difference in molecular size between the two proteins.

The increased retention for BSA as a function of the IgG concentration in the feed mixture can be explained by the effect of pore narrowing due to the interaction between

IgG molecules and membrane B. Concentration polarization should also be taken into consideration in such a case. However the effect of protein adsorption on the increase of hydrodynamic resistance can be much larger than the effect of concentration polarization when the pore size of a membrane is in the same order of magnitude as that of the proteins. In other words the effect of concentration polarization becomes negligible in such a situation. To support this hypothesis the relative flux reduction, 1 - RF, as a function of the IgG concentration is also examined. The term 1 - RF used here is defined as $1 - J_f / J_0$, where J_0 is the buffer flux and J_f is the flux at the end of the filtration process with the actual protein solution consisting of the two proteins. This solution flux reduction is a lumped parameter, which involves both the effects of concentration polarization and protein adsorption / deposition, and it differs from the buffer flux reduction which only takes protein adsorption or deposition into account. The results of the relative flux reduction are given in figure 2. The increase of the relative flux reduction follows the same trend as the increase in retention of the proteins. The two parameters may be correlated as a result of pore narrowing by protein adsorption on the pore wall of the membrane (see further on).

The filtration experiments were also carried out with a fixed IgG concentration while BSA concentration was varied. The results are given in figure 3. It is clearly shown in
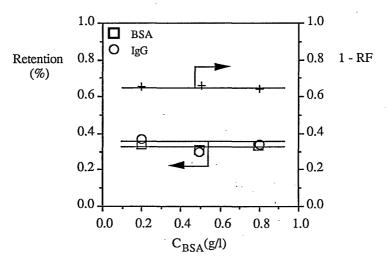

Fig. 3 The retention coefficient and (1 - RF) for membrane B as a function of the BSA concentration in the feed with a fixed 0.5 g/l IgG concentration.

figure 3 that the fluxes and the retentions for both proteins are essentially constant and not dependent on the variation of the BSA concentration applied. This result in combination with that given in figure 2 indicates that the presence of IgG is important regarding the flux reduction and the increased retention. Both flux and retention in figure 3 are obtained using a different batch of membrane B with a higher buffer flux than that used before. The buffer flux of this batch of membrane B is in the range of 1600 to 2000 ($1/m^2$.h.bar) and the membrane is only used for obtaining the data in figure 3. The observed higher flux reduction and higher retention for this membrane in comparison to those used earlier may result from the increased hydrophobicity of the membrane surface leading to a larger protein adsorption. The increased hydrophobicity is possibly caused by the different post-treatment procedures as has been described by Roesink *et al* [18].

For the purpose of comparison the effect of stationary adsorption of the proteins separately on the relative flux reduction for buffer (1 - RF_b), as defined in literature [17], was investigated. The influence of protein adsorption on flux reduction of the membrane showed a concentration dependence for both proteins (figure 4). It is noted that BSA adsorption gives less influence on flux reduction compared to IgG adsorption. Direct comparison of the flux reduction given in figure 4 with that given in figure 2 is not allowed because the former is purely a result of stationary adsorption whereas the latter involves hydrodynamic factors in the filtration process. Also figure 2 represents data for protein
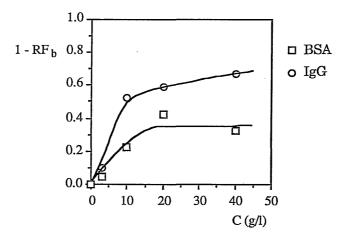

Fig. 4 The relative flux reduction of membrane B upon adsorption of the proteins separately determined for the buffer solution.

mixtures. Still the results shown in figure 4 can be useful for the interpretation of the flux reduction shown in figure 2 because it gives an indication to which extent protein adsorption may influence the filtration flux and by which protein. The one which has the higher affinity to the membrane will adsorb more, and consequently may contribute more to the effect of pore narrowing.

From these joint experiments it is evident that IgG interacts with membrane B whereas BSA interacts to a less extent. We conclude that IgG adsorption is essentially responsible for the increased retention and flux reduction during the filtration with the protein mixture.

The stationary adsorption experiments were also carried out with protein mixtures for 2 hours adsorption time. The results of the flux reduction ($1\text{-}RF_{b.m}$) with different IgG concentrations at a fixed BSA concentration are shown in figure 5 a, and the results with different BSA concentrations at a fixed IgG concentration are given in figure 5 b. For reasons of comparison the flux reductions during the filtration experiments are again presented in figure 5. Both figures show that the flux reduction originated from stationary adsorption of protein mixtures at low concentrations (bulk concentration during the
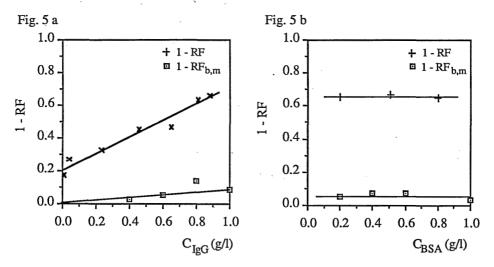

Fig. 5 a

Fig. 5 b

Fig. 5 Relative flux reduction ($1\text{-}RF_{b,m}$) measured for buffer solutions for membrane B upon adsorption of protein mixtures, together with ($1 - RF$) values measured during the filtration of protein mixtures. BSA and IgG concentrations are fixed at 0.5 g/l in figure 5 a and in figure 5 b respectively.

filtration process) on membrane B account for not more than ten percent of the total flux reduction. This suggests that the total flux reduction must result from a combined effect of protein adsorption and concentration polarization during actual filtration. Protein adsorption is in general concentration dependent. Concentration polarization accumulates rejected solutes, resulting in a higher concentration at the membrane surface than in the bulk solution. Therefore for a partially permeable membrane in a filtration process protein adsorption will occur, narrowing the pore size of the membrane. Concentration polarization will then be enhanced generating a higher protein concentration at the membrane surface for further protein adsorption.

It is observed in figures 2 and 3 that the retention for BSA is very close to that for IgG when the two proteins are present in a mixture. Assuming that the sieving effect is the mechanism causing the different retentions, IgG should show higher retention in comparison with BSA since the molecular size of IgG is larger than that of BSA. In the filtration experiments with single proteins membrane B showed less than 10 % retention for a 0.5 g/l BSA solution, and 60 - 70 % for a 0.4 g/l IgG solution. When only IgG is present in solution pores at the membrane surface will probably be narrowed severely due to IgG adsorption. The situation can be different when both BSA and IgG are present in a solution because BSA will also adsorb to the surface although to a smaller extent in comparison with IgG. Therefore the effect of pore narrowing will possibly become less severe than the case when only IgG is present. Consequently, the retention for IgG may be lowered compared to the case of single IgG. For BSA the retention rises mainly due to the effect of pore narrowing by IgG adsorption [19].

To gain an insight into the flux/retention behavior of membrane B, Hagen-Poiseuille's equation and Ferry's law were applied to estimate the relative flux reduction and the retention as a result of pore narrowing through adsorbed protein.

The Hagen-Poiseuille equation can be expressed as:

$$J = \frac{\varepsilon}{8} \frac{r^2}{\eta\ l} \frac{\Delta P}{\tau} \tag{1}$$

where J is the permeate flux through a cylindrical pore, ε is the surface porosity, r is the pore radius, ΔP is the transmembrane pressure, η is viscosity of the feed, l is the thickness of the active porous layer of a membrane and τ is the totuosity of the pores and is assumed to be one.

Ferry's law can be given as [20]:

$$R = 1 - 2(1 - \lambda)^2 + (1 - \lambda)^4 \qquad (2)$$

where R is the retention coefficient and λ is the ratio between particle size and pore size. This equation must be applied to a pore narrowing situation through protein adsorption which results in a partial or entire monolayer coverage on the pore wall.

From SEM, membrane B appears to have an active layer of 1 μm in thickness and a porosity of around 5%. Using these data together with the buffer flux of 1100 (l/m^2.h.bar), the average pore size of the membrane, calculated using the Hagen-Poiseuille equation, is 44 nm in diameter.

To use Ferry's law we must know the size of the particles; therefore the equivalent diameter of BSA and IgG is calculated using the Stokes-Einstein equation with the diffusivity of $6.9 * 10^{-11}$ (m^2/s) [21] for BSA and $4.0 * 10^{-11}$ (m^2/s) for IgG [22], resulting in a diameter of 6 nm for BSA and 11 nm for IgG. These data are then used in the evaluation of the relative flux reduction and the retention of the two proteins as a function of pore narrowing. Equation 1 (Hagen-Poiseuille) and equation 2 (Ferry) should be applied to membrane pores getting narrower through an increase in adsorption of IgG and BSA (especially IgG). This adsorption causes a decrease in the effective pore radius r and thus an increase in Δr which is defined as the variation in pore radius r caused by protein adsorption at the pore wall. When both proteins are present IgG will adsorb more stronger; so Δr is between 0 and 11 nm. For assumed values of Δr and effective pore radius ($r - \Delta r$) one can then calculate the filtration flux J_f, and 1 - RF and R for two particle sizes (IgG and BSA). In this way a curve like figure 6 is calculated. Figure 7 is a combination of the data from figure 6 (calculation) and figure 2 (experiments). As shown in figure 7, most of the experimental data are falling between the theoretical curves for BSA and IgG. This result implies that the effect of pore narrowing by protein adsorption on the wall of the membrane is responsible for the flux-retention behavior observed. The difference between the experimental results and the calculated data for the lower part of the plot in figure 7 may be due to the clogging of a few large pores.

6.3.2 Flux / rejection behavior of membrane C

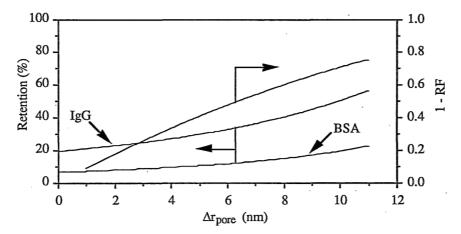Membrane C is a typical hydrophilic membrane. The filtration experiments, using

Fig. 6 The calculated retention coefficient and the relative flux reduction as a function of the pore narrowing factor Δr for membrane B, which results from an increasing IgG and BSA adsorption on the pore wall.
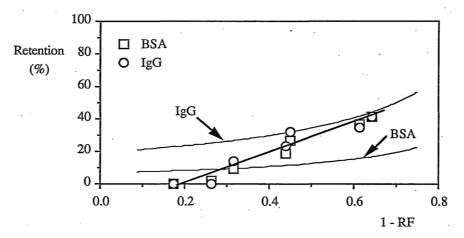

Fig. 7 Plots of retention coefficient versus relative flux reduction for the experimental results of membrane B and curves obtained by calculation.

membrane C with varied concentrations for one protein while constant for the other, were carried out to compare the results with membrane B. However, as mentioned before, the configuration is different in the two cases.

When filtration experiments were carried out using single protein solutions, membrane

C shows a few percent retention for BSA and around 70 % for IgG at a 0.5 g/l concentration, as can be seen in figure 8. The filtration fluxes are also shown in figure 8. The flux for BSA solution is nearly constant whereas the flux for IgG solution shows a decline. These results indicate that membrane C is retentive to IgG but almost not retentive
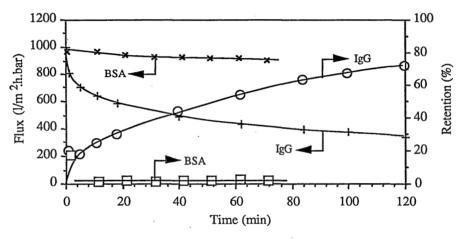

Fig. 8 Flux and retention as a function of time for membrane C with a 0.5 g/l single protein solution for BSA and IgG, respectively.

to BSA. However, when both proteins are mixed together as a feed, membrane C becomes retentive also to BSA. A typical example of such an experiment is shown in figure 9, in which the protein concentration in the feed was 0.5 g/l for BSA and 0.8 g/l for IgG. The retention for both BSA and IgG shows an increase in time during the filtration process, whereas a flux decline was observed in the mean time. After 2 hours of filtration time, the flux tends to level off.

A set of the results of the retention coefficients for both BSA and IgG, taken after 2 hours of filtration time, as a function of the IgG concentration are plotted in figure 10. In these experiments the BSA concentration was fixed at 0.5 g/l. It is clearly shown in figure 10 that the retention for both BSA and IgG increases with an increase of the IgG concentration in the feed. Logically, the relative flux reduction also follows the same trend. These results seem to suggest that the presence of IgG causes the increase of the retention for BSA. It is thought that these increases both in the retention coefficient and in the relative flux reduction are caused by concentration polarization as will be discussed below.
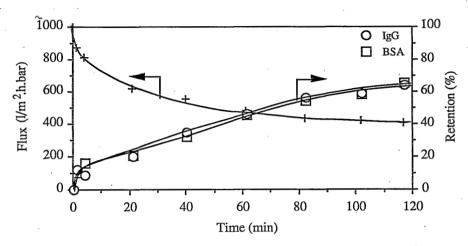
Fig. 9 Flux and retention as a function of time for membrane C with a protein mixture of 0.5 g/l BSA and 0.8 g/l IgG.
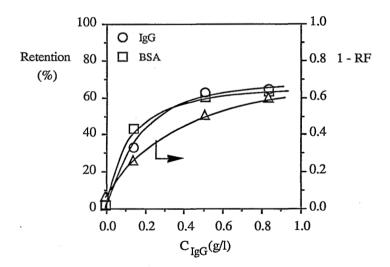

Fig. 10 Retention coefficient and relative flux reduction for membrane C, during the filtration of protein mixtures, as a function of the IgG concentration in the feed with a fixed 0.5 g/l BSA concentration.

To get further insight into the retention and flux behavior of membrane C the filtration experiments were also carried out with a fixed IgG concentration of 0.5 g/l while the BSA concentration varied. The results are given in figure 11. It can be seen in figure 11 that the
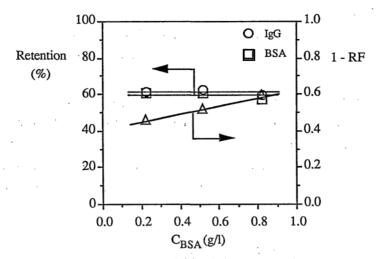
Fig. 11 Retention coefficient and relative flux reduction for membrane C, during the filtration of protein mixtures, as a function of the BSA concentration in the feed with a fixed 0.5 g/l IgG concentration.

retention for both proteins is nearly constant regardless of the increase of the BSA concentration, while the relative flux reduction shows an increase as the BSA concentration increases. This result is similar to the observation on membrane B, in which the retentions for BSA and IgG were not affected at all by the variation of the BSA concentration as shown in figure 3 although the mechanisms behind these results can be very different from each other. This retention behavior will be discussed below.

It is interesting to compare the different behavior in retention of BSA and IgG with varied IgG concentration between membrane B and membrane C. For the case of membrane B IgG adsorption is essentially responsible for the increased retention as has been discussed above. For membrane C it has a different story. Membrane C must be a non-adsorptive type of membrane to both BSA and IgG. This is shown by the following examples: For a sample of membrane C, after contact with a BSA solution of 0.5 g/l concentration, the buffer flux maintained the same level as for a fresh membrane. In a successive filtration experiment with a 0.5 g/l BSA solution, the flux did not show any decrease. The same experiments for membrane C with IgG solution did not show any influence of IgG contact on flux. Therefore, these results bring us to the conclusion that

membrane C is non-adsorptive to BSA and IgG at least in the range of the protein concentrations studied.

When adsorption of the proteins on membrane C is excluded as the cause of rising retention, concentration polarization comes into consideration. Since concentration polarization is sensitive to cross-flow velocity, a successive experiment of filtration of a protein mixture with the same concentration of 0.5 g/l for both BSA and IgG was performed at different stirring velocities with a constant pressure of 0.1 bar. The stirring velocity was changed in a sequence of four steps from zero to 500 r.p.m. The results of flux and retention as a function of time, after preconditioning of the membrane with the protein solution for one hour, are given in figure 12. The fluxes and the retentions for both
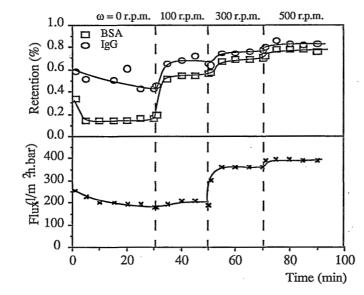

Fig. 12   Flux and retention as a function of time for membrane C with a protein mixture of 0.5 g/l BSA and 0.5 g/l IgG under four different stirring velocities (successive measurements).

BSA and IgG, taken at the end of each step, are also plotted against Reynolds number R_e as is shown in figure 13. For a stirred cell R_e is given as [23]:

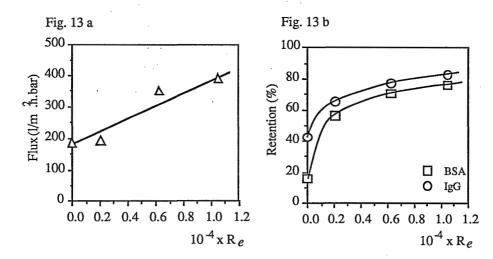$$R_e = \frac{\omega\, b^2}{\nu} \tag{3}$$

Fig. 13 a

Fig. 13 b

Fig. 13 Flux and retention as a function of the stirring velocity for membrane C with a protein mixture of 0.5 g/l BSA and 0.5 g/l IgG.

where ω is stirring velocity, b is the radius of the membrane used in the cell and ν is kinematic viscosity. It is observed from the two figures that the fluxes and the retentions for both BSA and IgG increase when stirring velocity increases. The increase in flux can be attributed to the reduced boundary layer thickness, and thus, the reduced filtration resistance by increasing stirring velocity. The effect of stirring velocity on retention may be two fold: the increase in flux may enhance protein penetration through the membrane, resulting in a decrease in retention; on the other hand, the increase of stirring velocity lowers the protein concentration at membrane surface C_w, resulting in an increase in retention [19]. The results of the increased retentions with an increase of stirring velocity suggest that the reduction of concentration polarization seems to have a more pronounced effect on the observed retention, while the flux-associated protein penetration seems to be less important. These results show clearly the influence of concentration polarization.

For unstirred ultrafiltration concentration polarization versus time can be described by a simple relationship between flux J and filtration time t as:

$$J = A * \frac{1}{\sqrt{t}} \qquad (4)$$

where A is a constant for a certain system. This relationship can be derived from either the

osmotic pressure model, the film model or the cake filtration model [24-26]. In an attempt to give a further support to the point that concentration polarization is the dominating factor when membrane C is used in the filtration experiments as mentioned above, an unstirred filtration experiment was performed with a protein solution of 0.8 g/l BSA and 0.2 g/l IgG. The results are analyzed using equation 4, and plotted as J^{-2} versus t in figure 14. It is clearly shown in figure 14 that the linear relationship does exist between the squared
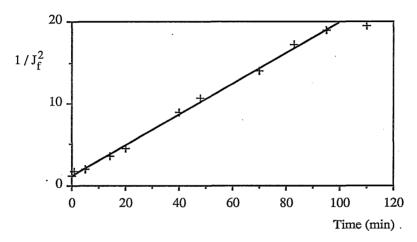

Fig. 14 The reciprocal flux (squared) as a function of time during the unstirred filtration experiment with a protein solution of 0.8 g/l BSA and 0.2 g/l IgG at a constant pressure 0.1 bar.

reciprocal flux and filtration time. Another experiment was carried out with a protein solution of 0.5 g/l BSA and 0.5 g/l IgG and the same type of membrane, with and without stirring during the filtration process. The results are shown in figure 15. The linear relation between J^{-2} and t shows up, and it appears to be valid at each level of stirring. A few data points fell in between the lines due to the transition from one stirring speed to another. According to these examples it can be concluded that the flux behavior of membrane C is mainly affected by the effect of concentration polarization.

Since membrane C is retentive to IgG but not to the same extent to BSA, a model of a protein-concentrated layer may be proposed to explain the retention behavior of membrane C mentioned above. For an ultrafiltration membrane which has a high retention to a macromolecule, it has been shown that concentration polarization is a fast process, e.g. C_w
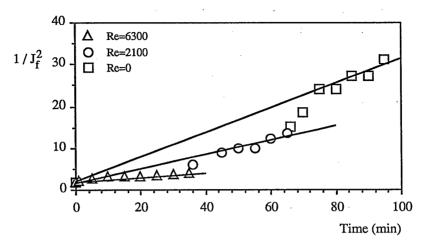
Fig. 15 The reciprocal flux (squared) as a function of time for different Reynolds number R_e which were changed in sequence during the filtration experiment with a protein solution of 0.5 g/l BSA and 0.5 g/l IgG at a constant pressure 0.1 bar.

may reach a plateau value in a matter of a few seconds [19, 21, 27]. Membrane C is not totally retentive to IgG so that the time needed to reach a plateau value of C_w may be longer than a few seconds. Still IgG molecules may be retained by the membrane much better than BSA molecules, and this results in a more concentrated IgG layer (not yet to be a gel layer) adjacent to the membrane surface. Such a IgG-concentrated layer will raise the resistance considerably towards the penetration of BSA molecules. Consequently the relative flux reduction and the retention for the two proteins increase with an increase in the IgG concentration, as shown in figure 10. When BSA concentration varies at a fixed IgG concentration the situation is different. The IgG-concentrated layer can be hardly influenced by the change of the BSA concentration. Therefore, the retention for BSA and IgG does not change when BSA concentration increases as is shown in figure 11. However an increase in the BSA concentration does result in an increase in the relative flux reduction because of the increase in the total protein concentration in the boundary layer near the membrane interface.

In the ACFF process carrier particles with affinity ligand immobilized have to be used in cross-flow filtration for the selective separation of a particular bound protein from a protein mixture. In this study it is clearly shown that an ultrafiltration membrane is not an appropriate choice for the ACFF process because a partial retention of one large protein

may result the formation of a concentrated layer which acts as a barrier to the non-rejected protein. To make the situation worse, the performance of a selected membrane may be modified by the carrier particles through deposition, which may in turn raise the retention for large protein molecules although the membrane itself does not show retention to any type of the proteins involved in the ACFF process.

6.4 CONCLUSIONS

It is confirmed that the retention of BSA by a membrane can be influenced by the variation of the IgG concentration. It is found that the relative flux reduction of membrane B, during the filtration of BSA and IgG solutions, is related to the increased retentions as a function of IgG concentration. In contrast, the increase of BSA concentration does not influence the retention of IgG. Adsorption experiments reveal that both BSA and IgG adsorb onto membrane B. The influence of IgG adsorption is more pronounced compared to that of BSA. Consequently, it is concluded that IgG adsorption on membrane B dominates the performance of this membrane.

Membrane C is a typical hydrophilic type of membrane. Therefore, it is expected that this membrane behaves differently in comparison with membrane B. Indeed, in the experiments it is found that the flux and the retention for both BSA and IgG is influenced by the variation of either IgG concentration or BSA concentration in the feed. The variations in shearing flow velocity change both flux and retention behavior of the membrane. Therefore, it is concluded that the changes of the retentions as a function of protein concentration solely results from concentration polarization.

According to this study it is preferred to use microfiltration membranes rather than ultrafiltration membranes in the ACFF process.

6.5 REFERENCES

1. Gebben B., D. van Houwelingen,W. Zhang, Th. van den Boomgaard, C.A. Smolders, Colloids and Surfaces B Biointerfaces, in preparation; chapter 2 of this thesis.
2. Zhang W., Z. Borneman, B. Gebben, Th. van den Boomgaard, C.A. Smolders, Colloids and

Surfaces B Biointerfaces, in preparation; chapter 3 of this thesis.

3. Chapter 5 of this thesis.

4. W.F. Blatt, A. Dravid, A.S. Michaels and L. Nelson, in "Membrane Science and Technology", J.E. Flinn (Ed.), Plenum Press, New York, NY, 1970, pp. 47.

5. K.C. Ingham, T.F. Busby, Y. Shahlestrom and F. Castino, in "Ultrafiltration Membranes and Applications", A.R. Cooper (Ed.), Plenum Press, New York, NY, 1980, pp.141.

6. H.J. Gurland, M.J. Lysaght, W. Samtelben and B. Schmidt, Nephron, 36 (1984) 173.

7.   U.R. Shettigar, H. Mann and A. Gressner, Artificial Organs, 6 (1982) 163.

8. C. Charcosset, M.Y. Jaffrin and L.H. Ding, J. Membr. Sci., 60 (1991) 87.

9. J.L. Nilsson, J. Membr. Sci., 52 (1990) 121.

10. A.D. Marshall, P.A. Munro and G. Trägårdh, Desalination, 91 (1993) 65.

11. A.G. Fane and J.M. Radovich, in "Separation Processes in Biotechnology", J.A. Asenjo (Ed.), Marcel Dekker, Inc., New York, NY, 1990, pp. 209.

12. W.S. Opong and A.J. Zydney, J. Colloid Interface Sci., 142 (1991) 41.

13. R.M. McDonogh, H. Bauser, N. Stroh and H. Chmiel, Chem. Eng. Sci., 46 (1991) 271.

14. S.P. Palecek, S. Mochizuki and A.L. Zydney, Desalination, 90 (1993) 147.

15. P. Heinemann, J.A. Howell and R.A. Bryan, Desalination, 68 (1988) 243.

16. K. Venkataraman, W.T. Choate, E.R. Torre, R.D. Husung, J. Membr. Sci., 39 (1988) 259.

17. E. Matthiasson, J. Membr. Sci., 16 (1983) 23.

18. H.D.W. Roesink, M.A.M. Beerlage, W. Potman, Th. van den Boomgaard, M.H.V. Mulder and C.A. Smolders, Colloids and Surfaces, 55 (1991) 231.

19. R.W. Baker and H. Strathmann, J. Appl. Polym. Sci., 14 (1970) 1197.

20. J.D. Ferry, J. Gen. Physiol., 20 (1936) 95.

21 G.B. van den Berg and C.A. Smolders, J. Membr. Sci., 40 (1989) 149.

22 A.V. Elgersma, PhD Thesis, Agricultural University of Wageningen, 1990.

23. B.D. Mitchell and W. M. Deen, J. Colloid Interface Sci., 113 (1986) 132.

24. M.W. Chdacek and A.G. Fane, J. Membr. Sci., 21 (1984) 145.

25. D.R. Trettin and M.R. Doshi, Ind. Eng. Chem. Fundam., 19 (1980) 189.

26. V.L. Vilker, C.k. Colton and K.A. Smith, AIChE J., 27 (1981) 637.

27. J.A. Howell and O. Velicangil, in "Ultrafiltration Membranes and Applications", A.R. Cooper (Ed.), Plenum Press, New York, 1980, pp. 217.

7

The Affinity Cross-Flow Filtration Process:

Membrane Aspects

W. Zhang, Z. Borneman, Th. van den Boomgaard and C.A. Smolders

SUMMARY

Downstream processing for protein purification is increasingly receiving interest in the commercialization of biotechnology for the tasks of producing proteins and enzymes in large quantity and with high purity. A novel separation process, Affinity Cross-Flow Filtration (ACFF), is being developed to meet this challenge. The ACFF process takes the advantage of high resolution from affinity adsorption and of large processing capacity in a continuous way from cross-flow filtration. Due to the formation of an affinity complex with a ligand-immobilized carrier particle, the protein of interest will be retained, while other proteins will be washed out. In the successive process step the target protein will be released by desorption. In this way the protein of interest is purified.

Both batch and continuous processes with a variety of carrier particles and ligand-ligate systems have been studied by others for the ACFF process. Most of the studies were focused on recovery and purity of the target proteins as the final product of the process. Relatively little has been done on the membrane side of the process. Filtration rate was regarded as the limiting factor in the ACFF process with respect to binding/dissociation kinetics. A new initiative is to use a non-porous core-shell latex particle to facility diffusion processes. In this study it becomes evident that by selecting a proper combination of protein/carrier particle/membrane it is possible to avoid the problem of flux decline during the separation process.

7.1 INTRODUCTION

Protein purification is an important step in the commercialization of biotechnology which not only aims at producing large quantities of purified proteins and enzymes but also

with high purity. With the advance of purification science, substantial progress has been made in using the affinity binding technique both in analytical and in large scale separation of proteins. This technique offers a high degree of specificity and provides an efficient extraction of a single product from a complex mixture typically formed in bioprocessing. Affinity chromatography, which was developed based on this principle, has become one of the most widely used protein purification procedures to deliver a product with a high purity and a good overall yield. This method, however, has several disadvantages that can hamper its application in large scale operation and will restrict its use to very costly products. These disadvantages are those associated with its low productivity, difficulty in scaling-up and in continuous operation [1].

Over the last decade, impressive advances have been made by subtly using affinity interaction in a different mode to solve the problems faced in affinity chromatography while providing products of the same degree of purity. Affinity cross-flow filtration (ACFF) is one of the most widely investigated novel affinity protein purification methods and has proven to be highly promising as an alternative process for affinity chromatography in downstream processing [2-7]. As the name suggests, the ACFF process combines the affinity adsorption technique with the cross-flow filtration process. Therefore, in principle, the ACFF process is capable to overcome the disadvantage of low throughput associated with the affinity adsorption process. A variety of carrier particles (or macroligands) has been used, including yeast cells, starch granules, agarose beads, dextran polymer molecules and unilamellar vesicles. Of importance in designing the carrier particles are: i) optimizing the specific surface area available for affinity binding; ii) minimizing non-specific binding of biomolecules to the carrier particles; iii) controlling the ligand density on the surface of the carrier particles.

Both batch and continuous processes have been studied for the ACFF process. Mattiasson and coworkers successfully used several types of carrier particles, e.g. heat-killed yeast cells, starch granules and silica nanoparticles, in the separation of a number of enzymes from crude extracts [8-11]. Luong et al. purified trypsin from chymotrypsin using a polymeric macroligand in a batch process with UF membranes with 90 % yield and 98 % purity [12-14]. A 45 % yield is obtained for the continuous process [15]. Choe et al. have also used starch granules and dextran to form the basis for carrier particles [16]. More recently, Herak and Merrill studied the ACFF process experimentally and theoretically with several target protein/ ligand pairs, e.g. HSA (and lysozyme)/Cibacron

Blue, IgG/Protein A and Horseradish Peroxidase/Concanavalin A [17, 18]. Their modeling work on the purifying stage of the ACFF process indicates that the question of release of target protein during the washing step is better represented by a model where no bound protein is released from the carrier particles than the one using an equilibrium hypothesis. Generally speaking, the observed slow kinetics of adsorbate release during the washing step should be applicable for most other systems as well. In most studies it was found that the target protein can be recovered in high purity while the biological activity is retained.

Although a number of investigations have been done for the development of the ACFF process, relatively little was said on the role of membranes in the ACFF process and its impact on the selection of carrier particles. Using a synthetic water-soluble, high molecular weight polymer (> 100,000 daltons) having an acrylamide backbone and side groups of aminobenzamide, which have an affinity for trypsin, Luong *et al.* found a retention coefficient for trypsin of more than 90 % during the purifying stage by a membrane with a MWCO value of 100,000 [15]. Mattiasson and co-workers performed a separation using an affinity carrier based on fumed silica with a diameter of 12 nm, which possesses a high specific surface area for ligand immobilization comparable to that of chromatographic beads. They pointed out that the limiting factor was the filtration rate, which could imply the occurrence of concentration polarization and/or fouling on the membranes used during the process [11].

In earlier chapters [19, 20] the preparation of core-shell latex particles with specific groups, and the adsorption characteristics of the functionalized particles, have been reported. Non-porous particles are thought to be a right choice for the ACFF process. The binding capacity will be not controlled by diffusion but merely by convection process. For reasons of comparison results are also given for porous agarose particles. A group specific ligand, Procion Blue HB™ which is a commercial name of well-known Cibacron Blue F3G-A, was chosen for this study. Bovine serum albumin (BSA) and bovine serum immunoglobulin G (IgG) were chosen as model proteins in this study. It is known from literature that the ligand has a high affinity for BSA and intermediate affinity for IgG [21]. The filtration behavior of particle suspensions in the presence or absence of protein, and the filtration behavior of protein mixtures using both adsorptive and non-adsorptive types of membranes have been demonstrated in chapter 5 and 6. In this chapter emphasis will be laid on the use of nonporous particles and membrane aspects in the ACFF process.

The ACFF process was carried out in a discontinuous mode with the BSA-IgG-

Cibacron Blue model system. As carrier particles both core-shell latex particles and agarose particles were tested.

7.2 EXPERIMENTAL

7.2.1 Materials

Bovine serum albumin (Boseral pur™, 40030) and bovine immunoglobulin G (Bovine Gamma Globulin™, 41979) were kindly supplied by Organon Teknika, The Netherlands.

The core-shell PS latices have been described in detail in Chapter 2 [19].

Superose 6 prep grade™ was purchased from Pharmacia LKB, Sweden and used as an example of a porous particle. The ligand-coupled Superose (cited as BS) was prepared according to the procedure described by Böhme [22]. The number average particle size of the BS particles, determined by SEM, was 17 μm.

The column material Protein G Sepharose 4 Fast Flow™ was obtained from Pharmacia LKB, Sweden. A Waters' HPLC system (Waters, U.S.A.) with UV detection was used for the determination of protein concentrations at 214 nm. The size exclusion columns, Shodex™ W803F, were also from Waters, U.S.A..

Three types of membranes are used in this study. Membrane B is the X-flow 0.2 ™ membrane in hollow fiber form, Membrane D is the X-flow 0.4 μm hollow fiber membrane; both have been supplied by X-Flow B.V., The Netherlands. Membrane E is PALL LoProdyne™ 3 μm flat sheet MF membrane obtained from Pall BioSupport Corp., U.S.A.. The characteristics of the membranes, determined by a Coulter Porometer and the measurements of water permeability, are represented in table 1.

7.2.2 Protein solution

Protein powder was dissolved in a 0.067 M Sörensen phosphate solution, pH = 7.4, ionic strength = 0.17 (without vehement stirring) for about 16 hours before use. The protein solution was stored at 4 °C. Just before use the solution was stirred for a short period of time (5 minutes). This procedure was followed in order to prevent shear induced aggregates [16]. The prepared protein solution was used within one day. All the protein solutions in the experiments were used immediately after a prefiltration with a Millipore Durapore 0.1 μm membrane to prevent interference from eventual aggregates present [23].

Table 1 *Characteristics of the membranes determined by a Coulter Porometer and by measurements of water permeability.*

Type	Manu-facturer	Material	Pore size (μm)			Water flux
			Min	Max	Mean	(l/m^2.h.bar)
B	X-flow	PES & PVP blend	ND	0.08	ND	1,100
D	X-flow	"	0.21	0.38	0.31	12,000
E	Pall	Nylon 66	1.9	3.0	2.4	71,000

ND - Not detectable.

A Waters' HPLC system with UV detection was used for the determination of the protein concentration at a wavelength of 214 nm. Protein analysis for the mixture of BSA and IgG was performed in such a way that a Protein G Sepharose 4 Fast Flow™ column was used to remove IgG from the solution and the BSA concentration was then measured. The IgG concentration was obtained by subtracting the part that was contributed by the BSA concentration from the total peak height, determined with a Shodex™ column.

7.2.3 Filtration apparatus

The lab-made modules for membrane B and D were used for the ACFF experiments. The module for membrane B contains 16 fibers with an inner diameter of 0.15 cm and a length of 31 cm, having a total surface area of about 230 cm^2. The module for membrane D contains also 16 fibers with an outer diameter of 0.25 cm and a length of 31 cm, having a total surface area of about 390 cm^2. The average operating pressure was 0.3 bar for membrane B, 0.1 bar for membrane D and E. The aim of using low operating pressure is to limit severe concentration polarization or deposition of the proteins which may otherwise occur on the membrane surface during the filtration process.

A Minitan™ cross-flow module from Millipore, with a surface area of 36 cm^2 (excluding the surface area occupied by the rubber separator), was used for the ACFF experiments with membrane E.

7.2.4 The stages of the ACFF process

The four stages of the ACFF process, affinity binding, purification, dissociation and

product recovery, cited as stage I to IV respectively, were performed successively using one experimental set-up. In the beginning of the experiments a mixture of 250 mg BSA and 250 mg IgG was loaded into the system with a processing volume of 550 ml for membrane A and 500 ml for the other membranes, containing 0.067 M phosphate buffer. The permeate was recirculated back to the feed in the cross-flow filtration system for about one hour. The samples were taken both in the feed and in the permeate for protein analysis. After one hour of recirculation of the protein solution, stage I starts with the addition of the ligand-coupled particles. The permeate was recirculated for another hour and samples were taken for the concentration analysis. For the samples taken from the feed side a Millipore Ultrafree™ filter was used to remove the particles prior to the HPLC analysis.

In stage II the diafiltration process was performed in which the permeate is discharged from the filtration system while phosphate buffer supplied with a peristaltic pump controlled by a level-controlling device is used to wash out unbound protein. This stage ends when at least a 5 times volume displacement of the processing volume was achieved.

In stage III, a solution of 20 mM sodium octanoate (by the addition of 11 ml of 1 M sodium octanoate solution) was established to dissociate the bound BSA. After addition of the dissociation solution the permeate was recirculated in the system for one hour to allow the dissociation process to come to completion. Then, in stage IV. the system was operated in a diafiltration mode to remove the dissociated BSA.

7.3 RESULTS AND DISCUSSION

As mentioned above the experiments for the batch operation of the ACFF process was performed in a sequence of the stages from stage I to stage IV using different membranes. Both core-shell latex particles and agarose particles were tested in the experiments. In the first section the results for agarose particles with three different membranes are presented as case studies (case 1 to 3 according to the membranes used). In case 1 the results for each stage of the experiments are given separately and in more detail, and then summarized into one plot to give a general impression of the process. In the following cases, only the summarized plots for all the stages are presented for reasons of ease of comparison. The results for core-shell latex particles are given in the second section.

7.3.1 Use of agarose particles

In case 1 the first membrane which has been used for the experiments was membrane B. Since this membrane has a mean pore size typically between ultrafiltration and microfiltration, it serves as a good example in testing the criteria for the selection of a proper membrane to be used in the ACFF process.

Flux decline together with changes in protein concentration in time, in stage I, are shown in figure 1. The flux decreased dramatically when the protein solution was loaded into the system(the first phase). Only a slight extra decrease could be observed when the particles were added into the system. The changes in the protein concentration given in figure 1
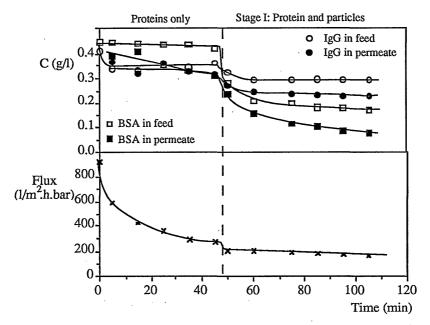

Fig. 1 Flux decline and changes in protein concentration in stage I of the ACFF process using membrane B with the BS particles (BS 17 μm).

show the difference of the adsorption and/or the deposition of the proteins on the membrane surface (in the first phase) and on the particles (in the second phase). As can be seen in figure 1, the BSA concentration in the feed hardly changed in the first phase, but a drastic decrease occurred upon the addition of the particles. This sharp decrease can be

attributed to the affinity binding of BSA on the particles. The IgG concentration dropped quite a bit within a few minutes after IgG was loaded into the filtration system. In the second phase, however, only a small extra decrease of the IgG concentration could be observed upon the addition of the particles.

It was found that the proteins were rejected by the membrane to some extent during the filtration process. A separate study reveals that IgG adsorption onto the membrane resulted in a increased retention (see chapter 6). This membrane is an adsorptive type for both BSA and IgG, and IgG tends to adsorb more strongly than BSA when both are present.

The changes in protein concentrations in stage II (washing) are shown in figure 2. A general impression is that all the unbound protein molecules are washed away provided
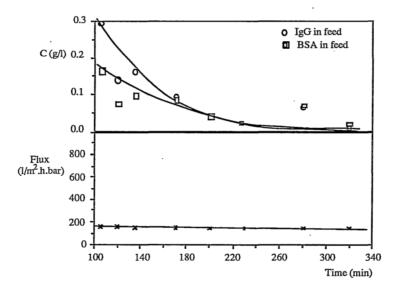

Fig. 2 Kinetic changes in flux and protein concentration in stage II of the ACFF process using membrane B with the BS particles (BS 17 µm).

the diafiltration process proceeded long enough, e.g., about 4 hours for a 95% removal of the unbound proteins in this case. The flux of the membrane in this stage was nearly constant.

The results of dissociation of the bound proteins using 20 mM sodium octanoate and the final washing-out of protein molecules from the particle suspension are shown in figure 3 in a summarized form of the total ACFF process. It was apparent that in stage III the

bound BSA could be dissociated rather efficiently using 20 mM sodium octanoate, while the bound IgG could not. Another observation is that the dissociated BSA can be removed from the filtration system through the diafiltration process in stage IV.
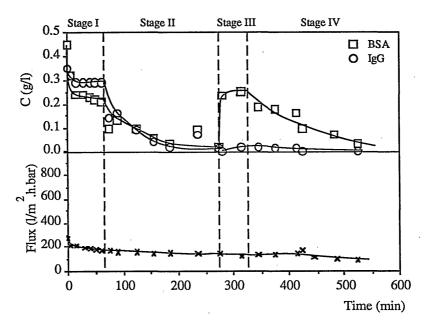

Fig. 3 *Kinetic changes in flux and protein concentrations (in the feed) in the four stages of the ACFF process using membrane B with the BS particles (BS 17 μm).*

In the ACFF experiments the mass balance for the proteins can be determined according to the changes of the protein concentrations in the feed, and are presented in mg/g drained gel in table 2. In total 32 mg protein per gram drained gel was loaded into the system. It appears that the membrane adsorbs about 2 mg BSA/g drained gel. The amount of BSA adsorbed on the particles was 18 mg/g drained gel, and 17 mg/g drained gel was recovered in the dissociation step. The recovery of the bound BSA was 53%, i.e. recovered protein against the total loaded protein, with a purity of more than 95 %. However, it has to be noted that the protein loading is not optimized against the amount of the carrier particles applied. Instead of the optimization an excess amount of proteins was loaded into the system for the purpose of demonstrating the efficiency of the membrane used in the washing stage of the ACFF process.

A large amount of IgG, 6.4 mg/g drained gel, was retained by the membrane, and only 4.9 mg/g drained gel was retained by the particles. In the dissociation stage hardly any IgG could be measured. This finding indicates that the bound IgG could not be removed effectively by the dissociation solution applied but stayed on the particles. This is in an agreement with the test tube results (see Chapter 3). However, it may not be a problem upon the reuse of the particles since BSA has the ability to displace preadsorbed IgG to a certain extent (see chapter 4 of this thesis).

As has been pointed out above that membrane B is an adsorptive type of membrane (see chapter 6 of this thesis), protein adsorption on the membrane will take place throughout the whole process as well as protein binding onto the ligand-immobilized particles. The two processes take place simultaneously which are therefore difficult to distinguish and has yet to be taken into account in the mass balance mentioned above.

In case 2, membrane D having a larger mean pore size in comparison with membrane B was tested as an alternative since membrane B to its disadvantage was proven to be of an adsorptive type. Membrane D has a selective layer at the outer surface of the fibers. Thus, the feed is supplied through the shell side of the module instead of the lumen side as used for membrane B. Nevertheless, the changes in concentration of BSA and IgG in the feed in the stages I, II and III, as shown in figure. 4, are comparable with those for membrane B. In stage I protein binding on the particles occurred. It appears that protein adsorption/deposition (especially IgG) onto the membrane occurs also which will be discussed in the following paragraph. In stage II the unbound proteins were removed via diafiltration. Finally, in stage III, upon the addition of sodium octanoate, the bound BSA molecules were released from the affinity complex while hardly any release of IgG was observed. When the flux behavior was examined a severe flux decline at the very beginning of the process indicates the occurrence of the fouling phenomenon. The actual flux during the process is not unreasonably low, and higher than in case 1. A further decrease in flux at the beginning of stage II has been observed in the ACFF experiments. The reasons for this flux reduction are not quite clear. One possibility could be that the deposition of particles or particulates on the membrane surface is dependent on protein concentration: a higher protein concentration prohibits particle deposition while a lower protein concentration does not prevent particle deposition. For membrane D it has been observed that the deposited particles were leaving the external membrane surface when a
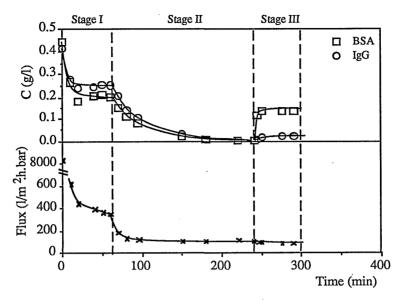
Fig. 4 Kinetic changes in flux and protein concentration in the four stages of the ACFF process using membrane D with the BS particles (BS 17 µm).

protein solution was added. Accordingly, it may be possible that upon the addition of buffer solution into the feed container during the diafiltration process the protein concentration in the feed is lowered, resulting in more particles deposited on the membrane surface, so that more pores will be blocked by these particles.

To understand the reason behind the drastic flux decline of membrane D, three filtration experiments were arranged using three solutions: 1) a 0.5 g/l BSA solution, 2) a 0.5 g/l IgG solution and 3) a mixture of 0.5 g/l BSA and 0.5 g/l IgG at the same operating pressure of 0.1 bar. The results for the filtration experiment with only BSA present showed no flux decrease and no retention was observed by the membrane in two hours. In contrast, the results for the filtration experiment with the IgG solution showed a severe flux decrease, as can be seen in figure 5. At the same time, the retention coefficient for IgG increased dramatically, reaching a value of more than 95% within 2 hours of filtration time. The filtration experiment with a mixture of BSA and IgG showed similar results as for IgG present alone in the solution, see figure 6. The difference between the two experiments was that the increase in retention for the protein mixture took much longer time to reach a value of 90% compared to that using IgG solution. According to these results, it is apparent that the flux decrease in the first stages of the ACFF process is merely caused by IgG and

not by BSA. A separate experiment for protein adsorption on membrane D was performed. The results revealed that no influence of adsorption of either BSA or IgG
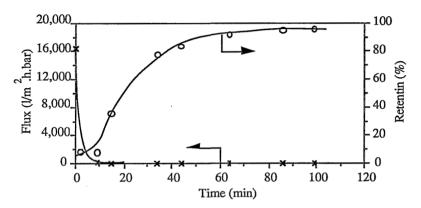

Fig. 5 Flux and retention behavior of membrane D with a 0.5 g/l IgG solution, at an operating pressure of 0.1 bar.
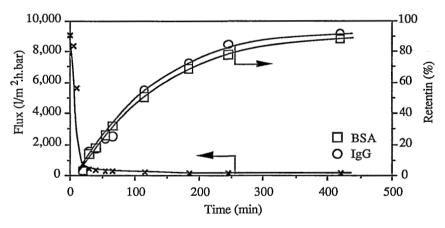

Fig. 6 Flux and retention behavior of membrane D with a mixture of 0.5 g/l BSA and 0.5 g/l IgG, at an operating pressure of 0.1 bar.

on buffer flux decline was observed. Therefore, the severe flux decrease may be attributed to the shear-induced protein aggregation (due possibly to the higher initial flux) and interfacial deposition of these aggregates.

When the protein pair BSA and lysozyme instead of BSA and IgG was used in the ACFF experiments with membrane D, the filtration flux showed only a limited decrease. At the end of the process the flux was still as high as 4000 (l/m^2.h.bar). This results gives a further evidence that IgG is causing the problems in case of membrane D giving a severe flux decrease.

The choice for hydrophilic hollow fiber membranes, which are commercially available, is rather limited. In contrast, there are numerous types of flat sheet membranes having a hydrophilic character. Therefore it was decided to use another membrane configuration in case 3. The results for flux decline and changes in protein concentration in the ACFF experiments using membrane E are given in figure 7. In stage I both BSA and IgG bound
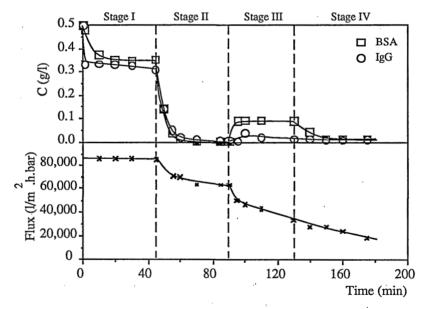
Fig. 7 *Kinetic changes in flux and protein concentration (in the feed) in the four stages of the ACFF process using membrane E with the BS particles (BS-17 μm).*

onto the particles. During the washing process in stage II all the unbound proteins were removed within 40 min. which is a rather fast process as compared to the cases 1 and 2. Upon dissociation using sodium octanoate BSA was released from the particles while only

very little IgG was released. Also shown in figure 7 is the flux behavior of membrane E. It is clearly shown that the flux decreased gradually during stage II to stage IV, which is regarded to be the result of the accumulation of protein-bound particles on the membrane surface. However, this flux decrease can be prevented by a kind of back flushing through flow management in which before each flux measurement the feed pump was stopped; as a result, the permeate flows back through the membrane to the feed side due to gravity forces (10 cm water height). This in turn removes the particles deposited on the membrane surface. When the pump was started again the flux was measured at the steady state. A typical example of such an experiment is given in figure 8. Besides the concentration
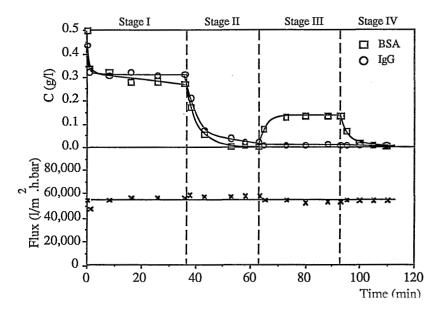

Fig. 8 Kinetic changes in flux and protein concentration (in the feed) in the four stages of the ACFF process using membrane E with the BS particles (BS-17 µm). The flux is kept constant by a special flow control (back flushing).

changes which reflect the binding / release of the proteins onto / from the particles, the interesting thing is that the filtration flux was kept high throughout the process which is a very encouraging result. This result does implys the necessity of the application of the back-flushing technique in the ACFF process.

7.3.2 Use of core-shell latex particles

In chapter 5 it has been observed that for the type of core-shell latex of smaller particle size, a severe flux decline as well as rising protein retention are inevitable due to the formation of a deposited particle layer, although the original membrane does not retain proteins. This has indeed been observed in the ACFF experiments using the BL particles of 0.22 µm in diameter. These disadvantages overbalance the benefit of using small-sized particles for a high surface area available for ligand immobilization. Therefore, the core-shell latex particles with a diameter of 1.96 µm were used in the ACFF experiments for the separation of BSA from a BSA/IgG mixture. The results of changes in flux and protein concentration using membrane B are given in figure 9. The changes in protein concentrat-
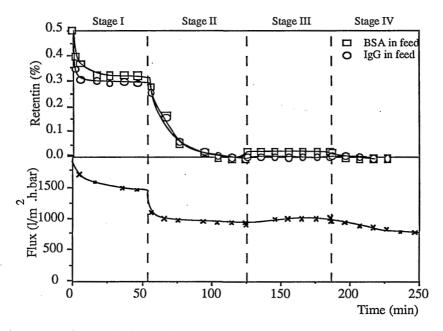

Fig. 9 Kinetic changes in flux and protein concentration (in the feed) in the four stages of the ACFF process using membrane B with the BL particles (BL-1.96 µm).

ions during the process are similar to the previous observations mentioned above. In stage I the concentration for both proteins decreases. This decrease is due largely to the binding / release on the membrane (see chapter 6). By counting the amount of protein present in the permeate throughout the washing stage, it appears that 80 % of the total loaded protein was

found in the permeate. The remaining 20 % proteins are partially bound to the particles, which can be found back upon release in stage III (4 % of the loaded protein and 3.8 mg/g latex particles), and partially adsorbed onto the membrane which could not be removed by the washing procedure. The washing stage was completed in one hour filtration time. During stage III only a small amount of BSA was recovered which is the result of the low surface area, and thus the low binding capacity of the larger BL particles. As a compensation for the low binding capacity the flux decline had largely improved and the flux kept relatively high throughout the filtration process. A flux decline at the beginning of stage II was observed in the ACFF experiments. The reasons for this flux reduction has been discussed above.

There are several mathematic models which can be used to describe the washing stage of the ACFF process [15, 17]. Depending on the state of the adsorbed proteins, two extremes can be distinguished, i.e. 1) no release of the bound proteins due to the dilution of the protein concentration by washing buffer because the binding is very strong; 2) the bound proteins on the surface are in equilibrium with the free protein in solution. For the first case an equation to describe the protein concentration C in the feed for a diafiltration process can be derived from a mass balance:

$$C = C_0 \exp \left(- (1 - R) \frac{V}{V_0} \right) \qquad (1)$$

where C_0 is the initial protein concentration, R is the retention coefficient, V_0 is the processing volume and V is the cumulative filtrate volume. For the second case a differential equation has to be used to take into account the change of the protein concentration in the feed due to protein binding/release onto/from the ligand-immobilized particles [17]:

$$V_0 \frac{dC}{dt} = - Q C (1 - R) - V_0 \phi \frac{d\Gamma}{dt} \qquad (2)$$

where Q is filtrate flow rate, t is time, ϕ is the volume fraction of the ligand-immobilized particles and Γ is the amount of the bound proteins on the ligand-immobilized particles. The term on the left hand side of the equation describes the changes of the protein concentrations in the feed, which are resulted from two sources as can be seen on the right

hand side of the equation. The first term on the right hand side of the equation gives the protein loss in the permeate during diafiltration and the second term accounts for the release of the bound proteins from the ligand-immobilized particles. When the second term is zero, meaning no protein release takes place, the integration of equation 2 results in equation 1. With the assumption that the bound proteins on the surface are in equilibrium with the proteins in the feed, the expression of $d\Gamma/dt$ can be derived from the following equation (see chapter 3):

$$\Gamma = \Gamma_m \frac{K_a C_e}{1 + K_a C_e} \tag{3}$$

where C_e is the protein concentration at equilibrium, K_a represents the binding strength between the protein and the ligand and Γ_m corresponds to a monolayer coverage of the bound molecules. In fact an equation for a two component system instead of a single component should be used for the differentiation of $d\Gamma/dt$. However, such a differential equation can not be solved analytically. Therefore equation 2 is solved in combination with equation 3 with the conditions that Q, ϕ, K_a and Γ_m are constant during the washing stage:

$$\frac{V}{V_0} = \frac{1}{(1-R)} \langle (1 + \phi \Gamma_m K_a) \ln (\frac{C_0}{C}) + \phi \Gamma_m K_a \ln (\frac{1 + K_a C}{1 + K_a C_0})$$

$$+ \frac{\phi \Gamma_m K_a^2 (C - C_0)}{(1 + K_a C) (1 + K_a C_0)} \rangle \tag{4}$$

With this equation the second case, i.e. the protein concentrations in equilibrium state can be modeled. The results of the model calculation for stage II, the washing stage, for the BL particles in the ACFF experiments are presented in figure 10. It can be seen in figure 10 a and b that the experimental data does not follow the calculated curves 3 which describes the diafiltration with $R = 0$ (in equation 1), but can be well described by the curves 2 when $R = 0.2$ for BSA and $R = 0.3$ for IgG are taken into account. These retention values for the proteins BSA and IgG by the membrane is reasonable as has been demonstrated in chapter 6. The model which describes the protein concentrations in the equilibrium state (equation 4), results in a similar curve (curve 1) to curve 2, when taking $R = 0.2$ for BSA and $R = 0.3$ for IgG. These modeling results may be explained by the fact that the binding interactions between the proteins and the ligand-immobilized particles are strong so that it

can equally well be described by the model corresponding to no protein release, while the similarity between the two models needs further study for a better understanding.
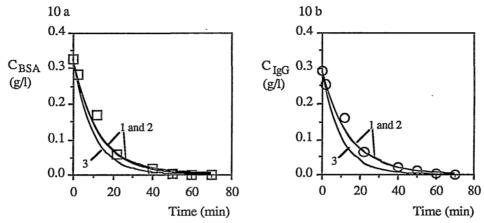

Fig. 10 *Model calculation for the protein concentrations in the washing stage of the ACFF process using membrane B with the BL particles (BL-1.96 µm). Curve 1 represents the model calculation at equilibrium (Eq. 1), curve 2 and 3 are obtained from the diafiltration theory with R = 0 for curve 3, and R = 0.2 for BSA and R = 0.3 for IgG in the case of curve 2.*

7.4 CONCLUDING REMARKS

Both BSA and IgG bind to the ligand-coupled particle. BSA shows a higher affinity compared to IgG. The bound BSA can be recovered using 20 mM sodium octanoate with a purity of more than 95 % whereas IgG can not. It is possible to avoid flux decline in the ACFF process by optimizing the combination of protein-particle-membrane.

The study on the Affinity Cross-Flow Filtration process in this thesis has come to the following conclusions:

- Microfiltration membranes with non-adsorptive characteristics are preferred while use of ultrafiltration membranes is not advisable.
- Larger porous particles with minimized non-specific protein adsorption have the advantages of providing larger surface area for ligand immobilization and thus have the potential for achieving higher binding capacity. In the meantime binding kinetics

for these larger particles can still be fast enough in comparison with the much smaller non-porous particles, while a higher permeate flux during filtration in the presence of proteins is possible.

- For non-porous type of particles a larger particle size means high permeate flux while protein binding capacity can be low. On the other hand a smaller particle size may lead to higher binding capacity while the filtration performance can be poor.

- Back flushing technique can improve filtration flux significantly.

7.5 REFERENCES

1. J.C. Janson, Trends Biotechnol., 2 (1984) 31.

2. C.R. Lowe, J. Biotechnol., 1 (1984) 3.

3. J.H.T. Luong, A.L. Ngugen and K.B. Male, TIBTECH, 5 (1987) 281.

4. N. F. Gordon, C.M.V. Moore and C.L. Cooney, Biotech. Adv., 8 (1990) 741.

5. J. -P. Chen, J. Fermentation and Bioengineering, 70 (1990) 199.

6. D. Sii and A. Sadana, J. Biotechnol., 19 (1991) 83.

7. B. Mattiasson, in "Chromatographic and Membrane processes in Biotechnology", C.A. Costa and J.S. Cabral (Eds.), Kluwer Academic Publishers, Amsterdam, 1991.

8. B. Mattiasson. and T.G.I. Ling, in "Membrane Separation in Biotechnology", W.C. McGreger (Ed.), Marcel Dekker, New York, 1986, pp. 99.

9. B. Mattiasson and M. Ramstorp, Ann. N.Y. Acad. Sci., 413 (1983) 307.

10. B. Mattiasson and M. Ramstorp, J. Chromatogr., 283 (1984) 323.

11. T.G.I. Ling and B. Mattiasson, Biotechnol. Bioeng., 34 (1989) 1321.

12. K.B. Male, J.H.T. Luong and A.L. Nguyen, Enzyme Microb. Technol., 9 (1987) 374.

13. J.H.T. Luong, K.B. Male and A.L. Nguyen, Biotechnol. Bioeng., 31 (1988) 439.

14. J.H.T. Luong, K.B. Male and A.L. Nguyen, Biotechnol. Bioeng., 32 (1988) 451.

15. J.H.T. Luong, K.B. Male and A.L. Nguyen, Biotechnol. Bioeng., 31 (1988) 516.

16. T.B. Choe, P. Masse and A. Verdier, Biotechnol. Lett., 8 (1986) 163.

17. D.C. Herak and E.W. Merrill, Biotechnol. Progr., 5 (1989) 9.

18. D.C. Herak and E.W. Merrill, Biotechnol. Progr., 6 (1990) 33.

19. B. Gebben, D. van Houwelingen, W. Zhang, Th. van den Boomgaard, C.A. Smolders, Colloids and Surfaces B Biointerfaces, in preparation; chapter 2 of this thesis.

20. a. W. Zhang, Z. Borneman, B. Gebben, Th. van den Boomgaard, C.A. Smolders, Colloids and Surfaces B Biointerfaces, in preparation; chapter 3 of this thesis.

b. Chapter 4 of this thesis.

21. G. Birkenmeier, in "Protein-Dye Interactions: Developments and Applications", M.A. Vijayalakshmi and O. Bertrand (Eds.), Elsevier Applied Science, London and N.Y., 1989, pp. 253.

22. H.-J. Böhme, G. Kopperschläger, J. Schulz, and E. Hofmann, J. Chromatogr., 69 (1972) 209.

23. A.C.M. Franken, J.T.M. Sluys, V. Chen, A.G. Fane and C.J.D. Fell, Proc. in the 5th World Filtration Congress, Nice, France, 1990, 207.

SUMMARY

In this thesis the Affinity Cross-Flow Filtration (ACFF) process is studied as a potential application for the large-scale separation and purification of proteins.

The ACFF process can be divided into four stages. In the first stage a mixture of proteins is introduced into a container in which a ligand-immobilized carrier particle is present. The target protein will be bound to the ligand-immobilized carrier particle. In this way an affinity complex is formed. In the second stage purification of the protein of interest takes place by using a cross-flow microfiltration unit to wash out the impurities. In the third stage a reagent is introduced into the system to release the target protein. A filtration unit is used to recover the target protein. In the final stage the carrier particle is regenerated and ready for the next cycle.

In chapter 2 polystyrene core-shell latex and the ligand-immobilized core-shell latex complex were investigated as affinity ligand carriers. The core-shell latex particles consisted of a hard polystyrene core surrounded by a hydrophilic shell with particle sizes ranging from submicron to micron. The hydrophilic copolymeric shell completely covers the hydrophobic surface of the polystyrene core. Cibacron Blue, a ligand for some proteins, has been coupled to the hydroxyl groups present in the shell of the particles through triazinyl arylation. The core-shell latex particles as well as the ligand-immobilized core shell particles are characterized by conductometric titration, electrophoresis, protein binding and diffuse reflection spectroscopy. The amount of immobilized ligand could be determined by a number of techniques. It was found that of these, diffuse reflection spectroscopy gave the most reliable information. The degree of ligand immobilization appeared to be linearly proportional to the ionic strength of the reaction medium. The immobilization of Cibacron Blue is accompanied by an increase in negative surface charge and an increase of colloidal stability while the electrophoretic mobility remained unchanged. Binding of BSA to these functionalized core-shell particles was found to be linearly proportional to the Cibacron Blue surface density. BSA binding and release could be controlled by the salt concentration and appeared to be completed within 10 minutes under unstirred conditions, without loss of colloidal stability of the particles.

In chapter 3 binding experiments for singular protein on the ligand-immobilized core-shell latex particles and ligand-immobilized agarose particles are performed for three different proteins under various conditions. The protein binding capability Γ_m and the

binding constant K_a were evaluated from binding isotherms using a type of Langmuir fit. Protein binding on the ligand-coupled particles with variable surface ligand density revealed that the binding capacities of the three proteins were linearly related to the surface ligand density. Bovine serum albumin (BSA), bovine serum immunoglobulin G (IgG) did not show any binding on the core-shell latex particles without a ligand. This was an indication of the absence of non-specific adsorption sites on the particles for these proteins. However, the third protein lysozyme adsorbed substantially onto the core-shell latex particles. This could be attributed to the presence of opposing charged groups on the interacting species. It was found that protein binding on the latex particles is a fast process with respect to that on the porous agarose particles. Binding of BSA and IgG was influenced drastically either by the change of pH or by a change of ionic strength. Release of the bound BSA could be achieved by addition of NaCl, sodium octanoate, or free dye to the solution. In contrast, release of the bound IgG could only be achieved by addition of NaCl.

The ligand release as a function of time is discussed in the appendix to chapter 3. For all preparations of the ligand-coupled latex particles, it was found that the concentration of free ligand in bulk solution increased slowly with storage time. The percentages of loss of the immobilized ligands for the longest time period measured, about one year, were found to be less than 5 %. This amount of ligand loss is too low to give any significant influence on the binding capacity of the particles.

In chapter 4 competitive binding between BSA and IgG, and between BSA and lysozyme, onto ligand-coupled latices was studied. It was found that BSA bound preferentially with respect to IgG throughout a range of various ratios of the two proteins. Preferential binding of lysozyme, with respect to BSA, was found for a broad range of different protein compositions. Dilution of the total protein concentration, with fixed protein ratios, did not influence the binding of BSA. The competitive binding of BSA over IgG on the ligand-coupled latices was sensitive to the ionic strength of the solution. Prediction of the isotherms was attempted using a competitive binding model. Small deviations of the theoretical curves from the experimental isotherms were observed.

In chapter 5 the microfiltration behavior of the protein solution, the particle suspension and the mixture of both was investigated. For the case of protein solution particular attention was given to the phenomenon of protein aggregation and its consequence to flux decline. Microfiltration of the ligand-immobilized carrier particles in the presence and absence of protein was studied using several types of membranes. A range of different

particle sizes were used to show the influence of the particle size on the steady state flux. This study makes it clear that in the ACFF process microfiltration membranes with large pore sizes should be preferred regarding the flux behavior

In chapter 6 two partially permeable membranes, one hydrophilic and the other less hydrophilic, were used. Flux reduction and retention measurements were performed with two different types of proteins (BSA and IgG). Experiments of protein adsorption on the membranes were performed as well. Membrane performance was reduced to a large extent due to protein adsorption which resulted in an increase in retention for the protein with their small dimensions. For the membrane which did not adsorb protein the increased retention for the small protein was the result of the increased resistance in the boundary layer due to concentration polarization of the larger protein.

In chapter 7 the ACFF process is carried out in a batchwise mode with the model protein-ligand systems using a few types of membranes. Both purity and recovery of the target protein, in the presence of a model impurity were examined. Emphasis of this chapter is laid on the use of nonporous particles and membrane aspects in the ACFF process. The bound BSA can be recovered using 20 mM sodium octanoate with a purity of more than 95 %. It is possible to avoid severe flux decline in the ACFF process by optimizing the process.

SAMENVATTING

Dit proefschrift behandelt de mogelijke toepasbaarheid van het 'Affinity Cross-Flow Filtration' (ACFF) proces voor het op grote schaal scheiden en zuiveren van eiwitten.

In het ACFF proces kunnen vier processtappen onderscheiden worden. In de eerste stap worden de zogenaamde dragerdeeltjes, met de daarop geimmobiliseerde liganden, in contact gebracht met een oplossing van verschillende eiwittten. Afhankelijk van de gebruikte ligand zal één bepaald eiwit zich specifiek binden aan de dragerdeeltjes. In de tweede processtap worden de dragerdeeltjes met het gebonden eiwit door middel van cross-flow microfiltratie afgescheiden van de rest van de eiwitoplossing. Vervolgens worden de te zuiveren eiwitten weer van de dragerdeeltjes gescheiden door toevoeging van een daartoe geschikt reagens. Met een tweede membraanfiltratiestap kan het eiwit in gezuiverde vorm verkregen worden. De vierde en laatste processtap omvat de regeneratie van de dragerdeeltjes, zodat deze hergebruikt kunnen worden.

Hoofdstuk 2 behandelt de geschiktheid van polystyreen core-shell latices als dragerdeeltjes. De deeltjes bestaan uit een harde kern van polystyreen omgeven door een hydrofiele schil van een copolymeer. De hydrofiele schil zorgt voor een volledige afscherming van de hydrofobe polystyreen kern. De core-shell deeltjes hebben een maximale grootte van enkele micrometers. Middels een koppelingsreaktie werd Cibacron Blue als model-ligand covalent gebonden aan de in de hydrofiele schil aanwezige hydroxyl-groepen. De core-shell deeltjes, met en zonder ligand, zijn gekarakteriseerd met verschillende technieken: conductrometrische titratie, electroforese, eiwitbindings-bepaling en diffusieve relflectie spectroscopie. De hoeveelheid geimmoboliseerde ligand bleek het beste met behulp van diffusieve reflectie spectroscopie bepaald te kunnen worden. Er werd een evenredig proportioneel verband gevonden tussen de hoeveelheid geimmobiliseerde ligand en de ionsterkte van het reaktiemedium. De immobilisatie van het Cibacron Blue gaat gepaard met een toename van de negatieve oppervlaklading en de kolloidale stabiliteit van de deeltjes terwijl de electrophoretische mobiliteit niet veranderd. De binding van het eiwit 'bovine serum albumine' (BSA) aan de ligand gebonden dragerdeeltjes bleek evenredig proportioneel te zijn met de hoeveelheid Cibacron Blue aan het oppervlak van de deeltjes. De mate van BSA binding kon worden beinvloed door variatie van de zoutconcentratie, dit had geen gevolgen voor de kolloidale stabiliteit van de deeltjes. De bindingsstap verliep volledig binnen 10 minuten.

Hoofdstuk 3 beschrijft de resultaten van bindingsexperimenten met drie verschillende eiwitten onder verschillende condities. Er is gekeken naar twee verschillende ligand geimmobiliseerde dragerdeeltjes: core-shell latex and agarose deeltjes. Voor de verschillende combinaties zijn de eiwitbindingscapaciteit Γ_m en de bindingsconstante K_a bepaald door het fitten van de gemeten isothermen aan de Langmuir vergelijking. Voor alle drie de eiwitten werd een lineair verband gevonden tussen de hoeveelheid gebonden eiwit en de hoeveelheid geimmobiliseerde ligand. BSA en bovine serum immunoglobuline G (IgG) vertoonden geen enkele binding aan de core-shell latex deeltjes zonder ligand; dit is een aanwijzing voor de afwezigheid van niet specifieke bindingsplaatsen voor deze eiwitten op de deeltjes. Het derde eiwit lysozym echter adsorbeerde in aanzienlijke mate aan de core-shell latex deeltjes. De adsorptie kan worden verklaard door de aanwezigheid van tegengestelde ladingen op het lysozym en op de core-shell latices. Voor alle drie de eiwitten verliep de bindingsstap sneller voor de core-shell deeltjes dan voor de agarose deeltjes. De binding van BSA en IgG werd drastisch beinvloed door veranderingen van de pH en de ionsterkte. Deadsorptie van het gebonden BSA kon worden bereikt door toevoeging van NaCl, natrium octanoaat of door toevoeging van niet geimmobiliseerde ligand. IgG kon alleen worden gedeadsorbeerd met behulp van NaCl.

In de appendix van hoofdstuk 3 worden de resultaten van stabiliteitsstudies met de ligand geimmobiliseerde latex deeltjes beschreven. Er werd een lichte toename van de ongebonden ligand concentratie gevonden in de tijd. Na één jaar opslag was het verlies aan ligand minder dan 5%. De ligand geimmobiliseerde latex deeltjes vertonen ruim voldoende stabiliteit voor toepassing in een continue ACFF proces.

Hoofdstuk 4 behandelt de resultaten van competitieve bindingsexperimenten met BSA en IgG en BSA en lysozyme. BSA bindt preferentieel ten opzichte van IgG aan de ligand geimmobiliseerde core-shell latex deeltjes, voor een reeks van concentratie-verhoudingen van de beide eiwitten. Lysozyme bindt preferentieel ten opzichte van BSA. Verdunning van de totale eiwitconcentratie, zonder de verhouding in concentratie van de eiwitten te veranderen, bleek geen invloed te hebben op de binding van BSA. De preferentiele binding van BSA ten opzichte van IgG is afhankelijk van de ionsterkte. De waargenomen bindings-isothermen konden goed beschreven worden met een model voor competitieve binding.

De resultaten van microfiltratie-experimenten met eiwitoplossingen, suspensies van de core-shell latex deeltjes en met mengsels van beiden, staan beschreven in hoofdstuk 5.

Voor de eiwitoplossingen werd speciale aandacht geschonken aan het optreden van eiwitaggregatie en de invloed daarvan op de afname van de flux door de membranen. Er zijn filtratie-experimenten uitgevoerd met de ligand geimmobiliseerde dragerdeeltjes in aanwezig- en afwezigheid van eiwit met verschillende typen van membranen. Met name ook is gekeken naar de invloed van de deeltjesgrootte op de 'steady-state' flux door het membraan. De studies maken duidelijk dat voor het ACFF proces bij voorkeur microfiltratie-membranen met grote poriën moeten worden gebruikt.

Voor de metingen beschreven in hoofstuk 6 is gebruik gemaakt van twee verschillende semi-permeabele membranen; een hydrofiel en een minder hydrofiel type. Er zijn flux- en retentiemetingen uitgevoerd met oplossingen van de eiwitten BSA en IgG. Ook zijn eitwitadsorptie studies verricht. Beide eiwitten bleken te adsorberen aan het minder hydrofiele membraan. Zowel de retentie voor BSA als de flux bleken afhankelijk te zijn van de concentratie IgG. Er werd geen invloed waargenomen van de BSA concentratie. Beide eiwitten vertoonden geen adsorptie aan het hydrofiele membraan. De verhoogde retentie voor BSA kon in dit geval verklaard worden door het optreden van concentratiepolarisatie van het IgG.

Hoofstuk 7 beschrijft de resultaten van batch ACFF experimenten met verschillende typen membranen. Het hoofdstuk behandelt met name de membraanaspecten van het proces. Zowel de zuivering als de opbrengst van BSA in aanwezig- en afwezigheid van IgG zijn bestudeerd. Het BSA kan worden teruggewonnen met een zuiverheid van meer dan 95%. Door optimalisatie van de procesomstandigheden kon een drastische fluxafname voorkomen worden.

Curriculum Vitae

Wei Zhang was born on March 14, 1954 at Dalian (Liaoning), China. After graduation from high school in 1972 he spent some years on a farm in a mountainous countryside , and in a steal-iron factory. From 1978 to 1982 he studied in the Chemical Engineering Department of the Dalian University of Technology and obtained the degree of Bachelor of Engineering in 1982. Until 1986 he worked as a research assistant in the Dalian Institute of Chemical Physics, Chinese Academy of Sciences in the field of characterization of ultrafiltration membranes. The following two years he spent in the Division of Food Engineering, Chemical Center, University of Lund (Sweden) and he got his M.Sc. degree in Engineering in 1989. In April 1989 he joined the Membrane Technology group (under supervision of Professor Smolders and later Professor Strathmann) of the Chemical Technology Department at the University of Twente (The Netherlands) and worked in the field of affinity binding technique in combination with cross-flow filtration for large-scale protein separation and purification.